SYNTHETIC POLY(ETHYLENE GLYCOL)-BASED HYDROGELS FOR BIOMEDICAL APPLICATIONS

YAN LI

(B.Sc. in Pharmacy, China Pharmaceutical University)

A THESIS SUBMITTED

FOR THE DEGREE OF DOCTOR OF PHILOSOPHY

DEPARTMENT OF PHARMACY

NATIONAL UNIVERSITY OF SINGAPORE

2013

DECLARATION

I hereby declare that the thesis is my original work and it has been written by me in its entirety. I have duly acknowledged all the sources of information which have been used in the thesis. This thesis has also not been submitted for any degree in any university previously.

_____

Yan Li

25 Dec 2012

ACKNOWLEDGEMENT

I would like to express my sincerest gratitude to my supervisors, Dr. Ee Pui Lai Rachel and Dr. Yi-Yan Yang for their patience, guidance and support over the course of this research. They are constant inspirations and their suggestions were invaluable towards the completion of this work. I would also like to thank our collaborator Dr James L. Hedrick from the IBM Almaden Research Centre for the inspiring discussions and his invaluable contributions to our research.

I would like to acknowledge the Department of Pharmacy at the National University of Singapore and the Institute of Bioengineering and Nanotechnology (IBN), A*STAR for the various opportunities that have helped to make this journey an educational as well as an enjoyable one.

I would like to thank all past and present members of the Drug and Gene Delivery Group at IBN, A*STAR, especially: Ms Amalina Bte Ebrahim Attia, Dr Ashlynn Lee, Ms Cheng Wei, Mr Chin Willy, Mr Ding Xin, Dr Gao Shujun, Dr Jeremy Tan, Mr Ke Xiyu, Dr Liu Lihong, Dr Liu Shao Qiong, Dr Majad Khan, Dr Nikken Wiradharma, Dr Ng Victor, Dr Ong Zhan Yuin, Ms Qiao Yuan, Ms Sangeetha Krishnamurthy, Dr Shrinivas Venkataraman, Ms Teo Pei Yun, Mr Voo Zhi Xiang, Dr Wu Hong, Dr Yang Chuan, Ms Yong Lin Kin and Ms Zhang Ying for their helpful discussion, sharing of knowledge and most importantly their constant encouragement throughout the years. Special thanks go to all past and present members of Dr. Ee's research lab in the Department of Pharmacy,

especially to Dr Leow Pay Chin, Dr Tian Quan, Miss Luqi Zhang, Miss Bahety Priti Baldeodas, Miss Ying Wang and Mr Jasmeet Singh Khara for their kind help and advice.

I would like to dedicate this research work to my family. To my parents, who have always encouraged me to pursue my dreams and never give up. From them I have learned to be the best that I can be. To my brother, who is my guide and greatest friend. Last but not least, I would like to thank all my friends in Singapore and worldwide for their constant friendship and company during my graduate studies.

LIST OF PUBLICATIONS AND PRESENTATIONS

Publications:

Yan Li, Chuan Yang, Majad Khan, Shaoqiong Liu, James L. Hedrick, Yiyan Yang and Pui Lai Rachel Ee, Nanostructured PEG-Based Hydrogels with Tunable Physical Properties for Gene Delivery to Human Mesenchymal Stem Cells, Biomaterials 2012 33(27):6533-41

Yan Li, Kazuki Fukushima, Amanda Engler, Daniel J. Coady, Shaoqiong Liu, Yuan Huang, John S.Cho, Yi Guo, Lloyd S. Miller, Pui Lai Rachel Ee, Weimin Fan, Yi Yan Yang and James Hedrick, Broad-spectrum antimicrobial and biofilm disrupting hydrogels: stereocomplex-driven supramolecular assemblies, Angewandte Chemie International Edition 2012 52(2):674-8

Shao Qiong Liu, Chuan Yang, Yuan Huang, Xin Ding, Yan Li, Wei Min Fan, James L. Hedrick, and Yi-Yan Yang, Antimicrobial and Antifouling Hydrogels Formed In Situ from Polycarbonate and Poly(ethylene glycol) via Michael Addition, Advanced Materials, 2012 24(48):6484-9

Conference presentations

Yan Li, Chuan Yang, Shaoqiong Liu, Pui Lai Rachel Ee, James L. Hedrick and Yi-Yan Yang, Nanostructured synthetic hydrogels as scaffolds for cell delivery, The 5th SBE International Conference on Bioengineering and Nanotechnology (ICBN) 2010, 1-4 Aug 2010, Singapore. Poster presentation.

Yan Li, Chuan Yang, Majad Khan, Shaoqiong Liu, Pui Lai Rachel Ee, James L. Hedrick and Yi-Yan Yang, Nanostructured synthetic hydrogels as scaffolds for cell and gene delivery, Material Research Society Fall Meeting & Exhibit (MRS) 2011, 28 Nov-2 Dec 2011, USA. Oral Presentation.

Yan Li, Pui Lai Rachel Ee, James L. Hedrick and Yi-Yan Yang, Stereocomplex hydrogel with supramolecular structures for vancomycin delivery to treat MRSA-induced skin infection, European Material Research Society (EMRS) 2012 Fall Meeting, 17-20 Sep 2012, Poland. Oral Presentation.

TABLE OF CONTENTS

SUMMARY

Synthetic poly(ethylene glycol) (PEG)-based hydrogels have been widely used as a highly valuable class of biomaterials for various biomedical applications due to their inherent biocompatibility, biochemical inertness and ease of meeting specific requirements through functional tailoring. The overall goal of this thesis is to design, develop and evaluate the application of synthetic PEG-based hydrogels in two different biomedical applications: tissue engineering and antimicrobial therapeutics.

In tissue engineering, we hypothesized that genetic manipulations of human mesenchymal stem cells (hMSCs) in a nanostructured hydrogel microenvironment will provide an effective approach to improve cell delivery for tissue engineering.

To test our hypothesis, we explored two specific aims:

Aim 1: Synthesize and characterize injectable PEG hydrogels with micellar nanostructures incorporated. Here we described the rationale of incorporating micellar particles into PEG-based hydrogels with key features of tuning the physical properties of the hydrogels such as swelling ratio, porosity and degradability. We successfully demonstrated that the physical properties of the hydrogels could be tuned predictably and thus enabled the subsequent study of biological interaction between the PEG-based hydrogel scaffold and encapsulated cells.

Aim 2: Evaluate cell viability and gene transfection efficiency of hMSCs encapsulated in the nanostructured hydrogels. Here we further evaluated the hydrogel scaffold for both cell survival and gene transfection. We demonstrated that our synthetic bolaamphiphile was superior to poly(ethylenimine) (PEI) as non-viral gene carrier and hydrogels with 20% micelle content provided the optimal microenvironment for both cell survival and gene transfection. Therefore, incorporating micelles into hydrogels is a good strategy to control cellular behavior in a three dimensional hydrogel environment for tissue engineering.

For antimicrobial therapeutics, we hypothesized that hydrogels with cationic polymers incorporated provide an excellent formulation for clinical use in eliminating various microorganisms and biofilms.

To test our hypothesis, we explored three specific aims:

Aim 1: Synthesize and characterize cationic polymers for the formation of stereocomplex PEG hydrogels with supramolecular structures. Here we first described particle size and toxicity of the three cationic polymers followed by the evaluation of physical properties of the cationic polymer incorporated hydrogel including stereocomplex formation, stiffness and supramolecular structures. It was demonstrated that polymer with optimal hydrophobic/hydrophilic balance was the least toxic and cationic polymer containing hydrogel formed through stereocomplexation with shear-thing property and ribbon-like supramolecular structure were observed.

Aim 2: Evaluate the antimicrobial and antibiofilm activities of the hydrogel with cationic polymer incorporated *in vitro*. Here we evaluated the antimicrobial and antibiofilm activities of the hydrogel with different amount of cationic polymer incorporated *in vitro*. We showed that these hydrogels exhibited broad spectrum antimicrobial activities against both Gram-positive and Gram-negative bacteria, fungus and various clinically isolated drug-resistant pathogens. Moreover, they were capable of dispersing biofilms formed by *S. aureus*, methicillin resistant *S. aureus*, *E. coli* and *C. candida*. The mechanism of antimicrobial and antibiofilm action was found to be through the physical disruption of the bacterial cell membrane.

Aim 3: Investigate the *in vivo* activity of our hydrogel using the fungal keratitis animal model. Here we tested the antibiofilm activity of the hydrogel on the fungal keratitis animal model *in vivo*. It was demonstrated that our hydrogels were comparable or superior to commercially available antibiotics Amphotericin B, evidenced by the significant decrease in fungal recovery and hyphae invasion without any display of toxicity in healthy eyes. Therefore, these cationic hydrogels showed great potential for clinic use in eliminating various microorganisms and biofilm infections.

In conclusion, the findings of this thesis supported the hypothesis specified in each application and well-defined synthetic PEG-based hydrogels served as a promising platform in meeting the specific requirements in our intended applications in tissue engineering and antimicrobial therapeutics.

List of Tables

List of Schemes

List of Figures

List of Abbreviations

AMP	Antimicrobial peptide
BCA	Bicinchoninic acid
CMC	Critical micelle concentration
CFU	Colony forming unit
DMEM	Dulbecco's Modified Eagle Medium
DMSO	Dimethyl sulfoxide
DS	Differential scanning calorimetry
ECM	Extracellular matrices
ESC	Embryonic stem cell
EPL-MA	Epsilon-poly-L-lysine-graft-methacrylamide
FBS	Fetal bovine serum
HA	Hyaluronic acid
HDF	Human dermal fibroblast
HDP	Host defense peptides
hMSCs	Human mesenchymal stem cells
iPSC	Induced pluripotent stem cell
LCST	Low Critical Solution Temperature
MIC	Minimum inhibitory concentration
MRSA	Methicillin-resistant *Staphylcoccus aureus*
MSCGM	Mesenchymal stem cell growth medium
PBS	Phosphate buffered saline
P(D,L)LA	Poly(D, L-lactide)
PDLA-CPC-PDLA	Poly(D-lactide)-charged polycarbonate- poly(D-lactide)
PEC	Polyelectrolyte complex
PEG	Poly(ethylene glycol)
PEG-AC	Tetra acrylate-terminated PEG
PEGDA	Polyethelyne glycol diacrylate
PEGDMA	Polyethelyne glycol dimethacrylate
PEGMA	Polyethelyne glycol methacrylate

PEG-SH	Tetra sulfhydryl PEG
PEI	Poly(ethylenimine)
ROP	Ring-opening polymerization
RLU	Relative light units
SEM	Scanning electron microscope
TBE	Tris/Borate/EDTA
TE	Tris ethylenediaminetetraacetate
TEM	Transmission electron microscope
TEOA	Tricthanolamine
TSB	Tryptic soy broth
TU	N-(3,5-trifluoromethyl)phenyl-N'-cyclohexylthiourea
VRE	*Vancomycin-resistant enterococci*
VS-PEG-PC	Vinyl sulfone-PEG-polycarbonate
XRD	X-ray diffraction
YMB	Yeast mould broth

CHAPTER 1. INTRODUCTION

1.1 What are hydrogels?

Hydrogels are, by definition, crosslinked polymeric networks with the ability to hold water as the continuous phase in the space between the polymeric chains. Water holding capacity of the hydrogel is dependent on the presence of hydrophilic groups such as amide (-CONH), hydroxyl (-OH) and carboxylic (-COOH) group found in the polymer backbone or as side chains. The integrity of hydrogels in water is maintained mainly due to the molecular interactions, including covalent and non-covalent forces between individual polymeric components present in the three dimensional network.

Polymeric hydrogels may be classified in different ways according to the nature of materials (natural vs synthetic), preparation methods (physical vs chemical) and biodegradability. The diverse material sources and preparation methods have significant implications on the physical properties of the hydrogels, such as three dimensional network, controllable mechanical properties, biodegradability and biocompatibility. The versatility of hydrogels has been demonstrated in a wide range of applications as food additives [1], pharmaceutics [2, 3] and environmental applications [4]. Due to their biocompatibility and the ease of tuning their physical properties, researchers have intensively exploited hydrogels for biomedical applications, including drug and cell delivery [5], wound healing [6] and tissue engineering [7] over the last 2 decades.

The aim of this chapter is to introduce readers to the nature of hydrogel materials, the preparation of hydrogels, their physical properties and finally their application in specific biomedical applications.

1.2 Materials of hydrogels

Polymer hydrogels for biomedical applications can be of either natural, synthetic origin or a combination of these two types of material. For example, alginate and chitosan are the two most widely used natural hydrogel materials which have gained substantial importance over the years [8, 9]. Collagen, gelatin and hyaluronic acid (HA) are natural components of extracellular matrix and have been successfully used as hydrogels for stem cell differentiation [5, 10, 11]. These natural polymers closely mimic targeted tissue structure because they are either components of or similar to the targeted living body in various macromolecular properties. Moreover, they interact with the targeted tissue in a favorable manner by presenting receptor-binding ligands and cell-triggered enzymatic degradation. Despite these advantages, it is difficult to tailor mechanical and degradability of these natural hydrogels in order to meet different requirement of specific applications. Furthermore, usage of these natural materials has been seriously restricted due to the potential risk of immunological reactions and pathogen transmission [12].

Apart from natural polymers, synthetic polymers provide an alternative and effective way for hydrogel formation and their broad applications. Hydrogels prepared from synthetic polymers differ in their properties due to various chemical structures, synthesis strategy and controllable hydrogel preparation techniques. In synthetic hydrogels, gel physical

properties and biological interactions between the hydrogel and living body are readily controlled, and therefore have significant advantages over natural polymers. For example, Benoit et al have successfully manipulated hydrogel degradation rate by changing the content of degradable macromere poly(lactic acid)-b-poly(ethylene glycol)-b-poly(lactic acid) endcapped with methacrylate groups (PEG-LA-DM) in the hydrogel to enhance osteoblast function and mineralized tissue formation [13]. Liu et al has prepared arginine-glycine-aspartic (RGD) peptide-containing hydrogels with tunable physicochemical and biological performance by varying fabrication temperatures. Specifically, increasing RGD concentration significantly enhanced cell attachment and proliferation in the hydrogel scaffold [14].

Many synthetic polymers, such as poly (D,L-lactic-*co*-glycolic acid) (PLGA) [15], poly (hydroxyethyl methacrylate (pHEMA) [16] and poly (ethylene glycol) (PEG) [17, 18], have been used in the formulation of hydrogels. Among these materials, poly (ethylene glycol) (PEG) hydrogel is one of the most widely used materials in biomedical applications due to their high compatibility, nontoxicity, low immunogenicity and highly water-swollen network. Functional groups, such as acrylate and methacrylate can be easily incorporated with PEG to form hydrogel network in the presence of appropriate photoinitiator or crosslinker. For instance, Bryant et al have prepared a poly(ethylene oxide) dimethacrylate hydrogel with varying thickness using UV photoinitiator for cartilage regeneration [19, 20]. Kim and team have mixed copolymer methacrylic acid (MMA) with PEG-PEGMA using tetra (ethylene glycol) dimethacrylate as crosslinker for insulin release [21]. More importantly, significant progress has been made to improve

cell-hydrogel interactions through the addition of cell adhesion peptides and enzymatically degradable entities. For example, the addition of RGD peptides as adhesive points has been utilized to promote stem cell proliferation in PEG hydrogels [22]. Lutolf et al has synthesized enzymatically degradable PEG hydrogel crosslinked by cysteine-containing matrix metalloprotease (MMP) oligopeptides for various applications [23, 24]. Therefore, PEG hydrogels with tunable physical properties and desirable biological interaction with the living body serve as superior hydrogel materials for various biomedical applications.

1.3 Preparation methods of PEG hydrogels

PEG hydrogels are commonly prepared by crosslinking either in a physical or chemical way. According to Hoffman, chemical hydrogels are permanent gels stabilized by covalently crosslinked networks [25], whereas physically crosslinked hydrogels do not rely on covalent bond formation and are generally formed through physical interactions, such as hydrogen bonding, molecular entanglement and ionic interaction. For example, Percec et al has blended hydrophobic aromatic poly(ether sulfone) and hydrophilic Poly(2-ethyl-2-oxazoline) polymers to form a physical hydrogel via hydrogen bonding [26]. Aqueous PVA solution turned into a highly elastic physical hydrogel in the process of freeze-and-thaw due to the formation of PVA crystalline, which acts as physical crosslinking points in the network [27]. Although these physically crosslinked hydrogels have been widely used in various medical applications, [10, 28], one significant limitation of these hydrogels is their poor mechanical strength attributed to the weak

physical interactions. It is also difficult to obtain stable physically crosslinked hydrogel with tunable degradation rates.

*C*hemical crosslinked hydrogels are generally obtained via photopolymerization, click chemistry and Michael addition polymerization. Although the resulted chemically crosslinked hydrogels are more robust and stable than physical hydrogels, an important concern about chemically crosslinked hydrogels is the potential cytotoxicity caused during the hydrogel formation. In a typical photopolymerization reaction, acrylate functionalized PEG monomer was polymerized using UV and visible light [29, 30]. One major limitation of this method is the poorly controlled structure due to radical chemistry. On the other hand, the copper-mediated 1,3-cycloaddition reaction of an azide with an ethynyl (known as Click Chemistry) [31] represents a class of reaction, which is fast and efficient, and allows for the fabrication of hydrogels with improved mechanical properties as compared to those synthesized through photopolymerization. However, it relies on copper ion as catalyst, which is cytotoxic when used in biomedical applications.

In contrast, Michael addition chemistry, which was first exploited by Hubbell and coworkers [32], can be used to form PEG hydrogels under physiological conditions. In a typical reaction, macromers containing terminal thiol groups are reacted with multi-arm PEG macromers with acrylate or vinyl sulfone end groups to form stable thioether linkages through michael-type conjugate addition (Scheme 1). It does not require any initiator or catalyst in the reaction. Various Michael addition hydrogels have been reported, including hydrogels formed from PEG tetra-acrylate and thiol-modified dextran

[33], PEG diacrylate with thiol-modified hyaluronan [34]. Moreover, as this reaction proceeds under physiological conditions, thiol groups in the proteins and other biomolecules can participate and provide a convenient way to incorporate bioactive substance into the hydrogels. Thus, Michael addition serves as a promising approach to synthesize injectable hydrogels and have been widely used for cell and gene delivery [35] and tissue engineering [23]. In short, it is crucial to choose specific preparation techniques according to the intended end-applications.

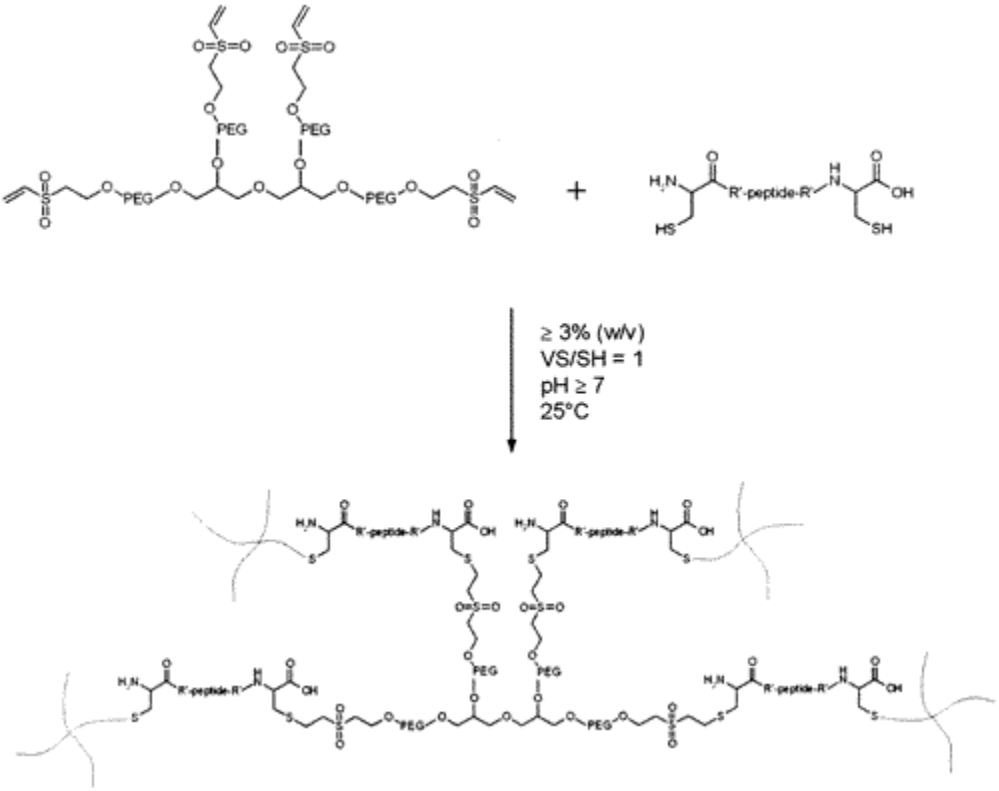

Figure 1.1 Synthesis scheme for the stepwise copolymerization of biomolecules containing free thiols on Cys residues with end-functionalized PEG macromers bearing conjugated unsaturated moieties. Image reproduces with permission from [36]. Cpoyright (2012) Elsevier.

1.4 Physical properties of hydrogels

Since hydrogels can be used in various biomedical applications which require different properties, it is important to characterize the mechanical properties of hydrogels. The strength of the hydrogel can be tuned by incorporating crosslinker, comonomers and increasing degree of crosslinking. However, there is an optimum mechanical strength for different applications. For example, soft hydrogels are preferred for neural regeneration [37] whereas bone tissue engineering requires hydrogel scaffolds to be more robust [38]. Too high a mechanical strength may lead to brittleness and less elasticity, the latter of which is important to provide flexibility to the hydrogel and facilitate the interaction between the hydrogel and target tissue. Thus it is important to strike a balance between mechanical strength and flexibility for the appropriate use of hydrogels.

Apart from mechanical strength of the hydrogels, a networked structure also plays a key role in biomedical hydrogel applications. These networks have a three dimensional structure and are crosslinked in a well-defined order. Hydrogel swelling generally results in a reduction in mechanical strength. Porosity of the hydrogels in return affects the hydrogel swelling and mechanical strength. These parameters are highly intertwined and an optimal balance between them is always essential for specific hydrogel application.

Shear thinning is another important property of hydrogel for biomedical applications. For example, injectability is a major requirement for minimal invasive surgery. Injectable hydrogel can be easily mixed with various therapeutics and cells before crosslinking and applied through a syringe to readily take the specific shape of target sites, providing

excellent interface between the hydrogel and tissue [39]. Moreover, remodelability is also desirable for topical applications [40].

Since the interaction between the hydrogel and targeted tissue is on both macroscopic mechanical and microscopic biological level, it is of great importance of study the degradability and biocompatibility of the hydrogels. The desired degradability of the hydrogel depends on specific applications and it is important to design and control degradation rate according to the unique requirement. There are three main degradation mechanisms: hydrolysis [41], enzymatic cleavage [42] and dissolution [43]. Most of the synthetic hydrogels adopt a hydrolysis degradation of ester bond at a constant rate [44, 45]. Moreover, hydrogels need to be biocompatible with the targeted tissue in order to be used safely. All polymers applied for biomedical applications and their degraded residues need to pass an *in vitro* cytotoxicity and *in vivo* toxicity test to determine the suitability for biological applications.

1.5 Biomedical applications of hydrogels

Wichterle and Lim first described the polymerization of (hydroxyethyl methacrylate) (HEMA) monomer in the presence of water and other solvents in 1960 to obtain a soft, elastic, water-swollen, clear gel. This innovation served as a prelude to the application of hydrogels in the soft contact lens industry, and to the modern field of biomedical hydrogels as we know it today [46]. Interest and applications for hydrogels have since steadily grown over the last fifty years from soft contact lens to diagnostics [47], therapeutic devices [48] and implants [49]. Specifically, hydrogels prepared from PEG

and their derivatives such as polyethelyne glycol methacrylate (PEGMA), polyethelyne glycol dimethacrylate (PEGDMA) and polyethelyne glycol diacrylate (PEGDA) have been applied in a wide range of biomedical industries, including drug and protein delivery [50], cell encapsulation and delivery [51], wound dressing [52] and tissue regeneration [53]. To our interest, this thesis is focused mainly on the applications of PEG-based hydrogels in the latter field of tissue engineering and another novel area in antimicrobial therapeutics.

1.5.1 Tissue engineering

Tissue engineering has received much attention as a potential strategy to overcome many developmental or degenerative diseases worldwide [54, 55]. For successful tissue engineering, three components are essential - appropriate cell source, scaffold and appropriate microenvironment.

1.5.1.1 Cell sources

Stem cells have been widely used to regenerate diseased and damaged tissues in the past decade. These cells can be found in embryonic or adult tissues or derived from adult somatic cells that have been reprogrammed via gene transfer. The pluripotent ability of embryonic stem cells (ESC) enables them to differentiate into any type of cells and reproducible generation of differentiated cell lineages has been reported [56]. However, the ethical debate on using ESC has put a serious limitation in its application. Induced pluripotent stem cell (iPSC), first produced from mouse cells in 2006 and from human

cells in 2007, has marked a great advance in stem cell research [57]. It allows researchers to induce pluripotent stem cells without using the ethically controversial embryonic stem cells. However, the uncertainty and risk due to gene silencing associated with reprogramming iPSC from somatic cells has greatly limited its application in humans [58]. On the other hand, human mesenchymal stem cells (hMSCs) act as appropriate cell source given that they can be expanded with high efficiency and induced to differentiate into different lineages under defined culture conditions [59-61]. Moreover, hMSC is an autologous cell source that can avoid immune rejection associated with heterologous cells. There is also less concern with ethical issues and the risk of teratoma formation associated with ESC [62]. These properties make hMSCs desirable candidate cell source for tissue engineering.

1.5.1.2 Scaffolds

In classic tissue engineering, hMSCs are encapsulated on/in to a three-dimensional scaffold in the presence of bioactive signals to induce differentiation, and the resulting constructs are then transplanted as a replacement tissue for regenerative repair [63]. An ideal three-dimensional scaffold for tissue engineering should be able to provide a well defined microenvironment to promote cell adhesion, proliferation and differentiation with good biocompatibility and biodegradability for clinical usage. Hydrogels as injectable delivery vehicles for cells and genes in the area of tissue engineering have been intensively studied in the past decades [25, 64, 65]. In particular, *in situ* forming hydrogels are attractive scaffolds because of their high water absorbing capacity, three dimensional properties that well mimic some of the physicochemical aspects of natural

tissues and ability to deliver cells and genes through a minimally invasive way to the desired site.

Although naturally derived biomaterials such as hyaluronic acid (HA) and collagen have been widely used as hydrogel scaffolds due to the good cell attachment properties [66, 67], their application has been restricted because of the potential risk of infectious diseases [12]. In this respect, synthetic hydrogels which provide biocompatible scaffolds with tunable physiochemical and mechanical properties can be better candidates. Poly (ethylene glycol) (PEG)-based hydrogels with low immunogenicity and tunable properties has been one of the mostly studied synthetic polymers for tissue engineering [68-70]. In addition, the remarkable versatility of PEG macromer chemistry facilitates the incorporation of bioactive signals into the scaffolds for stem cell anchorage and controlled differentiation [71].

The physical properties of PEG hydrogels can be tuned by changing the concentration of precursor material, the degree of crosslinking [72, 73] or using different degradable crosslinkers [74, 75]. However, most injectable PEG hydrogels are not able to remodel their structures when space is needed for cell growth, leading to limited cell proliferation. To overcome this problem, nanostructuring of scaffolds has recently been suggested to impart important structural cues and the subsequent interaction between the material and cells [76]. Nano-sized polymeric micelles can be formed from block or grafted amphiphilic polymers. With a crosslinkable functional group conjugated at one end of the hydrophilic block of the copolymer, a micelle can be formed with the functional groups

distributed on the surface of the micelle, which are accessible to crosslinking. These micelles can be utilized as a multi-arm crosslinker with great flexibility to prepare PEG hydrogels with tunable physicochemical and mechanical properties. Murakami Y et al [77] has successfully utilized an aldehyde-terminated crosslinkable micelle self-assembled from PEG-poly (D, L-lactide) as a multi-arm crosslinker to provide fast gelation property and good mechanical property for homeostasis glue.

1.5.1.3 Bioactive cues

Besides physical properties, a host of bioactive cues has been discovered to guide hMSC differentiation, thus making PEG hydrogels not only a 3D scaffold for supporting stem cells, but also an active microenvironment for tissue regeneration. These signaling molecules include, but are not limited to: 1) paracrine signal factors such as transforming growth factor-β [78], bone morphogenetic protein [79], fibroblast growth factors and the Wnt family [80]; 2) transcriptional regulators such as the Sox family [81]; 3) extracellular matrix components such as collagen and proteoglycans like versican [82]. Their induced commitment and differentiation of mesenchymal stem cells are modulated by the concentration of protein and the duration of exposure [83].

Specific or a combination of these signaling factors supplemented in the medium has been used to optimize the repair process in order to form stable and functional tissues [84]. Most of them are recombinant proteins with short half-lives, and are difficult to be effectively administered and maintain appropriate concentrations [85]. Gene transfer method has the potential to overcome these challenges by delivering therapeutical genes

to the right defect site via viral or non-viral gene vectors for sustained local expression of desired bioactive signals [86]. An ideal gene vector can efficiently deliver the gene of interest to the target cells and enable controlled and sustained gene expression for the desired biological effect.

Although viral gene vectors have been widely utilized in tissue engineering due to their high efficiency [87], they suffer from potential immunogenicity and insertion mutagenesis. Non-viral vectors, on the other hand, are easier to synthesize and modify which can cater to specific applications with low immunogenicity and safe to use [88]. Natural and synthetic materials such as cationic polymers [89], inorganic nanoparticles [90] and carbon nanotubes [91] as non-viral gene carriers have been intensively explored. Among them, cationic polymers are the most attractive because they can be easily tailored to suit special requirements. High molecular weight branched polyethylenimine (PEI, 25 kDa) has been widely used as a ‘golden standard’ of non-viral gene vectors. However, its application has been limited due to its high cytotoxicity. There is a pressing need in finding the optimal gene carrier with high gene delivery efficiency yet low cytotoxicity. In this thesis, we thus attempt to address this gap by incorporating a novel cationic polymer into our hydrogel scaffold to allow for high transfection yet low toxicity for concurrent gene and cell delivery in tissue engineering.

1.5.2 Antimicrobial applications

As mentioned above, hydrogel materials have been widely used in tissue engineering as extracellular matrix substitution by providing a suitable physical and biological

microenvironment for host cell function. However, these materials may also serve as an ideal environment for opportunistic bacteria on biomedical implants [92].

It has been reported that biomaterial-centered infections account for around 45% of all the nosocomial infections [93] and remained as a serious ongoing problem, regardless of advanced sterilization methods. These infections developed first through the bacterial adhesion and subsequent biofilm formation at the implantation site. When this happens, complicated surgical intervention to remove and/or replace the implant with possible function loss is needed and often inevitable [94]. Although preoperative sterilization and aseptic procedure help to limit the material-associated infections, there is a valid concern that the harsh sterilization conditions such as high temperature and irradiation may alter the material properties and destroy the therapeutics encapsulated, ultimately undermining the performance of the biomaterial [95].

1.5.2.1 Antimicrobial agents

Although antibiotics are the mainstay in the treatment of infections [96], recent studies have reported a less than desired efficacy against implant-associated infections [97]. There is also concern that such failure in treating implant-associated infections with conventional antibiotics may sooner or later result in antibiotic resistance in the pathogens [98]. These pathogens may acquire multidrug resistance through genetic mutation such as expression of drug altering enzymes and drug degrading enzymes, or drug efflux pumps capable of ejecting the antibiotics from the bacterial cells [99]. It has been reported that infections caused by multidrug resistant microorganisms failed to

respond to conventional antibiotics and raised high risk of death [100]. Thus there is an urgent need to develop new antimicrobial agents with mechanisms of action that are different from that of conventional antibiotics to overcome antibiotic resistance.

Antimicrobial peptides (AMP) were first discovered in early 1980s by Boman et al through the study of natural defensive system of the multicellular organisms [101]. These peptides are widely distributed throughout the animal and plant kingdoms and more than one thousand candidates have been identified on record in the AMP database [102]. These candidates are generally cationic amino acids capable of approaching negatively charged bacterial cell membrane through electrostatic interaction and hydrophobic amino acids for insertion into lipid domain of bacterial membrane to lyse the bacterial cells membrane [103, 104]. This physical interaction presents an unique mechanism in bacteria killing, not easily overcome by the development of drug resistance via classical means. However, having that said, it has also been reported that few bacterial species has acquired AMP-resistance by genetically reducing the peptides-binding sites or secreting digestive proteases to destroy peptides [105].

Inspired by the efficiency and versatility of AMP in killing pathogens, antimicrobial polymers are being developed as new class of alternative antimicrobial agents [106]. a number of strategies have been adopted by chemists for antimicrobial polymer synthesis. There are several important parameters to be considered in designing these macromolecules including: hydrophobic/hydrophilic balance, cationic density, molecular weight and biodegradability [107, 108]. Firstly, amphiphilicity greatly affects the

interaction between the polymers and cellular membrane and the further selectivity of bacteria over mammalian cells [109]. Secondly, changing cationic density was reported to be used as an alternative method to tune amphiphilicity of the polymers. By increasing charge density while keep hydrophobic domain constant, Tew et al successfully reduced hemolytic activity of poly(norobornene) [110]. Thirdly, molecular weight affects both efficiency and toxicity of the antimicrobial polymers. The efficiency of antimicrobial polymers were reported to increase [111], decrease [109] and adopt a parabolic shape [110] with increasing molecular weight, depending the composition of the polymer and the nature of pathogens. Moreover, nanostructured antimicrobial polymers with great degradability have recently received great attention due to the enhanced antimicrobial activity by increasing the local charge density through nanostructure formation [112]. The high versatility and efficiency of antimicrobial polymers offer great promise to enhance the current antimicrobial treatments. However, these antimicrobial polymers lack of specificity towards bacterial cells and thus induce nonspecific toxicity to mammalian cells. Therefore there is an increasing need to develop antimicrobial agents with broad-spectrum antimicrobial activities and negligible toxicity to mammalian cells.

1.5.2.2 Antimicrobial mechanisms

Understanding the antimicrobial mechanism will provide important insight for better design of new antimicrobial agents with broad-spectrum antimicrobial activity and no toxicity to mammalian cells. In contrast to conventional small molecular antibiotics which pathogens develop resistance easily through mutation [113], synthetic macromolecular antimicrobials are reported to adopt a physical membrane disruption

mechanism (Figure 1.2) to minimize the likelihood of pathogen developing resistance. Based on studies of AMP, two sub-classified mechanisms have been proposed: pore forming and non-pore forming mechanisms [114, 115]. Pore-forming AMP perpendicularly inserts into the bilayer of microbial cell membrane and induces stable pores of around 10 nm in the outer layer of the cell membrane, disturbing the homeostasis of the cell metabolism and resulting in cell death [116]. On the other hand, non-pore forming AMP interacts with microbial cell membrane in a parallel manner and generally induce massive disruption of the cell membrane [117]. In both of these two mechanisms, AMP induces physical disruption to the microbial cell membrane structure and reduces the possibility of developing drug resistant microbes.

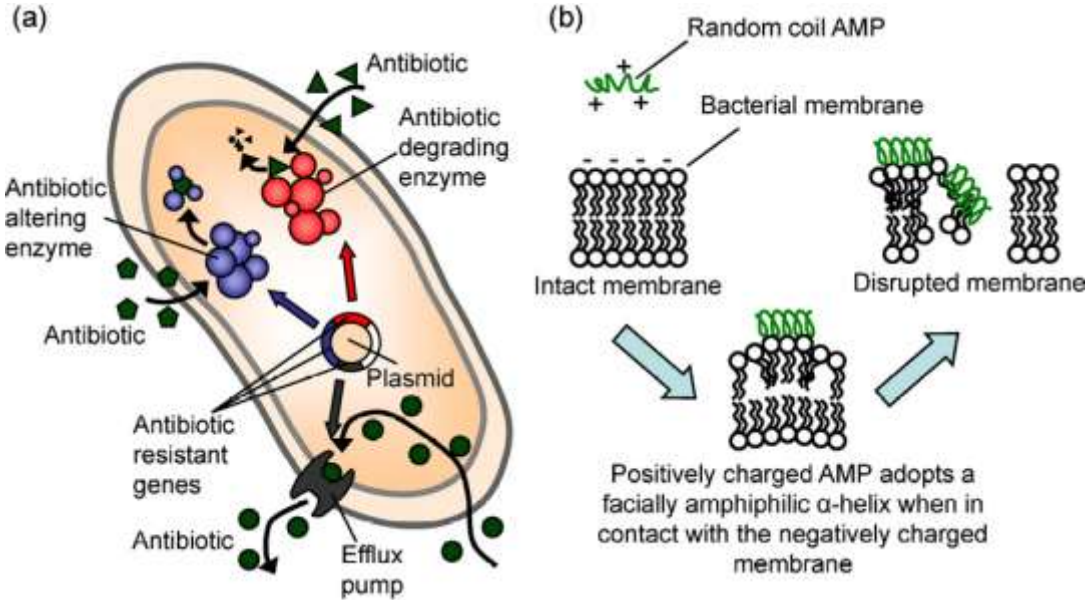

Figure 1.2 Comparison in functional mechanism between small molecular antibiotics and macromolecular antimicrobials. (a) Mechanisms of antibiotic resistance in bacteria and (b) mechanisms of membrane-active antimicrobial peptides. Image reproduces with permission from [108]. Cpoyright (2012) Elsevier.

1.5.2.3 Antimicrobial hydrogels

In order to reduce biomaterial-associated infections, hydrogel materials with antimicrobial activity have recently emerged as a rising trend to address these problems due to their wide application in biomedical applications [118, 119]. Typically, antimicrobial agents such as antibiotics, silver ions and niric oxide were loaded and released from hydrogels through active release strategies. For example, Wu et al has reviewed implanted medical devices with controlled drug released for infection prevention [120]. On the other hand, anti-infective silver, nitric oxide, known for their broad spectrum antimicrobial activity and nontoxicity to mammalian cells, have also been widely studied [121, 122]. Local administration of antimicrobial agents allows for selection of specific antimicrobial agent towards different pathogens at the implant sites. This approach not only enhances antimicrobial efficacy but also reduces the potential for systemic toxicity. However, their applications have been limited due to short half time of the cargoes in biological milieu for controlled release.

Hydrogels with intrinsic antimicrobial activity has recently attracted great attention and risen as a promising alternative strategy to address these problems. Salick et al has recently described a hydrogel scaffold formed from self-assembling peptide with inherent antimicrobial activities against both Gram-positive and Gram-negative bacteria while at the same time allow mammalian cell proliferation during co-culture [123]. The antibacterial activity was attributed to the lysine-rich polycationic surface which disrupts the bacterial cell membrane upon contact. These β-hairpin peptide hydrogels have further been proven by the same group to be able to kill methicillin-resistant *Staphylococcus*

aureus [124]. Beside peptides, polyelectrolyte hydrogels prepared through ionic interaction between cationic chitosan and anionic γ-poly(glutamic acid) exhibited antibacterial activity against *E. coli* and *S. aureus* yet promoted cell proliferation for potential biomedical applications [125]. However, hydrogels made through ionic interaction may lack proper mechanical stability and the risk of dissolution of the system for specific biomedical application. Recently, Li et al has reported an antimicrobial hydrogel coatings based on dimethyldecylammonium chitosan (with high quaternization)-graft-poly (ethylene glycol) methacrylate (DMDC-Q-g-EM) and poly (ehylene glycol) diacrylate [126]. These hydrogels were formed and coated using photoinitiators and the proposed mechanism of the antimicrobial activity is by attracting the anionic microbial membrane section into the internal pores of the hydrogel like an 'anion sponge'. The major disadvantage of hydrogel prepared from peptides and chitosan is the short half life and the possible risk of immunogenicity. Therefore, hydrogels made from synthetic materials with broad spectrum antimicrobial activity and biocompatibility are highly needed. Moreover, these antimicrobial hydrogels have great potential in treating biofilm-related infectious diseases by providing high local dosage of antimicrobial agents yet introducing low systemic toxicity.

1.5.2.4 Antibiofilm

Biofilm, consists of bacteria and self-secreted extracellular polymeric substances (EPS) [127], differ from free planktonic microorganism in distinct structural and biochemical properties (Figure1.3). Biofilm-associated infections are responsible for more than 85% of surgical devices associated infections [128] and have become one of the leading causes

of the surgical device implantation failure [129-133]. In addition, bacterial biofilms make wound management and healing very difficult [134]. These biofilms tend to grow on inert surface or dead tissue and often at a too slow growth rate to develop overt symptoms [135].

Although conventional antimicrobial agents are able to inhibit and/or kill the planktonic microorganisms, most of them remain ineffective in treating biofilm-associated infections [136, 137]. Host defense mechanism is incapable to kill the bacteria within biofilm and the resulted biofilms are extremely resistant to conventional antibiotics. Several mechanisms are reported to respond to the inherent resistance of biofilm to antimicrobial agents. Firstly, antimicrobial agents fail to penetrate the full depth of the biofilm [138]; secondly and most importantly, bacteria embedded in the biofilm is undergoing different metabolic state and slower growing rate due to the nutrient limitation in the biofilm as compare to planktonic bacteria cells [139]; thirdly, some of the cells in biofilm adopted a biologically programmed and protected biofilm phenotype to grow on a surface, and the complexity of the biofilm structure help to mimic the tissue of higher organisms [140]. Due to the insufficiency of standard antibiotic treatments, new approaches for preventing and treating drug-resistant infections need to be continually investigated. It is also one of our aims in this thesis to address this need with a new formulation of cationic hydrogels with broad spectrum antimicrobial activities in eliminating biofilms.

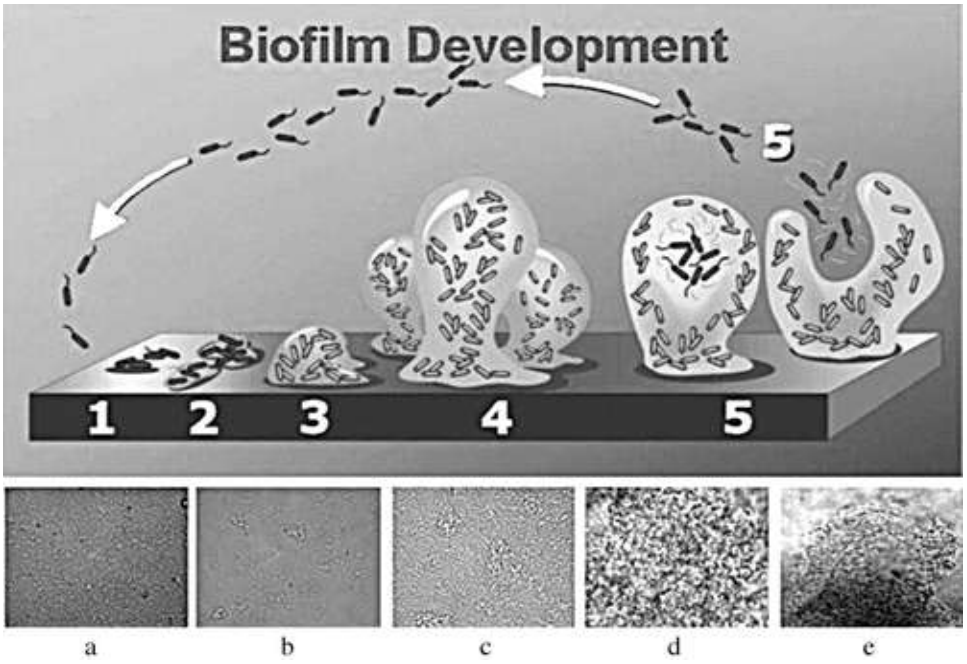

Figure 1.3 Diagram showing the development of a biofilm as a five-stage process. Stage 1: initial attachment of cells to the surface. Stage 2: production of EPS resulting in more firmly adhered "irreversible" attachment. Stage 3: early development of biofilm architecture. Stage 4: maturation of biofilm architecture. Stage 5: dispersion of single cells from the biofilm. The bottom panels (a-e) show each of the five stages of development represented by a photomicrograph of *P. aeruginosa* when grown under continuous-flow conditions on a glass substratum. Image reproduced with permission from [141]. Copyright (2002) Elsevier.

CHAPTER 2. HYPOTHESIS AND AIMS

Tissue engineering technologies have risen in recent years as important strategies for the replacement and reconstruction of dysfunctional and degenerative tissues. The emerging field of tissue engineering combines the principles of engineering, biology and medicine for the development of functional tissue and cell substitutes. An ideal scaffold should be able to support cell-cell and cell-matrix interactions and degrade at a rate that synchronizes with the new tissue being regenerated over time. In this respect, *in situ* forming hydrogels are attractive options because of their injectability, high water absorbing capacity and three dimensional properties which mimic the physicochemical aspects of natural tissues. In this study, our aim is to synthesize nanostructured hydrogels with tunable physical properties to closely mimic an optimal microenvironment for cell and gene delivery. To provide an appropriate microenvironment, current research has been focused on using specific or a combination of signaling factors supplemented in the growth medium to provide bioactive signals. However, most of these bioactive molecules are recombinant proteins which can be easily degraded *in vivo* and a sustainable release is thus required. To overcome these challenges, we investigated a novel strategy combining the benefits of gene transfection methods in our synthetic PEG-based nanostructured hydrogel scaffolds to create a cohesive system to guide cell behavior. **The hypothesis in this project is that genetic manipulations of hMSCs in a nanostructured hydrogel microenvironment will provide an effective approach to improve cell delivery for tissue engineering.**

To test this hypothesis, we propose 2 specific aims:

1) Synthesize and characterize injectable PEG hydrogel with varying amounts of micelle incorporated

2) Evaluate cell viability and gene transfection efficiency of hMSCs encapsulated in the nanostructured hydrogels

On the other hand, bacterial infections associated with the increasing utilization of biomaterial have attracted researchers' attention and the bottleneck to treat biomaterial-associated infections lies with the lack of broad spectrum antimicrobial and antibiofilm agents with less likelihood of drug resistance development and high selectivity to bacterial cells over mammalian cells. Of various antimicrobial agents, macromolecules have recently attracted immense attention in antimicrobial applications. These polymers balance charge and hydrophobicity to kill the pathogens through membrane disruption in order to avoid the development of drug resistance. In recent years, local delivery of existing antimicrobial agents by hydrogels greatly increased the antimicrobial efficacy to minimize the possible toxicity to mammalian cells and targeted the specific pathogen at the infection site to reduce the development of new strain of drug resistant pathogens. However, these hydrogels lack desirable shear thinning property for injection or topical applications. Moreover, degradability of the hydrogel remains as a valid concern in the clinical application of these hydrogels. To address these issues, we investigated a new strategy in combining the advantages of macromolecular antimicrobial polymers and remoldable hydrogel system to treat microbial infections. **Herein we hypothesized that stereocomplex hydrogels with cationic polymer incorporated provide a broad spectrum of antimicrobial and antibiofilm activities both *in vitro* and *in vivo*.**

To test this hypothesis, we propose 3 specific aims:

1) Synthesize and characterize cationic polymers and stereocomplex PEG hydrogel with supramolecular structure

2) Evaluate the antimicrobial and antibiofilm activities of the hydrogel with cationic polymer incorporated *in vitro*

3) Investigate the *in vivo* activity of our hydrogel using the fungal keratitis animal model

Work performed to carry out each specific aim is outlined as following: In chapter 3, we designed and synthesized hydrogels with different micelle contents to provide scaffolds with a wide range of physical property such as swelling ratio, porosity and degradability. Subsequently, the effect of micelle content on cellular behavior in the three dimensional hydrogel scaffold was explored in terms of cell survival and transfection. An optimal hydrogel scaffold with the highest cell viability and gene transfection was found to provide the best microenvironment to guide cell behaviors. In chapter 4, three cationic antimicrobial polymers were firstly screened in physical properties and toxicity test to obtain the best candidate for hydrogel incorporation. Hydrogels with cationic polymers incorporated were then formed through stereocomplexation and tested on various pathogens, including Gram-positive and Gram-negative bacteria, fungus and their biofilms. The potential hydrogel with broad spectrum antimicrobial and antibiofilm activities was further tested on a fungal keratitis animal model and showed comparable results as the commercially available antibiotic Amphotericin B. Lastly, in chapter 5,

conclusions and future perspectives derived from this thesis were provided in both application of tissue engineering and antimicrobial therapeutics.

The successful completion of this thesis has broadened the applications of synthetic PEG-based hydrogels and contributed in developing new strategies for hydrogels development in biomedical applications. The promising findings in this thesis should shed light on further research in designing well defined synthetic PEG-based hydrogel to meet specific requirements of different biomedical applications.

CHAPTER 3. NANOSTRUCTURED PEG-BASED HYDROGELS WITH TUNABLE PHYSICAL PROPERTIES FOR GENE DELIVERY

3.1 Background

Artificial scaffolds that can physically support cell infiltration and biologically direct cell behavior remain a challenge in tissue engineering. An ideal 3-D scaffold for tissue engineering should be able to provide a well defined microenvironment to promote cell adhesion, proliferation and differentiation with biodegradability and good biocompatibility. Poly (ethylene glycol) (PEG)-based hydrogels, as injectable vehicles with low immunogenicity and tunable physicochemical properties, has received much attention in the area of tissue engineering [142]. However, traditional PEG-based hydrogels are randomly crosslinked and are short of the structure complexity that existed in the natural extracellular matrices (ECMs) [143]. Recently, nanostructured scaffolds have been suggested to impart important structural cues on the subsequent interactions between the material and cells [144]. For example, Zhang et al [145] reported a nanoscale hydrogel network self-assembled from peptide nanofiber with ~20 nm in diameter. These gels mimic natural ECM that is composed of an intricate interweaving of protein fibers with diameter ranging from 10 to several hundreds of nanometers. Chondrocytes seeded in these peptide hydrogels maintained their phenotype throughout 4-week period of *in vitro* culture, and developed a cartilage-like ECM rich in type II collagen and proteoglycans. In addition, physical incorporation of polymeric micelles into PEG hydrogels was also used to tune the storage modulus, thereby influencing cell behavior in the hydrogel [146]. Here we, for the first time, proposed a new strategy by covalently incorporating nanosized polymeric micelles self-assembled from an amphiphilic block

copolymer of PEG and biodegradable polycarbonate into PEG hydrogel networks (Scheme 3.1). With a crosslinkable vinyl group at the hydrophilic end (PEG) of the block copolymer, micelles can be formed with vinyl groups present on the shell, which are accessible to thiol groups of four-arm PEG for crosslinking *via* Michael addition. Moreover, hydrogels formed with flexible multi-arm micelle served as an improved approach for cell and gene delivery as comparison to hydrogels formed from rigid two-arm PEG crosslinkers, which has reported by Shaoqiong Liu from our group [147].

Human mesenchymal stem cells (hMSCs) are multipotent cells that can self-renew and differentiate into multiple cell lineages, making them an attractive cell source for tissue engineering. Gene transfer in the hydrogel has the potential to overcome the shortage of protein production associated with protein delivery through providing sustained expression of desired bioactive signal [148]. A number of non-viral gene carriers such as cationic polymers [149], peptide [150] and lipid [151] have been introduced to hydrogels for gene transfection due to the low immunogenicity and high safety as compared to viral carriers [152]. However, it is challenging to attain high gene transfection efficiency and low cytotoxicity in the hydrogel scaffold. Hence, there remains a practical need to develop effective gene delivery systems in the hydrogel.

In this study, customized hydrogels with specific physical properties for cell adhesion and gene delivery is presented based on a formulation approach, where the constructs that are used are chemically incorporated into the gel. More specifically, we report biodegradable micelles-containing PEG hydrogels synthesized *via* Michael addition

chemistry, in which cationic bolaamphiphile/DNA complexes were physically encapsulated for gene transfer into hMSCs. The incorporation of the nanosized micelles provided an excellent means to tune physical properties of the hydrogels. RGD peptide was also chemically built into the hydrogel networks to enhance cell adhesion (Scheme 3.1). The effect of micelle content on various physical properties such as swelling ratio, mechanical strength and porosity, and on the subsequent cell behaviors including viability and gene expression efficiency of hMSCs incorporated inside the hydrogels was investigated. A small molecular weight symmetrical cationic bolaamphiphile was used as a non-viral gene transfection vector [153]. Polyethylenimine (PEI, 25 kDa), known as the gold standard for *in vitro* gene transfection, was employed as a positive control. Luciferase-encoding plasmid was used as a reporter gene to study the effects of the 3-D environment and micelle content on gene expression efficiency in hMSCs.

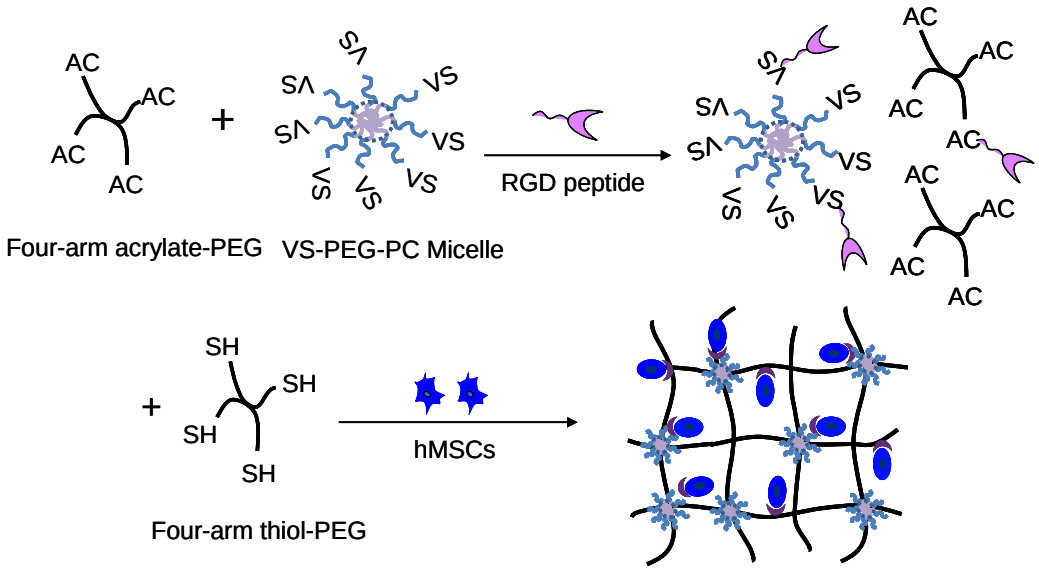

Scheme 3.1 Synthetic scheme of micelle-containing peptide/PEG hydrogel. VS-PEG-PC micelles were formed in advance by dissolving the polymer directly in 0.3 M triethanolamine buffer (pH 8.0) and stabilized overnight before adding to the hydrogel precursor solution. RGD peptide was chemically built into the hydrogel networks for cell adhesion. Gelation was done in 37 ℃ incubator.

3.2 Material and Methods

3.2.1 Materials

All reagents were purchased from Sigma-Aldrich and used as received unless otherwise noted. Tetra acrylate PEG (M_n 10,000 g/mol) and tetra sulfhydryl PEG (M_n 10,000 g/mol) were purchased from Sunbio Corporation (South Korea). RGD peptide (Mn 845.9 g/mol) with the sequence of Ac-GCGRGDSPG-$CONH_2$ was obtained from GL Biochem (Shanghai) Ltd (China). SH-PEG-OH (M_n 5000 g/mol, PDI 1.03) was purchased from RAPP Polymere GmbH (Germany). Sparteine was stirred over CaH_2, distilled in vacuum twice, and then stored in glove box. *N*-(3,5-trifluoromethyl)phenyl-*N*'-cyclohexylthiourea (TU) was prepared according to our previous protocol [154]. TU was dissolved in dry THF, stirred with CaH_2, filtered, and freed of solvent *in vacuo*. Phosphate-buffered saline (PBS) and tris ethylenediaminetetraacetate (TE) buffer were obtained from 1st BASE Pte Ltd (Singapore) and diluted to the intended concentrations before use. Luciferase-encoding plasmid was bought from Carl Wheeler, Vical (U.S.A). 1 kb DNA ladder was purchased from New England Biolabs, while ethidium bromide solution was obtained from Biorad Laboratories (U.S.A.). Reporter lysis buffer and luciferin substrate were purchased from Promega (U.S.A.) and bicinchoninic acid (BCA) protein assay reagent was purchased from Pierce (U.S.A.). Plasmid DNA encoding the 6.4 kb firefly luciferase gene driven by the cytomegalovirus (CMV) promoter was obtained from Carl Wheeler, Vical (U.S.A.), amplified in *Escherichia coli* DH5α and purified using Endofree Giga plasmid purification kit from Qiagen. Human bone marrow mesenchymal stem cells (hMSCs) and mesenchymal stem cell growth medium (MSCGM) were obtained from Lonza (U.S.A.).

3.2.2 Synthesis of VS-PEG-PC polymer

Amphiphilic diblock polymer (vinyl sulfone-PEG-polycarbonate, i.e. VS-PEG-PC) was synthesized by Dr. Chuan Yang from the Institute of Bioengineering and Nanotechnology (IBN). The polymer is capable of self-assembly into nanosized micelles in aqueous solution with crosslinkable vinyl sulfone group on the micelle shell.

3.2.3 Micelle formation and characterization

VS-PEG-PC micelles were formed in advance by dissolving the polymer directly in 0.3M triethanolamine buffer (pH 8.0) and stabilized overnight. Critical micelle concentration (CMC) of the polymer in triethanolamine buffer was estimated by fluorescence spectroscopy using pyrene as a probe [155]. Fluorescence spectra were recorded on a LS 50B luminescence spectrometer (Perkin-Elmer, U.S.A) at room temperature (25 ± 2°C). Typically, 10 μL pyrene in acetone solution (6.16×10^{-5} M) was added to containers and the acetone was left to evaporate. Polymer solutions (1 mL) at various concentrations were added into the containers and left to equilibrate for 24 hours. The final pyrene concentration in each sample was 6.16×10^{-7} M. The intensity (peak height) ratios of I_{337}/I_{334} from the excitation spectra were evaluated as a function of polymer concentration. The CMC was taken from the intersection between the tangent to the curve at the inflection and tangent of the points at low concentrations. Hydrodynamic diameter of the micelles was measured using a Zetasizer (3000 HAS, Malvern Instrument, U.K) at room temperature (25 ± 2°C). Micelle morphology was observed under a FEI Tecnai G^2 F20 transmission electron microscope (TEM) using an acceleration voltage of 200 KeV. To prepare the TEM sample, several drops of micelle solution at a concentration of 1000 mg/L containing 0.2% (w/v) of phosphotungstic acid were placed on a formcar/carbon-

coated 200 mesh copper grid and left to dry under room temperature (25 ± 2°C) prior to TEM observation.

3.2.4 Synthesis of micelles-containing PEG hydrogels

In a typical hydrogel preparation (e.g. 20% micelle), tetra acrylate-terminated PEG (PEG-AC) (2.6 mg, 0.26 μmol) was dissolved in 21.5 μl of 0.3M triethanolamine buffer (pH 8.0) to make a 12 (w/v)% precursor solution. 5.4 μl of VS-PEG-PC micelle solution (12 (w/v)%) as prepared in Section 3.2.3 was added to the precursor solution, followed by the addition of 10 μl of RGD solution (5 mg/ml) with final concentration of 1 mM. The reaction solution was kept in a 37°C incubator for 30 min. 23.2 μl of tetra sulfhydryl PEG crosslinker in triethanolamine buffer (12 (w/v)%) was then added to the mixture to make 1:1 molar ratio of SH in tetra sulfhydryl PEG and (AC+VS) (sum of acrylate groups in tetra acrylate PEG and vinyl sulfone groups in VS-PEG-PC). The final precursor concentration was 10 (w/v) %. The reaction mixture was kept in 37 °C as three 20 μl drops and hydrogel formed in minutes.

3.2.5 Physical characterization of hydrogels

As reported previously by our laboratory [74], the gelation time was determined by the vial tilting method. When the sample showed no flow, it was regarded as a gel. The hydrogels were placed in PBS buffer at 37 °C for 24 hours and weighed periodically, swelling ratio was calculated from the formula: Swelling ratio = $(W_w-W_d)/W_d$, where W_w

represents the weight of swollen gels, W_d represents the weight of the freeze-dried gels. All samples were analyzed in triplicate.

The internal morphologies of the freeze-dried gels were observed using a field emission scanning electron microscope (FESEM, Model JSM-5600, Japan). The hydrogels were immediately frozen in liquid nitrogen prior to freeze drying to keep the morphology intact. The cross-sectioned hydrogels were mounted on metal holders and vacuum coated with a platinum layer before SEM examination.

Rheology experiments were performed at room temperature (25 ± 2°C) using a control-strain rheometer (ARES 100FRTN1, Rheometric scientific). The dynamic storage modulus (G') and loss modulus (G'') were examined as a function of frequency from 1 to 100 Hz. The measurements were carried out at strain amplitude (γ) of 5% to ensure the linearity of viscoelasticity. Gel yield was calculated from the formula: Gel yield = W_d/W_i, where Wd represents the weight of the freeze-dried gels, and W_i represents the weight of the total starting materials. All samples were analyzed in triplicate.

3.2.6 Culture and encapsulation of hMSCs in the hydrogels

hMSCs were cultured in Mesenchymal Stem Cell Growth Medium (MSCGM) (Lonza, U.S.A) and incubated at 37 °C, 5% CO_2 incubator. The medium was changed every other day. Cells were harvested with PBS containing 0.025% (W/V) trypsin and 0.01% EDTA, centrifuged and subcultured to passage 4 in the MSCGM medium. Hydrogels for the study of cell encapsulation were also prepared according to the protocol described in

Section 3.2.4. The cells were resuspended in 20 µl of MSCGM medium and then mixed with the gel precursors prior to crosslinking. Cell density was 10 million per ml. Droplets of hydrogel were kept in 37 °C incubator and formed within minutes. The gels were then transferred to a 96 well plate and cultured in 150 µl of MSCGM medium. Medium was changed hourly for the first 2 hours and every day for the following 2 days.

To visualize the distribution of hMSCs inside the PEG hydrogel, confocal images were obtained using a LIVE/DEAD$^{@}$ viability/cytotoxicity kit (Invitrogen, U.S.A). Briefly, 10 µL of ethidium homodimer-1 and 5 µL of calcein AM from the kit were diluted with 10 mL of PBS to make the staining solution. Each gel was stained with 100 µL of the staining solution for 30 min at room temperature (25 $\pm$ 2°C) in the dark and imaged with an inverted confocal microscope (Carl Zeiss, U.S.A)

3.2.7 Cell viability in the hydrogels

The viability of hMSCs in the hydrogel was quantified by MTT assay in triplicate. This assay is based on the cleavage of MTT (a yellow tetrazolium salt) into insoluble purple formazan crystals by the mitochondrial enzymes of viable cells. MTT solution was added to the hydrogel and incubated for 4 hours. The hydrogel constructs were then collected and homogenized in 400 µL of DMSO with tissue ruptor (Qiagen, U.S.A). An aliquot of 100 µL was taken from each well and transferred to a fresh 96-well plate. The plates were then assayed at 590 nm with a microplate reader (Tecan, Switzerland). The results were expressed as a percentage of the cell viability in the hydrogel without the micelles.

3.2.8 Characterization of polymer/DNA complex

The particle size and zeta potential of the complexes were measured using the Zetasizer (3000 HAS, Malvern Instrument, U.K). Gel electrophoresis was performed to evaluate the DNA binding ability of the cationic bolaamphiphile. Cationic bolaamphiphile/DNA complexes containing 1.5 μg of luciferase-encoded plasmids were prepared with various N/P ratios ranging from 2 to 14. The complexes were electrophoresed on 1% agarose gel (stained with 4 μL of 0.5 μg/mL ethidium bromide per 50 mL of agarose solution) in 0.5×TBE buffer at 80 mV for 60 min. The gel was then analyzed on a UV illuminator (Chemi Genius, Evolve, Singapore) to show the position of the complexed DNA relative to that of naked DNA.

3.2.9 Gene transfection in 2D cell culture plate

Gene transfection of bolaamphiphile/DNA complexes was performed in 24-well plates. The cell were seeded at a density of 5 $\times 10^4$ cells/well and cultivated in 500 μl growth medium for luciferase transfection. After 24 hours incubation, the culture medium was replaced with fresh medium and the complex solution (50 μl) containing 2.5 μg luciferase reporter gene was added to each well. After 4 hours incubation, the culture media were replaced with the fresh medium and incubated for 24 hours before being washed with 0.5 ml of PBS. Reporter lysis buffer (0.2 ml) was then added to each well to lyse the cells. The cell suspension was subjected to 2 cycles of freeze (-80 ℃, 30 min) and thaw (on ice), then centrifuged at 13,000 rpm at 4 ºC for 10 min to remove the cell debris. 20 μl of supernatant of the cell lysate was mixed with 100 μl of luciferase substrate and the relative light units (RLU) was measured using a lumimometer (Lumat LB9507, Berthold,

Germany), and normalized to protein content measured using BCA protein assay (Pierce). Naked DNA was used as negative control and PEI at N/P ratio 10 was used as positive control in this experiment.

3.2.10 Cytotoxicity studies of polymer/DNA complex in 2D cell culture plate

Cytotoxicity of bolaamphiphile/DNA complexes was performed in 96-well plates. Briefly, hMSCs were seeded at a density of 1 $\times 10^4$ cells/well and cultivated in 100 µl of growth medium. The culture medium was replaced with fresh medium after 24 hours incubation. Following that, 10 µl of complex solution was added into each well. After 4 hours, the culture medium was replaced with fresh medium and incubated for another 24 hours. The medium was then replaced with 100 µl of fresh medium together with 10 µl of MTT solution (5 mg/ml) and incubated for 4 hours. The medium was removed and 150 µl of DMSO was added to dissolve the formazan crystal formed. The resulted purple solution (100 µl) was taken and absorbance reading was measured at 550 nm and 690 nm using a microplate reader (PowerWave X, Bio-Tek Instruments). The difference of absorbance was taken and the results were expressed as a percentage of that of the negative control.

3.2.11 Gene transfection in 3D hydrogels with different micelle content

Cationic bolaamphiphile/DNA complexes containing 1.5 µg of luciferase-encoded plasmids with a series of N/P ratios were added to each hydrogel. Cationic bolaamphiphile/DNA complexes were formed by adding equal volume of bolaamphiphile solution into DNA solution, and incubated for 30 min. The complexes were then mixed

with hMSCs and incubated for 15 min at room temperature (25 ± 2°C). The cell suspension was then encapsulated into polycarbonate micelles-containing PEG hydrogels by mixing with the gel precursors prior to crosslinking. The gels were formed within 15 min at 37°C. The gels were transferred to a 96 well plate, and the medium was changed hourly for the first 2 hours and every day for the following 2 days. On the 4th day, the gel was washed twice with PBS and homogenized in 200 mL of reporter lysis buffer. The relative light unit (RLU) was measured using a luminometer (Bio-rad, U.S.A) and was normalized to protein content measured using the BCA protein assay (Bio-Rad, U.S.A). PEI/DNA complexes were used as a positive control and naked DNA was employed as a negative control. PEI/DNA complexes were made at N/P 10 as at this N/P ratio they induced high gene expression efficiency, yet provided more than 50% cell viability.

3.2.12 Cytotoxicity studies of polymer/DNA complex in 3D hydrogels

Cell viability in the hydrogel after gene transfection with the cationic bolaamphiphile/DNA complexes was tested by MTT assay in triplicate (Section 3.2.10). On the 4th day, the gel was washed twice with PBS. MTT solution was added to the hydrogel and incubated for 4 hours. The constructs were then collected and homogenized in 400 mL of DMSO with tissue ruptor (Qiagen, U.S.A). The results were expressed as a percentage of the cell viability in the hydrogel without the bolaamphiphile/DNA complexes incorporated.

3.2.13 Statistical analysis

All data are presented as mean ± SD. The statistical significance of the data was evaluated by two-tailed Student's t-Test. $P<0.05$ was considered statistically significant.

3.3 Results and discussion

3.3.1 Synthesis of VS-PEG-PC polymer

Vinyl sulfone-functionalized PEG-b-polycarbonate (VS-PEG-PC, Scheme 3.2) is an amphiphilic diblock copolymer synthesized by Dr. Chuan Yang from the Institute of Bioengineering and Nanotechnology (IBN). The detailed synthesis and characterization of the diblock copolymer is shown in Appendix A.

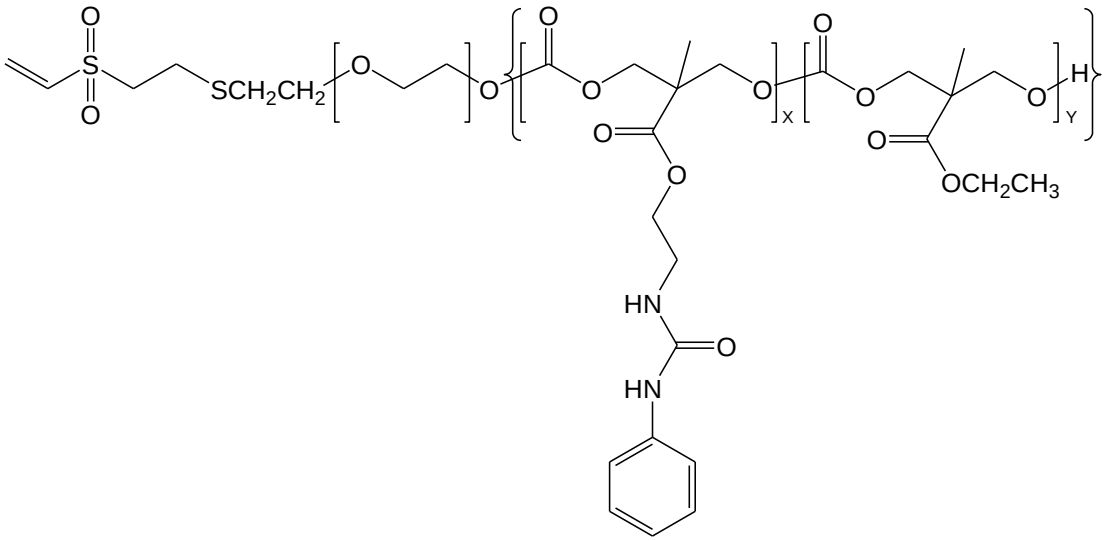

Scheme 3.2 Chemical structure of Vinyl sulfone-PEG-b-polycarbonate.

3.3.2 Micelle formation and characterization

VS-PEG-PC has a very low critical micelle concentration (CMC), which is about 7.1 mg/L in DI water, indicating that it can easily self-assemble into micelles by simply dissolving into water at very low concentrations. The CMC value of the polymer decreased to 1.6 mg/L (Figure 3.1) in TEOA buffer because of the presence of salts in the buffer. The particle size of the micelles in DI water was 56 nm with a narrow polydispersity index of 0.19. As shown in Figure 3.2, VS-PEG-PC self-assembled into distinct spherical nanoparticles as a result of the combination of hydrophobic and hydrogen-bonding interactions within the hydrophobic blocks of poly(urea-*random*-ethyl carbonate). The particle size estimated from the TEM pictures was in agreement with that obtained from dynamic light scattering analysis. To investigate if the formation of the polymeric micelles was affected by other precursors during the hydrogel formation, the particle size of the micelles was measured in the presence of tetra acrylate PEG. It was found that the presence of tetra acrylate PEG did not affect the micelle size, indicating that the micelles were most likely intact during the hydrogel formation. The nanosized micelles embedded in the hydrogel may offer great advantages in directing cell behaviors by mimicking the intricate nanoscale structure of the natural ECM [156].

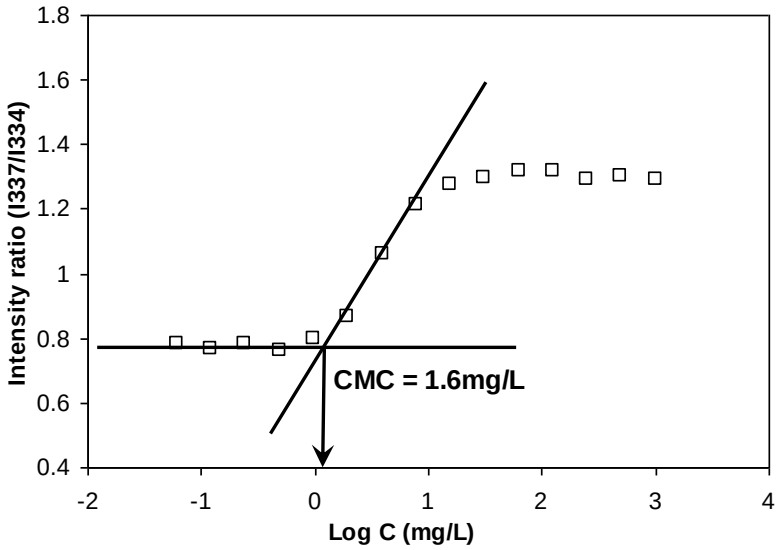

Figure 3.1 Determination of critical micelle concentration (CMC) of VS-PEG-polycarbonate. VS-PEG-PC micelles were formed and stabilized overnight before measurement.

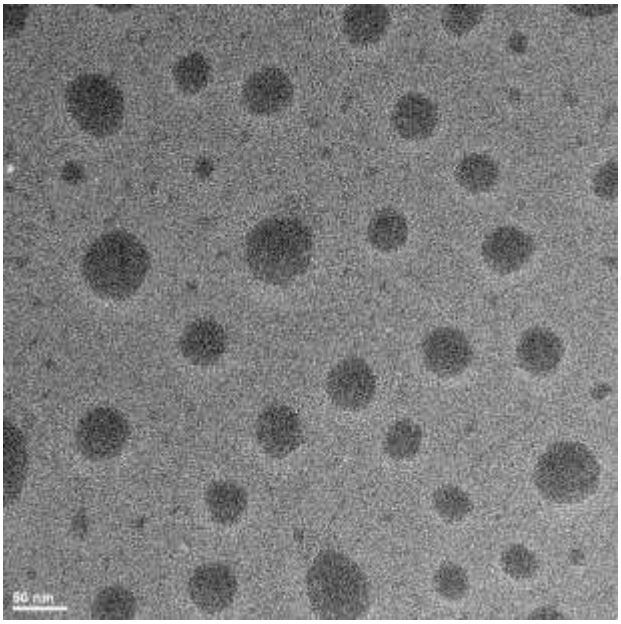

Figure 3.2 A typical TEM image of micelles prepared using VS-PEG-PC in DI water with polymer concentration of 0.5 mg/mL. Scale bar: 50 nm.

3.3.3 Synthesis and physical characterization of micelle-containing hydrogels

Michael addition chemistry offers the possibility of obtaining hydrogel *in situ* under mild physiological conditions, which avoids the use of toxic initiators and UV exposure involved in the photo polymerization process. Therefore, it was employed to synthesize micelle-containing PEG hydrogels. Both a tetra acrylate PEG solution and the vinyl sulfone-functionalized polycarbonate (VS-PEG-PC) micelle solution were mixed, followed by the addition of a thiol-containing RGD peptide (a cell adhesion receptor binding motif). Gelation occurred within minutes upon the introduction of tetra sulfhydryl PEG.

Table 1 summarizes the physical properties of hydrogels formed with different micelle contents. The storage modulus (Ge) of the micelles-incorporated hydrogels ranged from ~900 Pa to ~3000 Pa., indicating that stiffness of the hydrogels can be adjusted by varying the micelle content. Ge was not affected significantly when the micelle content was 20% or 40% as compared to hydrogels without micelles ($P>0.05$). For instance, the Ge values of the hydrogels without micelles (Gel 1) and with 20% (Gel 2) and 40% (Gel 3) micelles were 2522, 2691 and 2475 Pa, respectively. We have previously reported that Ge of PEG/RGD hydrogel decreased with increasing RGD contents because of the presence of elastically ineffective dangling RGD ends in the hydrogels [74]. However, this effect may be compromised by the presence of well-defined VS-PEG-PC micelles with multiple crosslinkable units. Notably, storage modulus and gel yield decreased significantly when the micelle content was increased to 60% (Gel 4) and 80% (Gel 5). The decreased Ge and gel yield can be directly related to lower crosslinking density of

hydrogel networks, which was caused by the decreased molar concentration of -SH and (AC+VS) crosslinkable groups. In addition, the lower crosslinking density at higher micelle contents led to increased gelation time.

Gel number	Micelle (VS) content (%)	PEG-AC content (%)	Ge (Pa)	Gel yield (%)	Gelation time (min)
1	0	100	2522 ± 56	97.8 ± 4.8	3.0
2	20	80	2691 ± 51	92.7 ± 3.3	5.5
3	40	60	2475 ± 30	90.2 ± 3.6	7.0
4	60	40	1855 ± 71	79.5 ± 1.0	9.5
5	80	20	902 ± 27	75.3 ± 2.8	15.0

Table 3.1 Physical properties of hydrogels. (Stoichiometry of (vinyl sulfone + acrylate) to thiol groups was 1.0 for all formulations. G′ value at frequency of 1 Hz was defined as G_e).

As shown in Figure 3.3, swelling ratio of the hydrogels increased with increasing micelle content, indicating more hydrated status. The higher swelling ratio of hydrogels with increasing micelle content may be due to their more porous structures (Figure 3.4). For example, when the content of micelles increased from 0 to 80%, the swelling ratio increased from 14.7 to 22.9.

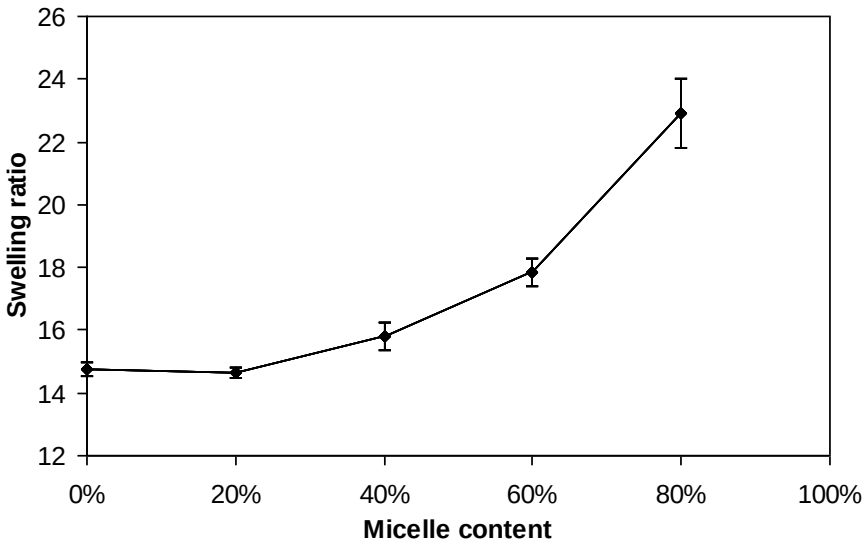

Figure 3.3 Effects of micelle content on the swelling ratio of the hydrogels. The hydrogels were placed in PBS buffer at 37 °C for 24 hours, swelling ratio was calculated from the formula: Swelling ratio = $(W_w-W_d)/W_d$, where W_w represents the weight of swollen gels, W_d represents the weight of the freeze-dried gels. All samples were analyzed in triplicate.

Figure 3.4 shows SEM images of internal structure of the freeze-dried hydrogels with different micelle content, which is characterized by high porosities. It is observed that the size of pores increased with increasing micelle content due to decreased crosslinking degree. In particular, when the content of the micelles was 80%, the pores inside the hydrogel were highly interconnected.

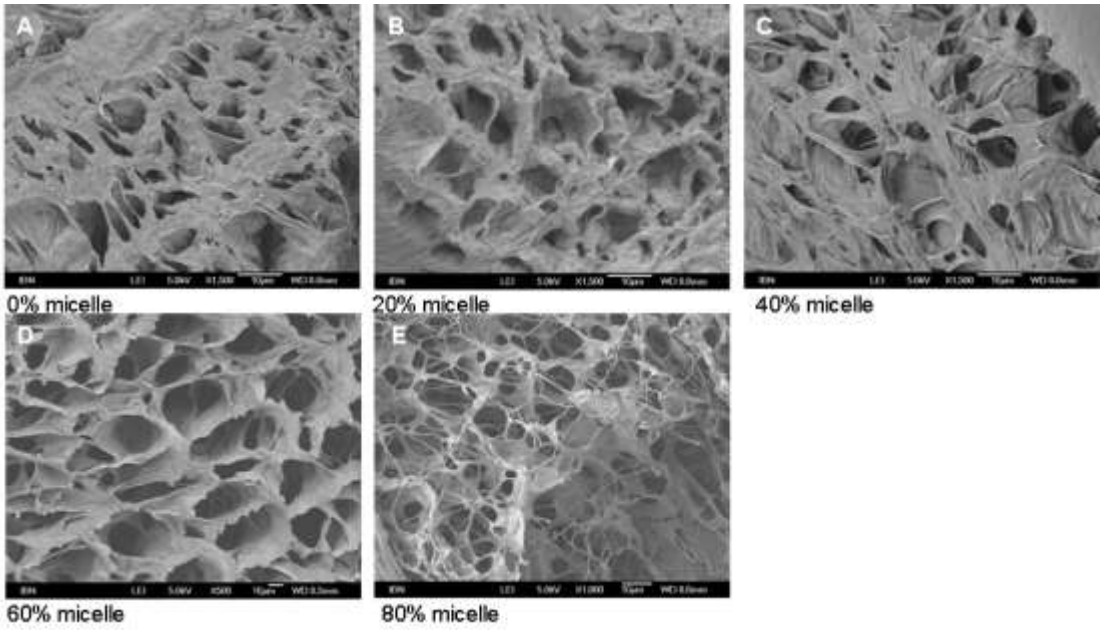

Figure 3.4 A typical SEM image of cross-sectioned hydrogel with different contents of micelles. The hydrogels were immediately frozen in liquid nitrogen prior to freeze drying to keep the morphology intact. (A) 0%, (B) 20%, (C) 40%, (D) 60% and (E) 80%. Scale bar: 10μm.

For an ideal biodegradable hydrogel system, the hydrogel should be able to degrade at an appropriate rate that synchronizes with the new tissue being regenerated over time. Hydrogel degradation was normally accompanied with increased weight loss, higher swelling ratio and decreased storage modulus [157]. A typical storage modulus profile over time for hydrogel with 20% micelles is illustrated in Figure 3.5. The Ge of Gel 2 decreased steeply during the first 5 days and slowed down to a constant rate up to 28 days, likely due to dissociation of the micelles, followed by the hydrolytic degradation of acrylate-PEG component. The gradual degradation profile and relative long degradation time of the hydrogel are of importance as temporary scaffold for tissue engineering.

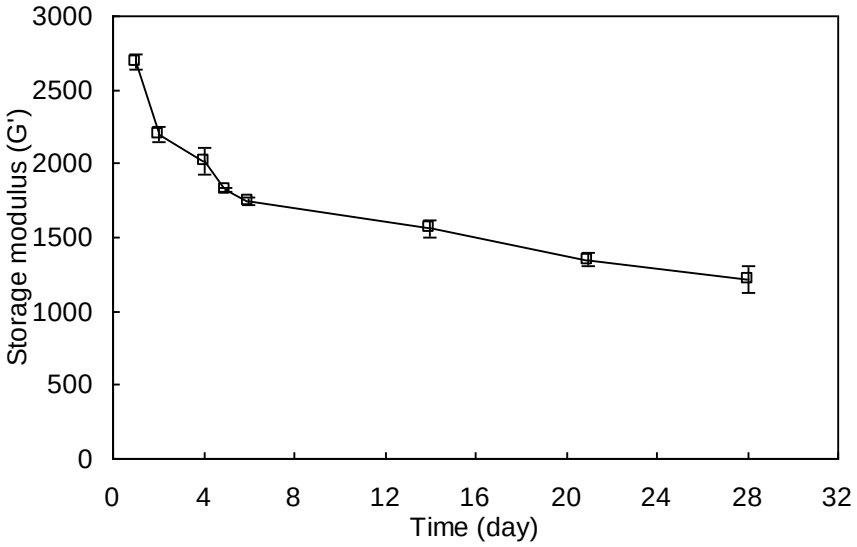

Figure 3.5 Storage modulus (Ge) of the hydrogel with 20% micelles changes as a function of time for 28 days. Hydrogels were incubated in PBS in 37 ℃ incubator and rheology measurement was carried out periodically.

3.3.4 Cell viability in the hydrogels

Previous studies have indicated that the cell behavior in the hydrogel is affected by several factors including stiffness, porosity and degradation rate of the hydrogel [158, 159]. These parameters are highly intertwined. In order to study the effect of micelles on cell behavior, cell viability assay was first performed. As can be seen from Figure 3.6, cell viability in the hydrogel with 20% and 40% micelles was significantly higher than that in the hydrogel without micelles ($P<0.005$). This may be because more space has been provided by micelles incorporated into the hydrogels, which in turn allowed for better hMSCs migration and proliferation. In addition, with more porous structures, the cells obtained more and faster oxygen and nutrient exchanges for cell proliferation, as compared to the less porous hydrogel without micelles. However, when hydrogels became softer as the micelle content increased to 60% and 80%, cell viability started to

decrease to that of the hydrogel without micelles. This may be because these hydrogels were too soft to support cell growth. Overall, the hydrogel with 20% micelles provided an optimal scaffold with a structure that is sufficiently stiff yet porous enough for cell migration and growth.

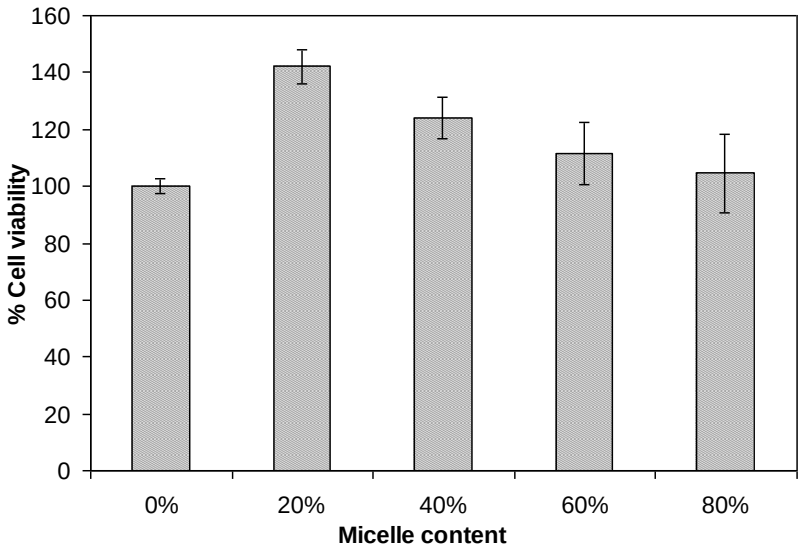

Figure 3.6 Effect of the micelle content on the viability of hMSCs in the hydrogel. hMSCs were incubated in the hydrogel for 4 days. MTT test was carried out by adding MTT solution to the hydrogel and incubating for 4 hours. The hydrogel constructs were then collected and homogenized with tissue ruptor. Aliquots of the solution were then assayed with a microplate reader. The results were expressed as a percentage of the cell viability in the hydrogel without the micelles.

Confocal images (Figure 3.7) further showed that cells encapsulated inside the hydrogel tend to adopt a rounded morphology - a phenomenon that agrees with previous findings [160]. hMSCs were evenly distributed especially in the hydrogels with 0 to 40% micelles. The number of live cells, as indicated green in the confocal images, was consistent with the cell viability assay, i.e. the highest number of viable cells was found inside the hydrogel with 20% micelles. A lower number of cells were observed in the hydrogels with 60% and 80% micelles possibly because dead cells were washed off during sample

preparation. Therefore, the hydrogel with 20% micelles was chosen for further evaluation on gene transfection, and the hydrogel without micelles was used as a control.

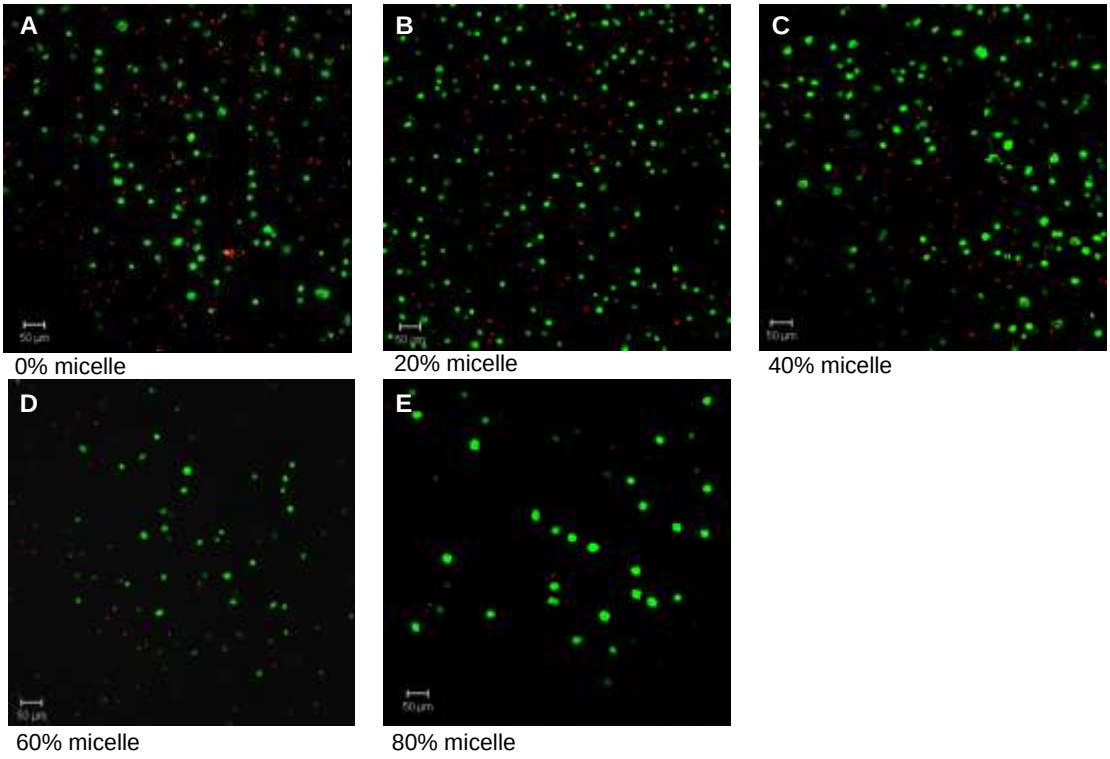

Figure 3.7 Confocal images of hMSCs incorporated in the hydrogels with different contents of micelle. LIVE/DEAD viability/cytotoxicity kit was used to stain hMSC in the hydrogels (A) 0%, (B) 20%, (C) 40%, (D) 60% and (E) 80%. Scale bar: 50 μm. Green represents live cells and red represents dead cells.

3.3.5 Characterization of polymer/DNA complex

The Bolaamphiphile polymer, MK397, is a cationic polymer synthesized as a gene vector by Dr. Majad Khan from the Institute of Bioengineering and Nanotechnology (IBN). It contains both primary and secondary amine for DNA binding and endosomal escape and amine bond for potential biodegradability. The detailed synthesis and characterization of the cationic bolaamphiphile polymer is shown in Appendix B.

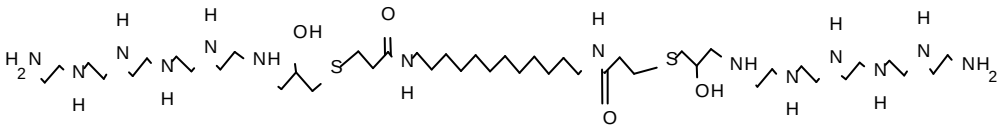

Scheme 3.3 Chemical structure of bolaamphiphile polymer (MK397)

Polymer/DNA complexes were formed by adding different volume of polymer solution into an identical volume of reporter gene solution at different N/P ratios. The particle size and zeta potential of the polyplexes were measured by Zetasizer at room temperature (25 ± 2°C). As shown in Figure 3.8, the particle size of the DNA complexes slightly increased at N/P 3 and gradually decreased to a level of below 200 nm from N/P 5 onwards. The Zeta potentials of the complexes increased with increasing N/P ratio and obtained a positive charge at N/P ratios higher than 5. The results from the agarose gel electrophoresis experiments showed that the bolaamphiphile polymer (MK397) exhibited strong DNA binding ability, and complete retardation of DNA was observed at N/P 2 (Figure 3.9). These findings clearly demonstrate that the bolaamphiphile polymer (MK397) condensed DNA efficiently into nano-sized particles, which are optimal for cellular uptake.

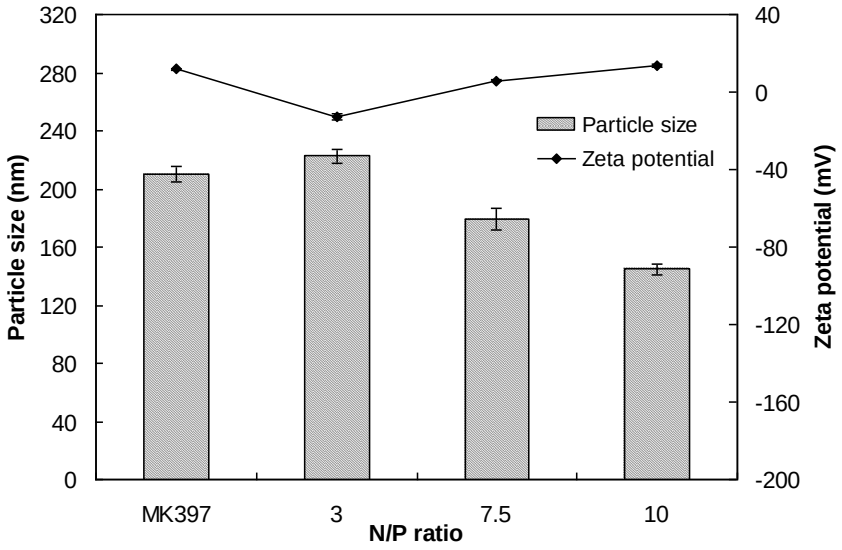

Figure 3.8 Particle size and zeta potential of bolaamphiphile/DNA complexes. Polymer/DNA complexes were formed by adding different volume of polymer solution into an identical volume of reporter gene solution at different N/P ratios.

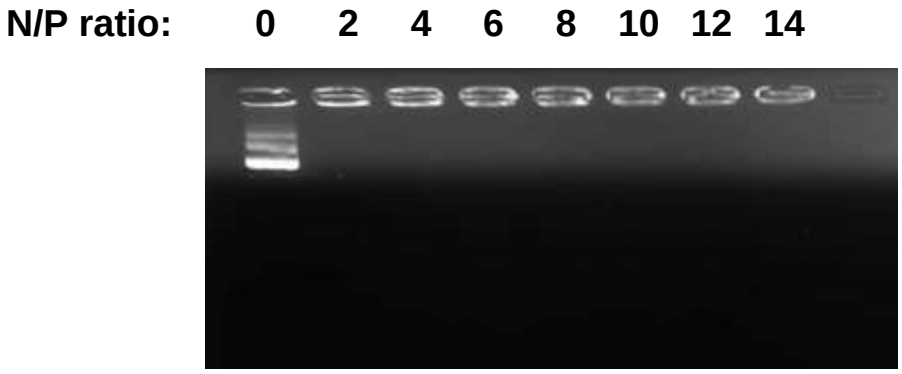

Figure 3.9 Electrophoretic mobility of DNA in bolaamphiphile/DNA complexes at N/P ratios specified. Lane 1: naked DNA; last lane: blank polymer. Cationic bolaamphiphile/DNA complexes were prepared and electrophoresed with various N/P ratios ranging from 2 to 14. The gel was analyzed on a UV to show the position of the complexed DNA relative to that of naked DNA.

3.3.6 Transfection efficiency in 2D cell culture plate

To examine the applicability of the bolamphiphile as an ideal gene vector for hMSC transfection, we first determined the transfection efficiency of MK397 over a range of N/P ratios in 2 dimensional cell culture plate.

As shown in Figure 3.10, no gene transfection was observed at N/P ratios 3 to 10 followed by a 1000 fold jump at N/P ratio 15. Transfection efficiency increased as the N/P ratio was increased from 10 to 20 and then reached a plateau. The highest transfection efficiency obtained was significantly higher than that achieved using PEI/DNA ($P<0.05$). Several reasons may be offered to explain why the bolaamphiphiles were so efficient in gene delivery. Firstly, the hydrophobic component in the bolaamphiphile enhanced gene binding and cell membrane penetration. More importantly, the presence of primary and secondary amine in bolaamphiphile greatly improved endosomal buffering capacity and thus enhanced DNA release from the complexes, which in turn helped prevent DNA from degradation in the harsh endosomal environment [161].

3.3.7 Cytotoxicity of polymer/DNA complex in 2D cell culture plate

An ideal non-viral gene delivery vector should show a low cytotoxicity to the target cells. The high cytotoxicity induced by PEI has largely limited its application in clinical settings, despite its high gene transfection efficiency [162]. The cytotoxicity profile of the bolaamphiphile was subsequently determined over a wide range of N/P ratios from 3 to 30. As shown in Figure 3.11, the bolaamphiphile/DNA complexes induced no cytotoxicity against hMSCs at N/P ratios below 10. Beyond N/P ratios of 10, however, a decreasing trend in cell viability was observed. Notably, the effect of the

bolaamphiphile/DNA on cell viability was comparable to that of the PEI/DNA complex at N/P ratio 15.

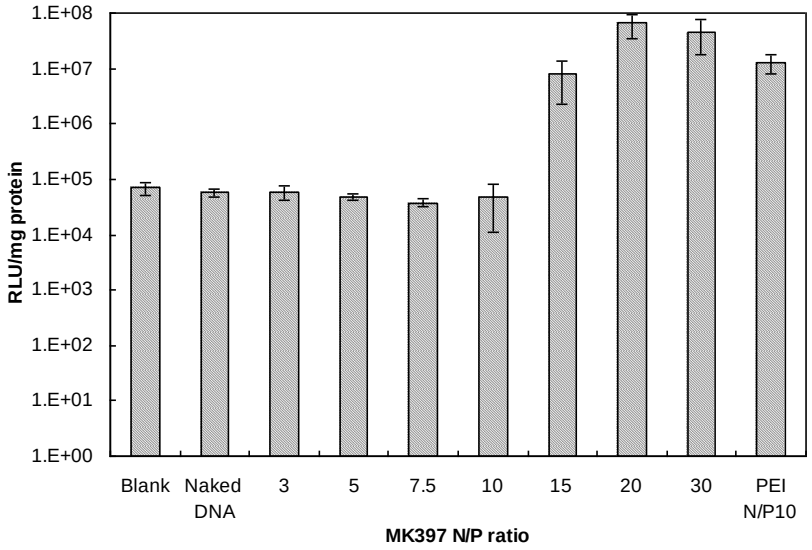

Figure 3.10 Gene transfection of bolaamphiphile/DNA complex in 2D cell culture plate. Complex solution was added into fresh media at various N/P ratios and incubated for 4 hours. hMSCs were further cultured for 4 days before carrying out the reporter gene analysis.

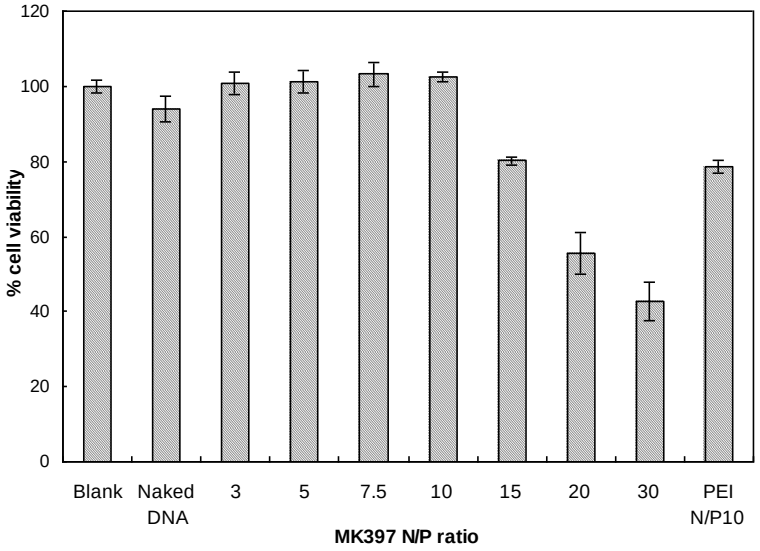

Figure 3.11 Cytotoxicity studies of bolaamphiphile/DNA complex in 2D cell culture plate. Complex solution was added into fresh media at various N/P ratios and incubated for 4 hours. hMSCs were further cultured for 4 days before carrying out the cell viability analysis by MTT assay.

3.3.8 Transfection efficiency in 3D hydrogels with different micelle content

It was reported that the non-specific interaction between the hydrogel component and PEI/DNA complexes affected the complex release and thus rendered the hydrogel as a local reservoir for the DNA complexes [163]. After determining the transfection efficiency of the cationic bolaamphiphile in the two dimensional environment, we next tested its gene transfection efficiency in the 3D hydrogels with different micelle content.

In both hydrogel scaffolds with 0% and 20% micelles, luciferase expression level induced by the cationic bolaamphiphile/DNA complexes increased with increasing N/P ratio from 3 to 7.5, with the maximal level observed at N/P 7.5 (Figure 3.12). The highest luciferase expression level mediated by the cationic bolaamphiphile/DNA complexes was significantly higher than PEI in both hydrogels with and without 20% micelles ($P<0.05$). For instance, the luciferase expression level induced by the cationic bolaamphiphile/DNA complexes at N/P 7.5 was 33 times higher than that mediated by PEI in the hydrogels with 20% micelles. This may be because the presence of hydrophobic components in the bolaamphiphile promoted cellular uptake of the complexes, leading to high gene expression efficiency.

The effect of micelle content on gene expression efficiency was further studied at the optimal N/P ratio of 7.5. As shown in Figure 3.13, luciferase expression levels in the hydrogel with 20% micelles was significantly higher than those in the hydrogel without micelles for the bolaamphiphile at all N/P ratios ($P<0.05$). The enhanced gene expression may be attributed to the higher cell viability in the hydrogel with 20% micelles. In

addition, porosity can play an important role in gene transfection in scaffolds [164]. A denser hydrogel network may prevent the cationic bolaamphiphile/DNA complexes from being in contact with the cells. However, the luciferase expression level in the hydrogels started to decrease as the micelle content increased from 40% to 80%. This may be attributed to a highly porous and soft scaffold structure that may not be able to support the interactions of the cells with the complexes.

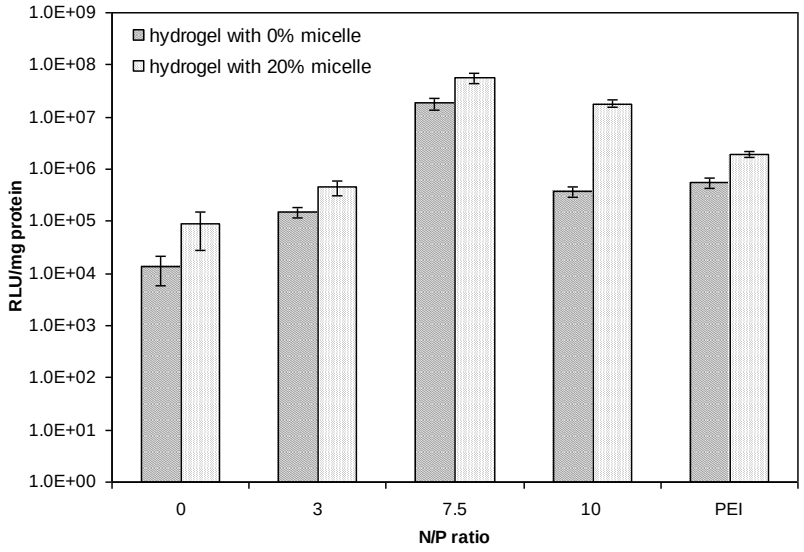

Figure 3.12 Luciferase expression level in the hMSCs incorporated in the hydrogels with and without 20% micelles. hMSCs mixed with complex solution at various N/P ratios were added into hydrogels and incubated for 4 hours. The hydrogel constructs were further cultured for 4 days before carrying out the reporter gene analysis.

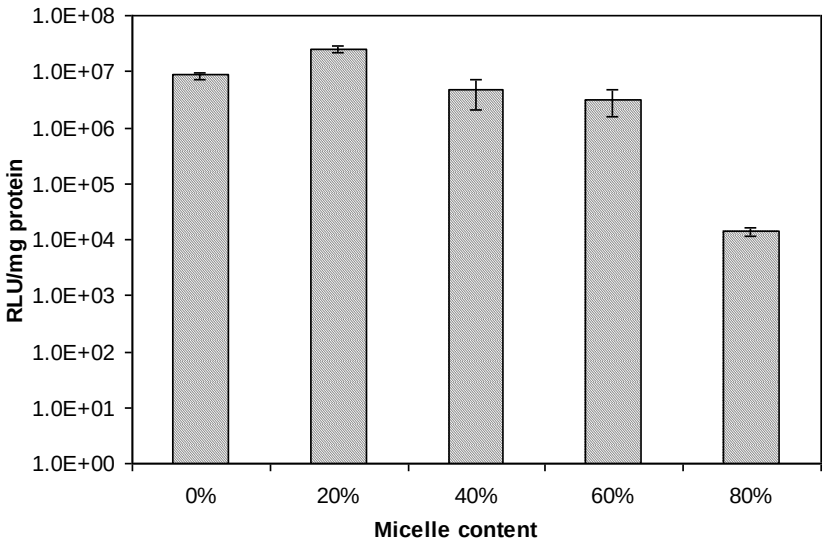

Figure 3.13 Luciferase expression level in the hMSCs incorporated in the hydrogels with different micelle content. hMSCs mixed with complex solution at N/P ratio 7.5 were added into hydrogels and incubated for 4 hours. The hydrogel constructs were further cultured for 4 days before carrying out the reporter gene analysis.

3.3.9 Cytotoxicity of polymer/DNA complex in 3D hydrogels

As aforementioned, cytotoxicity is an important parameter used to evaluate cationic polymers as non-viral gene transfection vectors. The cytotoxicity is believed to be related to gene transfection efficiency [165], and may be caused by electrostatic interaction with negatively charged glycocalyx of the cell surface [166]. Cytotoxicity of bolaamphiphile/DNA complex was much lower than PEI at N/P ratio below 15 in 2D cell culture plate (Figure 3.11). Lower N/P ratios were required to achieve successful gene transfection in the 3D hydrogel environment as hydrogels serve as a local gene reservoir with intimate contact with the encapsulated cells. As revealed in Figure 3.14, there was no significant cytotoxicity of the cationic bolaamphiphile/DNA complexes against hMSCs at all the N/P ratios from 3 to 10 ($P=0.3$-0.6). This was in sharp contrast to PEI, which induced much higher cytotoxicity against hMSCs in the hydrogels ($P<0.05$). The

cationic bolaamphiphile exhibited small particle sizes and relatively low zeta potentials after complexation with DNA, leading to little cytotoxicity at low concentrations. Collectively, hydrogels with 20% micelles provided optimized mechanical support, higher transfection efficiency and better cell viability.

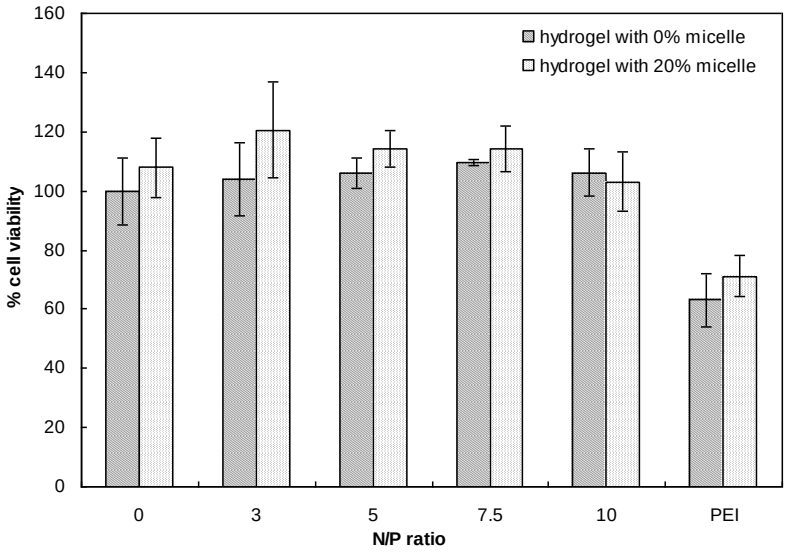

Figure 3.14 Viability of hMSCs in the hydrogel after incubation with bolaamphiphile/DNA and PEI/DNA for 4 days at various N/P ratios specified.

3.4 Conclusion

In this Chapter, we describe synthetic hydrogels made from PEG with micelles self-assembled from a biodegradable and crosslinkable polycarbonate-based amphiphilic block copolymer. Increasing the content of the micelles from 0 to 80% led to increased porosity and tunable mechanical property of the hydrogels. The hydrogel with 20% micelles provide the best balance among hydrogel stiffness, flexibility and porosity for cell survival, leading to the highest viability of hMSCs. The cationic bolaamphiphile/DNA complexes induce higher gene expression efficiency in the hydrogels than the PEI/DNA complexes, yet show no cytotoxicity. The gene expression

level in hMSCs in the hydrogel with 20% micelles was the highest as compared to that in the other hydrogels. Overall, the hydrogel with 20% micelles offers an optimal scaffold with ideal physical properties for cell growth and transfection. Therefore, incorporating nanoparticles into the hydrogels is a useful strategy to tune the physical properties of hydrogel scaffolds and subsequently control cellular behavior in a 3-D environment. These biodegradable hydrogels can be an excellent platform for cell and gene delivery in tissue engineering.

CHAPTER 4. STEREOCOMPLEX HYDROGEL WITH SUPRAMOLECULAR STRUCTURES FOR ANTIMICROBIAL AND ANTIBIOFILM ACTIVITIES

4.1 Background

As mentioned in Chapter 3, biomaterials have been widely used in tissue engineering and other biomedical applications. However, bacterial infections associated with the increasing utilization of biomaterial have attracted researchers' great attention and the bottleneck to treat biomaterial-associated infections lies with the lack of broad spectrum antimicrobial and antibiofilm agents with less likelihood of drug resistance development and high selectivity to bacterial cells over mammalian cells. To broaden the application of synthetic PEG-based hydrogels, we continued to explore the application of cationic hydrogels for antimicrobial and antibiofilm activities.

The development of antibiotic-resistant bacteria has caused a myriad of new challenges within the healthcare industry. Skin infections caused by drug-resistant Staphylcoccus aureus (MRSA) account for more than half of all reported cases of S. aureus skin infections in the United States [167]. Furthermore, due to the extremely high occurrence of MRSA infections it is estimated that 20,000 deaths occur annually [168]. Unfortunately, current problems associated with drug-resistant microbes extend far beyond Gram-positive bacteria such as MRSA. Perhaps even more distressing is the rapidly increasing antibiotic-resistance of Gram-negative bacteria, which was already suffering from inadequate treatments [169].

Considering that people afflicted with microbial infections generally receive treatment within hospitals, it should come as no surprise that nosocomial infections are becoming increasingly problematic for all patients regardless of malady [170]. Nowhere is this more evident than with post-operative infections. The introduction of drug-resistant bacteria during surgical procedures is thought to be the primary reason for complications. More specifically, bacteria easily colonize the surfaces of tissues and surgical devices (implants, orthopedics, catheters, etc.), and subsequently form biofilms. Bacterial biofilms consist of bacteria and self-secreted extracellular polymeric substances (EPS) [127] and are extremely resistant to conventional antibiotics mainly due to resistant gene expression in bacteria, limited diffusion and inactivation of antibiotics in EPS [171-173]. Biofilm formation is one of the leading causes of the surgical device implantation failure [129-133]. In addition, bacterial biofilms make wound management and healing very difficult [134]. Due to the insufficiency of standard antibiotic treatments, new approaches for preventing and treating drug-resistant infections need to be continually investigated.

Eukaryotic organisms have demonstrated an incredible ability to selectively target microbial infections without promoting rapid resistance development. Fundamental to this defense is the deployment of host defense peptides (HDPs) which utilize charge and facial amphiphilicity [174-177]. Through electrostatic interactions positively charged HDPs are attracted to the bacterial cell surface, followed by inserting into the cell membrane after recruiting additional peptide molecules, thus disintegrating the cell membrane and eventually lysing the cell. This discovery has led to cutting edge research into the development of soluble self-assembling synthetic cationic polymers designed to

mimic the HDP structure and action [178, 179]. However, application of such materials for localized function (such as placement on a skin infection) becomes problematic because of their rapid solubilization and subsequent removal. Therefore, there is a critical need to develop an antimicrobial material that has a low modulus, is readily remoldable and is conformable to a wide variety of surfaces and substrates.

Antimicrobial hydrogels are envisioned to be an integral weapon for combating drug-resistant infections. Since they exhibit many of the characteristics of water soluble polymers without being freely dissolved, such materials can remain in place under physiological conditions while still demonstrating antimicrobial activity. These attributes make them ideal for applications in wound healing, implant and catheter coatings, skin infections or even orifice barriers (such as placement into the nares for decolonization of MRSA). Several antimicrobial hydrogels including quaternized ammonium chitosan-graft-poly(ethylene glycol) methacrylate [180] or epsilon-poly-L-lysine-graft-methacrylamide (EPL-MA) [181] polyelectrolyte complex (PEC) hydrogel comprising chitosan as the cationic polyelectrolyte and co-poly(glutamic acid) (co-PGA) [182] and self-assembled peptide hydrogels [183] were reported with broad-spectrum activity. However, most of them were formed based on chitosan, a material that is extracted from crab shell, can cause immunogenicity and varies from batch to batch in quality and molecular size, or produced from expansive peptides. Therefore, there is a pressing need to develop antimicrobial hydrogels from synthetic, cost-effective and biodegradable materials with well-defined molecular structure. It must also be moldable/processable allowing in situ applications. This behavior is exemplified by attributes such as

physically cross-linked gels for drug delivery [184, 185] and/or stimuli responsiveness (pH, temperature, radiation, etc) [186-189] facilitating gel localization without compromising material properties. Furthermore, the antimicrobial hydrogel must also be stable and active for the duration of its purpose. However, upon completion of its intended use it should undergo natural biological remediation. With the high volume of poorly degradable single use healthcare items such as bandages, catheters, stents and many others already destined for landfills, the problem would be exaggerated by the addition of antimicrobial material that destroys bacteria and fungi responsible for slow landfill degradation.

Among biofilm-associated diseases, fungal keratitis is a leading cause of ocular morbidity worldwide and it is also a major eye disease in Asia and can cause sight loss [190]. Risk factors include epithelial abrasions as a result of contact lenses wearing [191], systemic or topical usage of corticosteroids and atopic diseases [192]. *Candida albicans* is one of the most frequently isolated pathogens [193]. Treatment for ocular fungal keratitis remains problematic partly because of the lack of effective therapeutical agents against fungal biofilms and partly due to the shortage of routine test of fungal isolates in the laboratory. Current antibiotics in clinic use include azole compounds such as voriconazole and polyenes such as Amphotericin B. Azole can be administered both intravenously and orally. Common side effects include reversible disturbance of vision, skin rashes and hepatic enzyme level elevation [194, 195]. Moreover, azoles are unstable for topical applications as eye drop [196]. On the other hand, usage of polyenes is largely limited due to their poor permeability through intact epithelium, stability and high

toxicity [197, 198]. Therefore, hydrogel with cationic polymer incorporated serves as an alternative and effective approach to treat fungal keratitis. By providing locally administration of antimicrobial polymeric macromolecules, hydrogels with low toxicity and high biocompatibility are able to remove biofilm without developing drug resistant bacteria to overcome the problems associated with the usage of common antimicrobial agents.

Herein, we describe a simple yet effective approach to generating charged hydrogels using non-covalent interactions to overcome the issues that existing antimicrobial hydrogels have. More specifically, we report a stimulus-responsive antimicrobial gel formed from stereocomplexes of biodegradable poly(L-lactide)-b-poly(ethylene glycol)-b-poly(L-lactide) (PLLA-PEG-PLLA) and a charged biodegradable polycarbonate triblock polymer (i.e. PDLA-CPC-PDLA). The stereocomplexes were found to exist as soluble micelles at room temperature in aqueous solution, however, upon heating to physiological temperature (~37°C) gel-like materials with distinctive supramolecular fiber/ribbon-like structures and shear-thinning behavior were formed. This drastic change in material properties was also accompanied by a large increase in antimicrobial activity which encompassed Gram-positive/Gram-negative bacteria and fungi, and drastically disrupted microbial biofilms.

4.2 Materials and methods

4.2.1 Materials

Staphylococcus aureus (ATCC 6538), *Escherichia coli* (ATCC 25922) and *Candida albicans* (ATCC 10231) were obtained from ATCC. Human dermal fibroblast (HDF) was obtained from ATCC. Dulbecco's Modified Eagle Medium (DMEM), fetal bovine serum (FBS), sodium pyruvate, penicillin-streptomycin were all purchased from Invitrogen (U.S.A). Tryptic soy broth (TSB) powder and yeast mould broth (YMB) powder were purchased from BD Diagnostics (Singapore) and used to prepare the microbial broths according to the manufacturer's instructions. Phosphate-buffered saline (PBS) at 10 × concentration was obtained from 1st BASE Pte Ltd (Singapore) and used after dilution to the desired concentration. Ethanol (analytical grade, 99%) and Glutaraldehyde (Synthetic grade, 50% in H2O) were purchased from Sigma-Aldrich (Singapore) and used as received. Rat red blood cells were obtained from Animal Holding Units of the Biomedical Research Centers (Singapore). Lotrafilcon A contact lenses were purchased from CIBA Vision with a power of +1.00 diopters. Cyclophosphamide, 1-heptanol and commercial antifungal agent Amphotericin B were obtained from Sigma-Aldrich (Switzerland). Tetracaine hydrochloride eye drops was obtained from Bausch & Lomb Pharmaceuticsa (Florida).

4.2.2 Polymer synthesis and characterization

4.2.2.1 Polymer synthesis

Polymers for hydrogel formation, PLLA-PEG-PLLA, PDLA-PEG-PDLA and PDLA-CPC-PDLA, were synthesized by Dr. James L. Hedrick in IBM, Almaden Research Center, U.S. Detailed synthesis and characterization of the polymers is shown in Appendix C.

4.2.2.2 Particle size and zeta potential

Polymer solutions were prepared in DI water at 1 mg/ml using PDLA-CPC-PDLA or PLLA-PEG-PLLA and PDLA-CPC-PDLA stereocomplex mixture in a 1:1 molar ratio of PDLA and PLLA. The polymer solutions were equilibrated for 1 hour. Particle size of the particles was measured using a Zetasizer (3000 HAS, Malvern Instrument, U.K.) at 25 °C. Each measurement was repeated three times. An average value was obtained from the three measurements.

4.2.2.3 Minimal inhibitory concentration (MIC) determination

The bacteria were grown in tryptic soy broth at 37 °C and yeast was cultured in yeast mould broth at 24 °C. The MICs of the polymers were measured using a broth microdilution method. Briefly, polymer stock solution was prepared by dissolving 25 mg polymer in 100 µL phosphate-buffered saline (PBS, pH 7.4) followed by a serial dilution into various concentrations using growth media. Subsequently, 90 µL of fresh growth media and 10 µL of polymer solution were added to each well. 100 µL of microorganism

solution at a concentration, which gave an optical density reading of ~0.1 at 600 nm, was added into each well. The cell cultures were then incubated for 8 hours and the optical density was monitored at 2 hours intervals. The MIC was taken at the concentration, at which no growth was observed. Broth containing cells alone was used as control.

4.2.2.4 Hemolysis assays

Fresh mouse red blood cells were washed with PBS for three times. 100 μL of red blood cell suspension in PBS (4% in volume) was placed in each well of 96-well plates and 100 μL of polymer solution with various concentrations was added to each well. The plates were incubated at 37 °C for 1 hour, followed by centrifuge at 1000g for 5 min. 100 μL of supernatant were transferred to 96-well plates, and hemoglobin release was monitored at 576 nm using a microplate reader (Bio-Teck Instruments, Inc). The red blood cell suspension in PBS was used as negative control. Absorbance of wells with red blood cells lysed with 0.5% Triton X-100 was taken as positive control of 100% haemolysis. Percentage of haemolysis was calculated using the following formula:

$$Haemolysis\ (\%) = \frac{O.D.\,576nm\ in\ the\ \ polymer\ \ solution - O.D.\,576nm\ in\ the\ PBS}{O.D.\,576nm\ in\ 0.5\%\ Triton\ \ X - O.D.\,576nm\ in\ the\ PBS} \times 100$$

4.2.2.5 Cytotoxicity assay

The cytotoxicity of the cationic polymers against human dermal fibroblast (HDF) was studied by standard MTT assay in triplicates. Briefly, HDF cells were seeded onto 96-well plates at density of 10 000 cells per well and allow to attach overnight before

treatment. The cells were then incubated with polymer containing growth media comprising of 10 μL cationic polymers and 100 μL fresh growth media for 12 hours at 37 °C. Subsequently, 100 μL of fresh growth media and 10 μL MTT solution (5mg/mL in PBS) were added to each well and incubated for 4 hours at 37 °C. Resultant formazan crystals formed were solubilized using 200 μL DMSO after removal of the growth media. An aliquot of 100 μL was taken from each well and transferred to a fresh 96-well plate. The plates were then assayed at wavelength of 550 nm and 690 nm using a microplate reader (Tecan, Switzerland). Percentage of cell viability was expressed as $[(A_{550}-A_{690})_{sample}/ (A_{550}-A_{690})_{control}] \times 100\%$in the wells without cationic polymers.

4.2.3 Hydrogel formation and characterization

4.2.3.1 Hydrogel formation

In the preparation of a typical hydrogel, PLLA-PEG-PLLA (3.5 mg, 0.45 μmol), PDLA-CPC-PDLA (0.5 mg, 0.03 μmol) and PDLA-PEG-PDLA (2.6 mg, 0.33 μmol) were dissolved in 50 μl DI water. The resultant hydrogel was kept in a 37˚C incubator for 5 hours. It should be mentioned that the molar ratio of PLLA to PDLA group was 1.0, and the final PLLA-PEG-PLLA concentration was 7 (w/v) %.

4.2.3.2 Differential scanning calorimetry

Differential scanning calorimetry (DSC) was performed using a TA Differential Scanning Calorimeter 1000 that was calibrated using high purity indium. Melting points were

determined from the second scan at a heating rate of 5 ℃/min following slow cooling (to remove the influence of thermal history) at a heating rate of 3 ℃/min.

4.2.3.3 X-ray diffraction analysis

X-ray diffraction analysis was performed on a PANalytical X-ray diffractometer (X'pert PRO) with Cu Kα radiation at 0.154nm. The hydrogels were lyophilized and mounted onto zero-background XRD holders.

4.2.3.4 Rheology

Rheology experiments were performed at room temperature (25 ± 2°C) using a control-strain rheometer (ARES G2, U.S.A). The dynamic storage modulus (G′) was examined as a function of frequency from 0.1 to 50 rad/s. The measurements were carried out at strain amplitude (γ) of 5 % to ensure the linearity of viscoelasticity. Viscosity of the hydrogel was examined as a function of shear rate from 0.1 to 1 1/s.

4.2.3.5 Fiber observation under optical microscopy, SEM, TEM

The morphologies of the hydrogel fibers were observed under Olympus microscope 1×71 with DP 70 camera (Japan). To prepare the sample, the hydrogel were prepared as described in section 4.2.3.1 and diluted to 5 mg/ml after incubating for 5 hours. 20 μL fiber solution was placed into a 96-well plate and observed under the microscope.

The morphologies of the hydrogel fibers and microorganisms after treatment with hydrogels were observed using a field emission SEM (JEOL JSM-7400F) operated at an accelerating voltage of 10 keV. For hydrogel fibers, the hydrogel were prepared as described in section 4.2.3.1 and diluted to 5 mg/ml after incubating for 5 hours. 20 μL of the fiber solution was placed on a copper tape, and air-dried at room temperature (25 ± 2°C). The copper tape was mounted on metal holders and vacuum coated with a platinum layer before SEM examination

Fiber morphology was also observed under a FEI Tecnai G^2 F20 transmission electron microscope (TEM) using an acceleration voltage of 200 KeV. To prepare the TEM sample, the hydrogel were prepared as described in section 4.2.3.1 and diluted to 5 mg/ml after incubating for 5 hours. 5 μL of the fiber solution was placed on a plasma treated formcar/carbon-coated 200 mesh copper grid and left to dry under room temperature (25 ±2°C) prior to TEM observation.

4.2.4 Antimicrobial activities *in vitro*

Hydrogels with and without cationic polymer were prepared as described in section 4.2.3.1. 30 μL of microorganism solution at a concentration, which gave an optical density reading of ~0.1 at 600 nm, was then added onto each hydrogel. Hydrogel without cationic polymer and DI water (pH 7.4) were used as negative controls. The cell hydrogel construct were then incubated for 8 hours and the optical density was monitored at 2 hours intervals. Stereocomplex cationic hydrogels were tested against gram-negative bacteria E.coli, gram-positive bateria S.aureus and fungus C. Albicans as well as various

clinically isolated microbes, including methicillinresistant S. aureus (MRSA, gram-positive), vancomycinresistant enterococci (VRE, gram-positive), P. aeruginosa (gram-negative), A. baumannii (gram-negative, resistant to most antibiotics), K. pneumoniae (gram-negative, resistant to carbapenem), and C. neoformans.

4.2.4.1 Killing efficiency

After 8 hours incubation, 20 µl of the microorganism with or without dilution using medium was taken out from the hydrogel and streaked on the agar plate. The agar plates were inverted and incubated in a 37 °C incubator for 24 hours. The number of colony forming unit (CFU) was counted and expressed in

$$Killing\ \ efficiency = \frac{cell\ \ count\ of\ \ control - survivor\, count\ on\ cationic\ \ hydrogel}{cell\ \ count\ of\ \ control} \times 100$$

4.2.4.2 SEM observation

The microorganisms grown in DI water alone or incubated on the hydrogel with or without cationic polymer were harvested by centrifuging at 4000 rpm for 5 minutes. They were washed with phosphate-buffered saline (PBS) and then fixed in PBS containing 5% formaldehyde for half an hour. The cells were further washed with DI water, followed by dehydration using a series of ethanol washes and drying at room temperature ($25 \pm 2°C$). The cell sample was placed on copper tape, which was mounted onto aluminum stud, and coated with platinum prior to SEM analysis.

4.2.4.3 Drug resistance stimulation study

Drug resistance was studied by repeatedly exposing microbes to antimicrobial agents at sub MIC concentration. In this study, we tested E. coli as a model microorganism. With the microdilution method mentioned in section 4.2.2.3, MIC of gentamicin, ciprofloxacin was monitored for consecutive 10 passages. At passage n, bacterial treated at sub-MIC (1/4 MIC at that specific passage) were revived and re-grown for subsequent MIC test (passage n+1). By monitoring the changes in MIC, MIC at passage n (MIC_n) was normalized to that of passage 1 (MIC_1) and drug resistance development was studied. Two conventional antibiotics with different growth inhibitory mechanisms ciprofloxacin (fluoroquinolone antibiotics) and gentamicin (aminoglycoside antibiotics) were chosen in comparison with hydrogel (Gel 1).

4.2.5 Antibiofilm activities *in vitro*

4.2.5.1 Biofilm growth on 96 well plate

S. aureus (ATCC 6538), *E. coli* (ATCC 25922) and *C. albicans* (ATCC 10231) were obtained from ATCC and clinically isolated methicillin-resistant *Staphylcoccus aureus* (MRSA) was obtained from a local hospital [199]. The bacteria were grown overnight in tryptic soy broth (TSB) at 37 °C and diluted in TSB to 1×10^6 cells/ml before use. 100 μl of the diluted cell suspension were then inoculated into each well of 96-well plate and cultured for 7 days. PBS was added to wash off the planktonic and loosely adhered cells before fresh medium were changed everyday.

4.2.5.2 Biomass assay

Biomass of the biofilm was analyzed using crystal violet staining assay after incubating the biofilm with hydrogels for 24 hours [200]. After removal of culture medium, the formed biofilm was gently washed with PBS three times to remove the planktonic cells. 100 μl of methanol was added to fix the biomass for 15 min, followed by 100 μl of crystal violet staining (0.1 w/v %) for 10 min. Excess of crystal violet was washed off thoroughly with DI water. The remaining crystal violet bound with the biofilm was extract by 33% glacial acetic acid and the absorbance was measured at 570 nm with a microplate reader (Tecan, Switzerland). The results were expressed as a percentage of the cell viability without treatment.

4.2.5.3 XTT assay

XTT assay was used for quantification of viable cells in the biofilms after the incubation of biofilm with hydrogels for 24 hours. XTT assay is based on the reduction of 2,3-bis(2-methoxy-4-nitro-5-sulfophenyl)-5-[(phenylamino)carbonyl]-2*H*-tetrazolium hydroxide (XTT) in the metabolically active microbial cells to a water soluble formazan [201]. Briefly, XTT solution (1 mg/mL) was prepared using PBS and filtered with 0.22 μm pore size filter. Menadione solution (0.4mM) was prepared and mixed with XTT solution at a ratio of 1:5 by volume right before each assay. At the end of treatment, medium was removed and biofilm were carefully washed with PBS three times to remove planktonic cells. 120 μl of PBS and 14.4 μl of the XTT-menadione solution was added to each well and incubated for 3 hours. An aliquot of 100 μL was then taken and transferred to a fresh 96-well plate. The plates were then assayed at 490 nm with a microplate reader (Tecan,

Switzerland). The results were expressed as a percentage of the cell viability without treatment.

4.2.5.4 SEM observation

The morphologies of the biofilm treated with control, control gel, gel 1 and gel 2 were observed using a field emission SEM (JEOL JSM-7400F) operated at an accelerating voltage of 10 keV. After incubation for 24 hours, the biofilms were gently washed with phosphate-buffered saline (PBS) once and then fixed in PBS containing 5% formaldehyde for half an hour. The cells were further washed with DI water, followed by dehydration using a series of ethanol washes and drying at room temperature (25 ± 2°C). The cell sample was placed on copper tape, which was mounted onto aluminum stud, and coated with platinum prior to SEM analyses.

4.2.6 Antibiofilm activities *in vivo*

4.2.6.1 Contact lens-associated keratitis model

4.2.6.1.1 Biofilm growth on contact lenses

The contact lens were washed once with 1×PBS and punched into small pieces of 2 mm in diameter before incubating at 37 ℃ in YM broth overnight. To grow *Candida albicans* biofilm, the contact lenses were cultured in 6 well plates with 4 mL yeast suspension (10^6 CFU/mL) and incubated at 22 ℃ for 5 hours. After incubation, the contact lenses were gently washed with PBS to remove the planktonic cells and immersed in fresh YM broth for 4 days at 22 ℃ with shaking at 100 rpm.

4.2.6.1.2 Mice source

Adult C57BL/6 mice (6-8 weeks, 18-22 g) were used for animal studies. 6 mice were housed in individual cage under standard condition. All eyes were examined to avoid any ocular pathology before experiment initiation. Experiment protocol was done with approval of the Institutional Animal Care and Use Committee of Biological Resource Centre, A-STAR, Singapore.

4.2.6.1.3 Keratitis model initiation

Black mouse keratitis model was established as our collaborator did [202, 203]. Briefly, the mice were firstly immune suppressed by cyclophosphamide (180 g/kg) for 2 days (sc) and anaesthetized by ketamine (150mg/kg) and xylazine (10mg/mL), I.P., followed by an additional topical anesthetic administration of 0.5% tetracaine hydrochloride eye drops before surgery. A 1 mm filter paper disk soaked with 99% of 1-heptanol was placed on the center of the cornea for 40 s and the cornea epithelium was removed atraumatically. After rinsing the eyes with PBS to remove remaining traces of 1-heptanol, a 2 mm contact lens with *Candida albicans* biofilm was then placed on the denuded cornea surface. The eye lids were closed with silk sutures in order to keep the contact lenses inside the eyes. After infection for 18 hours, eye ulcer with a leathery, tough and raised surface was observed due to fungi infection on the eyeball. A disease grading system from 0 (no disease) to 4 (severe disease) was established to evaluate model efficacy.

4.2.6.2 Biofilm susceptibility

The treatment was adopted from a study of Amphotericin B [204]. The infected mice were randomly assigned into 3 groups (saline group, 250 μg/mL Amphotericin B and hydrogel group, 8 mice in each group) with comparable median disease grades. After infection of 18 hours, the silk sutures and contact lenses were removed, 10 μL of eye drop was then administered to both eyes, and uninfected eyes with intact corneal epithelium were used as control. Topical administration was repeated at hourly interval for 8 hours. Photos were taken before and after the treatment. All mice were sacrificed after the last administration of eye drop. The treated eyes were collected immediately; three of them were fixed in 4% paraformaldehyde for histology assay and remaining five were collected for quantitative fungi recovery assay.

4.2.6.2.1 Fungi recovery assay

The eyeball was gently washed with PBS and homogenized in 3 mL PBS ground on ice for 6 cycles of 10 s using a tissue ruptor. Yeast cells were detached in PBS by ultrasonication for 3 min. After a serial dilution, 20 μL sampling aliquots were streak on LB agar plates and incubated at 22 ℃ for 48 hours before counting the colony forming unit (CFU). The percentage of fungi recovery was expressed as the number of CFU revived from treatment groups as compare to those revived from control group to determine the survival of *Candida albicans*.

4.2.6.2.2 Histopathology

Histological assay was utilized to evaluate the *in vivo* acute toxicity of the hydrogels after topical administration. Briefly, the fixed corneal were embedded in paraffin and sectioned to 5 μm. The resulted sections were stained using hematoxylin eosin, Groccott's methenamine silver and periodic acid Schiff reagents by standard protocol. The extent of stromal infiltration induced by fungal elements was examined by light microscopy ar the central corneal sections of each eye. Maximal penetration depth and total hyphal area in a defined area were measured.

4.2.7 Statistical analysis

All data are presented as mean ± SD. The statistical significance of the data was evaluated by two- tailed Student's t-Test. $P<0.05$ was considered statistically significant.

4.3 Results and discussions

4.3.1 Polymer synthesis and characterization

4.3.1.1 Polymer synthesis

Polymers for hydrogel formation, PLLA-PEG-PLLA, PDLA-PEG-PLLA and PDLA-CPC-PDLA, were synthesized by Dr. James L. Hedrick in IBM, Almaden Research Center, U.S using organocatalyzed ring opening polymerization (ROP) techniques [205-208]. The PLLA-PEG-PLLA triblock copolymers synthesized have very narrow molecular weight distributions (Scheme 4.1 A). Three separate PDLA-CPC-PDLA polymer compositions of different block length were studied; 1000-6000-1000 (PC1), 2000-13000-2000 (PC2) and 1500-6000-1500 (PC3) Scheme 4.1 B.

A

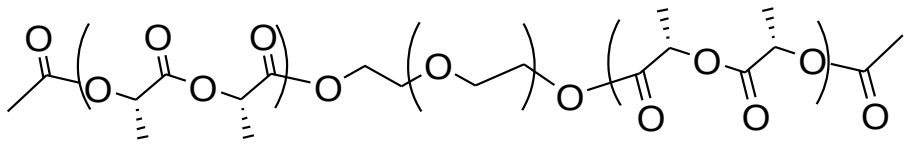

PLLA-PEG-PLLA

B

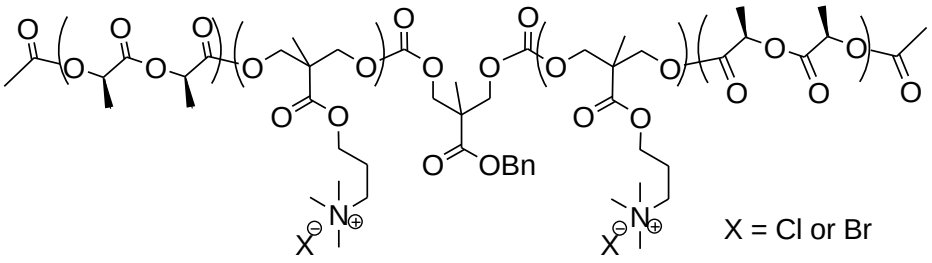

PDLA-CPC-PDLA
PC1 = PDLA1k-CPC6k-PDLA1k
PC2 = PDLA2k-CPC13k-PDLA2k
PC3 = PDLA1.5k-CPC6k-PDLA1.5k

Scheme 4.1 Chemical structure of P(D/L)LA-PEG-P(D/L)LA (A) and cationic polymer PDLA-CPC-PDLA (B). Three separate PDLA-CPC-PDLA polymer compositions of different block length were synthesized; 1000-6000-1000 (PC1), 2000-13000-2000 (PC2) and 1500-6000-1500 (PC3).

4.3.1.2 Particle size and zeta potential

The utilization of a central cationic block produced water soluble materials, which spontaneously formed spherical micelles ranging from 134 to 181 nm in size with zeta potentials between 25 and 69 mV (Figure 4.1).

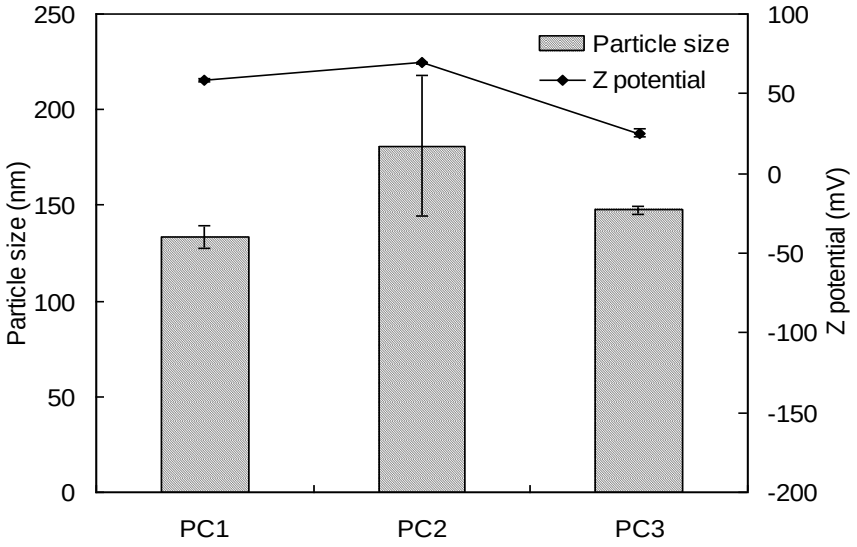

Figure 4.1 Particle size and zeta potentials of PDLA-CPC-PDLA copolymers. Polymer solutions were prepared in DI water at 1 mg/ml using PDLA-CPC-PDLA and equilibrated for 1 hour before measurement.

4.3.1.3 Minimal inhibitory concentration (MIC) determination

Despite having alkyl ammoniums, no antimicrobial activity was observed for PDLA-CPC-PDLA at concentrations below 10000 mg/L for all the three cationic polymers in solution form (Table 4.1).

Polymers	Gram-positive	Gram-negative
	S. aureus	***E. coli***
PC1 ($PDLA_{1k}$-CPC_{6k}-$PDLA_{1k}$)	10000	10000
PC2 ($PDLA_{2k}$-CPC_{13k}-$PDLA_{2k}$)	> 25000	> 25000
PC3 ($PDLA_{1.5k}$-CPC_{6k}-$PDLA_{1.5k}$)	> 25000	> 25000

Table 4.1 Minimum inhibitory concentrations (MICs) of cationic PDLA-CPC-PDLA triblock copolymers. The MICs of the polymers were measured using a broth microdilution method.

4.3.1.4 Hemolysis and cytotoxicity assays

The cationic triblock polymers were further tested for cytotoxicity against rat red blood cells and human dermal fibroblasts (HDF). It was found that PC2 was the least toxic among the three copolymers, and no hemolysis was observed for PC2 up to a concentration of 25,000 mg/L (Figure 4.2) while maintaining HDF cell viability above 80% (Figure 4.3).

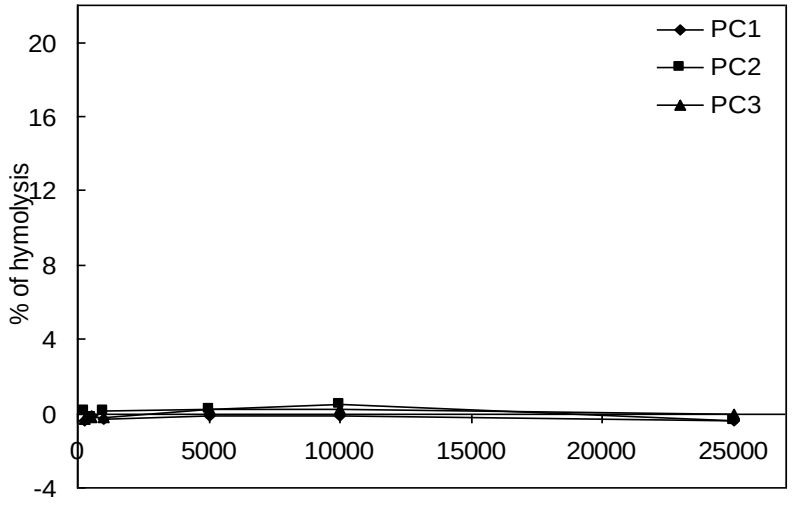

Figure 4.2 Hemolytic activity of cationic polycarbonate copolymers. Fresh mouse red blood cells were incubated with polymer solution for 1 hour. The red blood cell suspension in PBS was used as negative control.

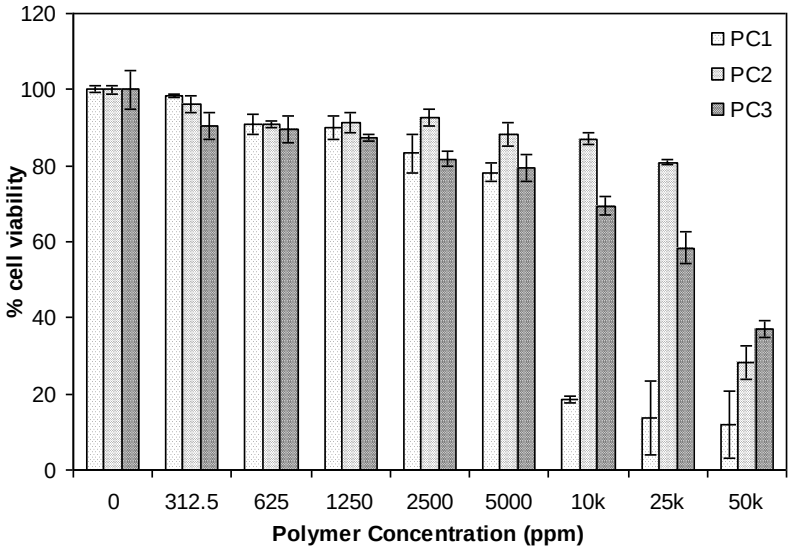

Figure 4.3 Viability of primary human dermal fibroblasts after incubation with cationic polycarbonate copolymers at various concentrations for 12 hours.

4.3.2 Hydrogel formation and characterization

4.3.2.1 Hydrogel formation

PDLA-CPC-PDLA (PC2) was then incorporated into PLLA-PEG-PLLA (0.85k-6k-0.85k) and PDLA-PEG-PDLA (1k-6k-1k) gels at different contents *via* stereocomplexation at 37°C with a total concentration of 13.2% w/v to impart antimicrobial function. Three different gel compositions where studied; Gel 1 (PLLA-PEG-PLLA, PDLA-PC-PDLA and PDLA-PEG-PDLA at 1:0.15:0.85), Gel 2 (PLLA-PEG-PLLA, PDLA-PC-PDLA and PDLA-PEG-PDLA at 1:0.3:0.7) and Gel 3 (PLLA-PEG-PLLA and PDLA-PC-PDLA at 1:1). The molar ratio of PLLA to PDLA was kept at 1:1. Upon dissolution in water, the PEG-based copolymers and their mixture having the opposite stereochemistry formed clear solutions (Scheme 4.2 b and d). Kimura et al. reported two distinctive gel processes occurred at temperatures of 37^{o}C and 75^{o}C and believed that the gel formation resulted

from the crystallization of collapsed PLA domains in water [209]. Similar to his findings, we observed a cloud point and gelation upon heating the polymer solution above 37°C (Scheme 4.2 c and e).

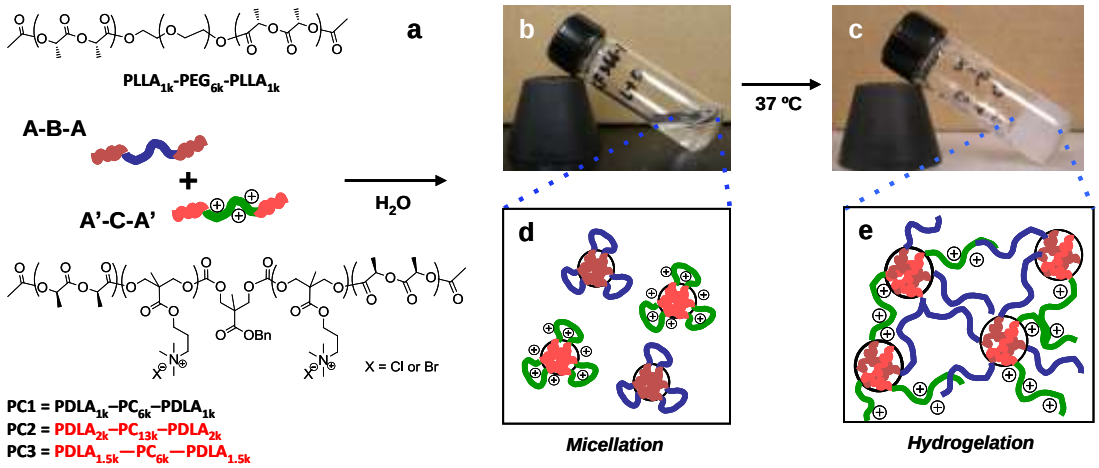

Scheme 4.2 Chemical structures of PLLA-PEG-PLLA and PDLA-CPC-PDLA (a) and pictures of 10 wt% solution at 25 ℃ (b) and at 37 ℃ (c). At 25 ℃ the solution is clear fluid and each polymer forms flower-type micelles in aqueous environment (d). Upon heating at 37 ℃ for 30 min, the solution turns into opaque gel based on stereocomplex formation between enantiomeric pure polylactide segments in the micelle cores (e).

4.3.2.2 Differential scanning calorimetry

Interestingly, this supramolecular gel did not show a melting point associated with the PLA component (Figure 4.4 B). Whereas for P(D/L)LA-PEG-P(D/L)LA of long P(D/L)LA block length and resulted stereocomplex, a melting point shift from 114 ℃ to 174 ℃ was clearly observed due to the stereocomplexation (Figure 4.4 A). Similar finding was reported by O'Reily that PEG-PLA block polymer micelles crystallized adjacent lactide blocks to form high aspect ratio nanostructures [210].

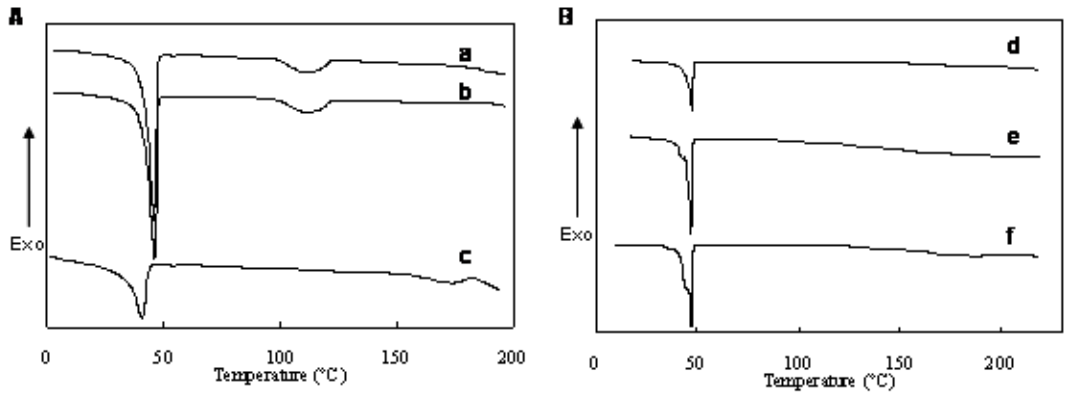

Figure 4.4 DSC of stereocomplexes. A. Stereocomplex of long PLA segment: a. PDLA-PEG-PDLA (2k-6k-2k), b. PLLA-PEG-PLLA (2k-6k-2k), c. PDLA-PEG-PDLA (2k-6k-2k) : PLLA-PEG-PLLA (2k-6k-2k) at 1:1 molar ratio; B. Stereocomplex of short PLA segment: d. PLLA-PEG-PLLA (0.85k-6k-0.85k), e. PDLA-PEG-PDLA (1k-6k-1k) and f. PDLA-PEG-PDLA (0.85k-6k-0.85k) : PLLA-PEG-PLLA (1k-6k-1k) at 1:1 molar ratio

4.3.2.3 X-ray diffraction analysis

X-ray diffraction (XRD) patterns of individual polymer and stereocomplexes were tested to further confirm the stereocomplexation. As shown in Figure 4.5, pure PLLA shows two intense peaks at 2θ of 16.9 ° and 19.3 °. The PLLA-PEG-PLLA shows both the peaks of PEG at 19.4 ° and 23.6 ° and those pronounced signals due to PLA stereocomplex formation at 12.0 ° and 20.6 °. This is consistent with what have previously reported in the literature [211].

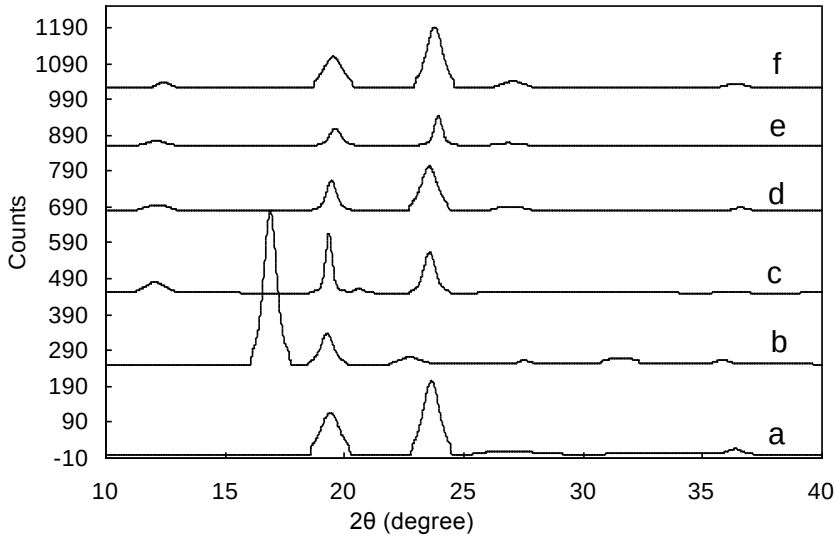

Figure 4.5 Wide-angle X-ray diffraction patterns of control polymers: a. PLLA-PEG-PLLA 850-6000-850 , b. PLLA 2000) and c. control Gel (PLLA-PEG-PLLA and PDLA-PEG-PDLA at 1:1 molar ratio), d. Gel 1 (PLLA-PEG-PLLA, (PDLA-PC-PDLA and PDLA-PEG-PDLA at 1:0.15:0.85), e. Gel 2 (PLLA-PEG-PLLA, PDLA-PC-PDLA and PDLA-PEG-PDLA at 1:0.3:0.7) and f. Gel 3 (PLLA-PEG-PLLA and PDLA-PC-PDLA at 1:1). The gels were formed at 7% w/v and freeze dried for experiment.

4.3.2.4 Rheology

Copolymers having lower PLA block lengths (e.g. Mn = 850 and 1000 g/mol), required for water dispersion without use of an organic solvent, formed opaque, low modulus and viscous solutions (13.2% w/v aqueous solutions) after incubation at 37 ^{o}C for 5 hours. As shown in Figure 4.6, storage modulus of stereocomplex was much higher than either of the isomer alone, indicating hydrogel formation. In addition, storage modulus of the hydrogel decreased as the incorporation of PC2 increased, depending on the amount of PC2 present in the system. It was reasoned that the fiber-like assemblies were forming through partial crystallization of the lactide domains[212], which reinforced the gel, manifesting higher moduli.

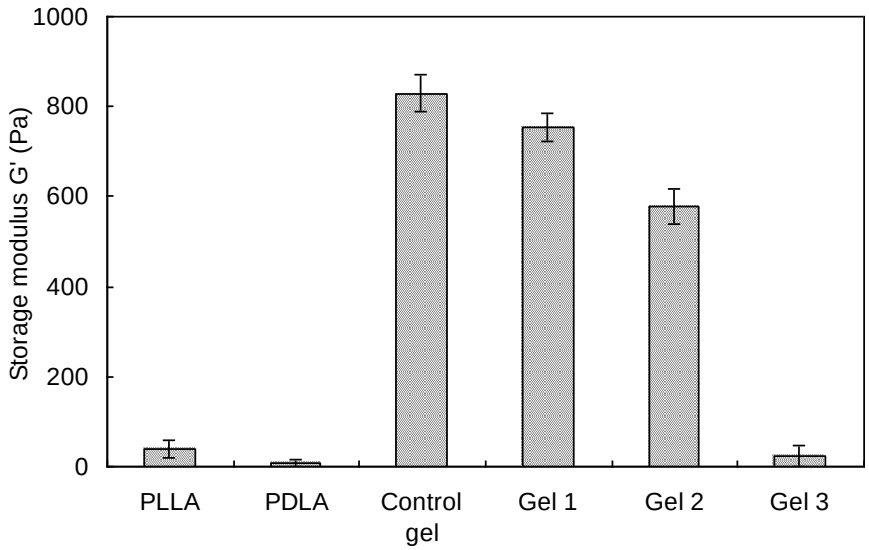

Figure 4.6 Storage modulus of individual polymer solutions and stereocomplex gels. Polymer concentration: 13.2% w/v. The dynamic storage modulus (G′) was examined as a function of frequency from 0.1 to 50 rad/s. The measurements were carried out at strain amplitude (γ) of 5% to ensure the linearity of viscoelasticity

Furthermore, regardless of PC2 content, modulus was found to increase with longer annealing times, supporting the idea of refining crystallization within the lactide blocks (Figure 4.7). The moduli were low for all three cationic gels (Gel 1, 2 and 3), reflecting the non-covalent nature of the gel-forming reacton. As such the gels were readily remoldable, and showed a significant drop in viscosity with increasing shear rate (Figure 4.8), indicating a unique ability to shear-thin. This likely resulted from the dynamic nature of the gel-forming reaction and/or the alignment for the supramolecular features. This unique attribute is thought to significantly facilitate the ease of deposition for applications such as skin infections, injectable gels and eye drops.

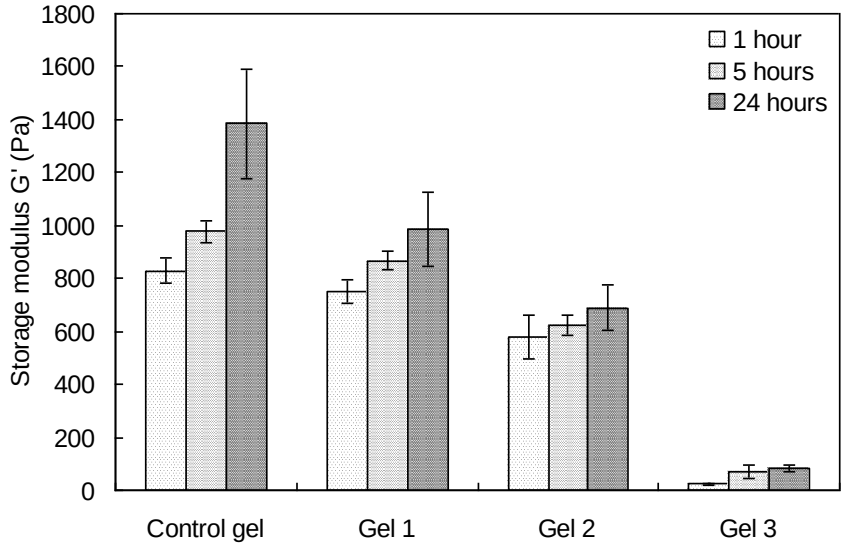

Figure 4.7 Rheology changes of the cationic hydrogels as a function of annealing time. Hydrogels were incubated in 37 ℃ incubator and rheology of the hydrogels was examined periodically at 1 hour, 5 hours and 24 hours.

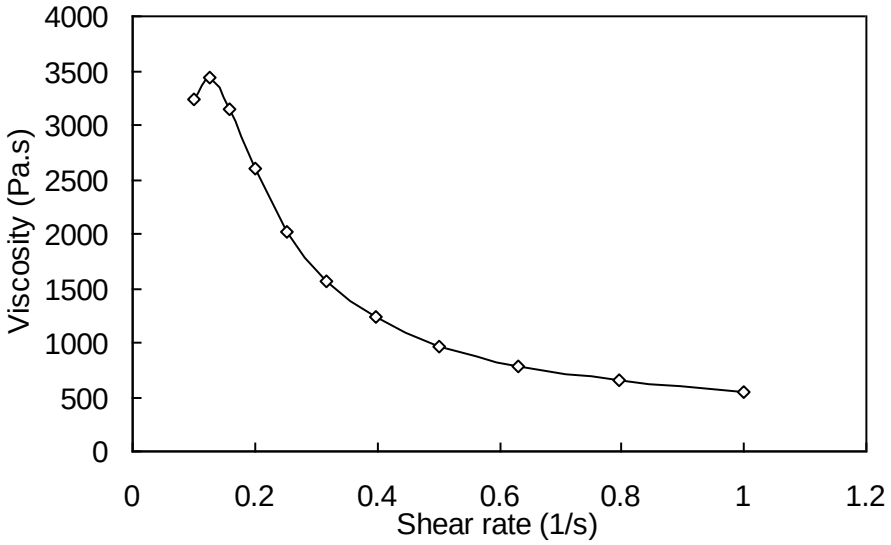

Figure 4.8 Viscosity of representative hydrogel as a function of sheer rate from 0.1 to 1 1/s. Hydrogels were incubated at 37 ℃ incubator for 5 hours before the viscosity measurements.

4.3.2.5 Fiber observation under light microscope, SEM and TEM

Imaging of the PLLA-PEG-PLLA with an optical microscope showed an abundance of fiber-like nanostructures, whereas PDLA-PEG-PDLA formed far fewer fiber-like assemblies (Figure 4.9). After combining PLLA-PEG-PLA with PDLA-PEG-PDLA after incubation 37 ^{o}C for 5 hours, short fibers were formed (Figures 4.9 and 4.10), but it was accompanied by gel formation and a much higher modulus than either of the isomers alone (Figure 4.6). Fiber length was determined by counting and measuring 100 fibers at 5 different areas of each sample.

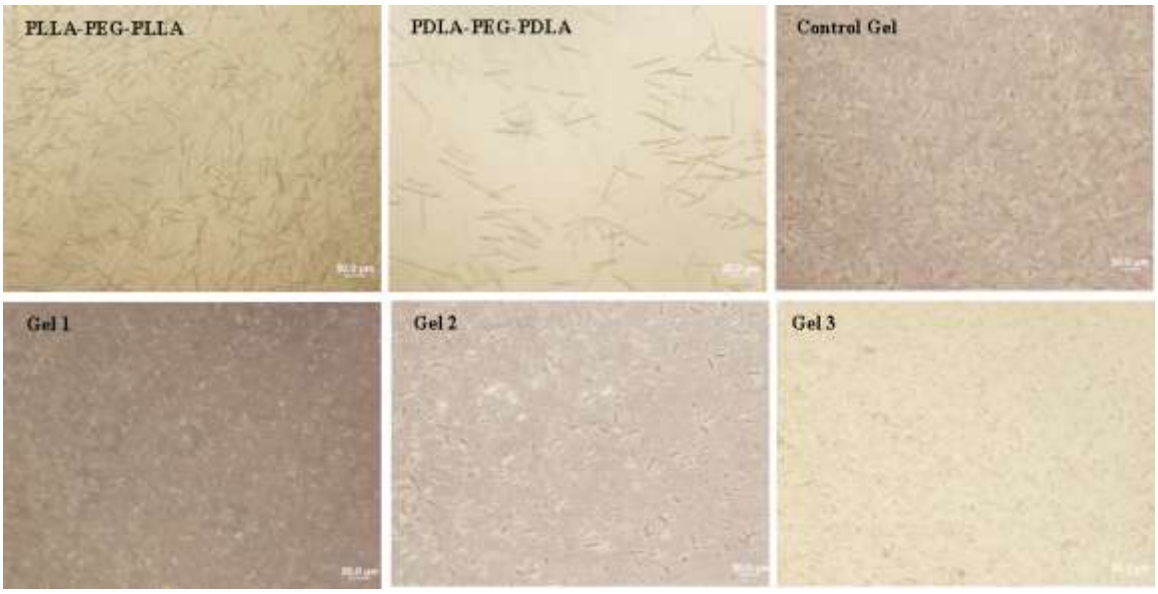

Figure 4.9 Optical micrographs of individual polymers and stereocomplex gels. Polymer concentration: 13.2% w/v. Scale bar: 50 μm. Hydrogels were diluted to 5 mg/ml for observation.

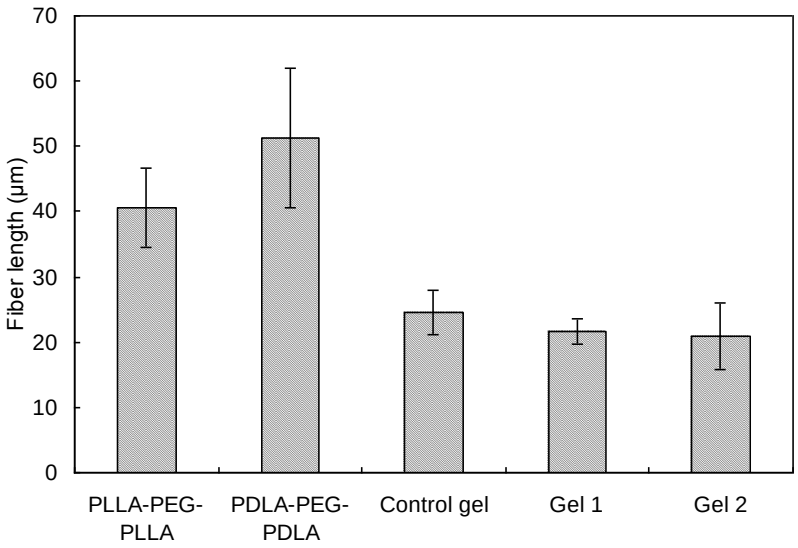

Figure 4.10 Fiber length of individual polymers and stereocomplex gels. Fiber length was determined by counting and measuring 100 fibers at 5 different areas of each sample.

Using transmission and scanning electron microscopies, major morphological changes were observed for the gels formed with stoichiometric equivalents of PDLA-CPC-PDLA and PLLA-PEG-PLLA (Gel 3) relative to the control gel prepared from PLLA-PEG-PLA/PDLA-PEG-PDLA (Gel 3 in Figure 4.11 and 4.12). Nonetheless, numerous fibers with similar length were also seen in PLLA-PEG-PLA/PDLA-PEG-PDLA/PC2 gels with lower amounts of PC2 (Gel 1 and Gel 2 in Figure 4.11 and 4.12).

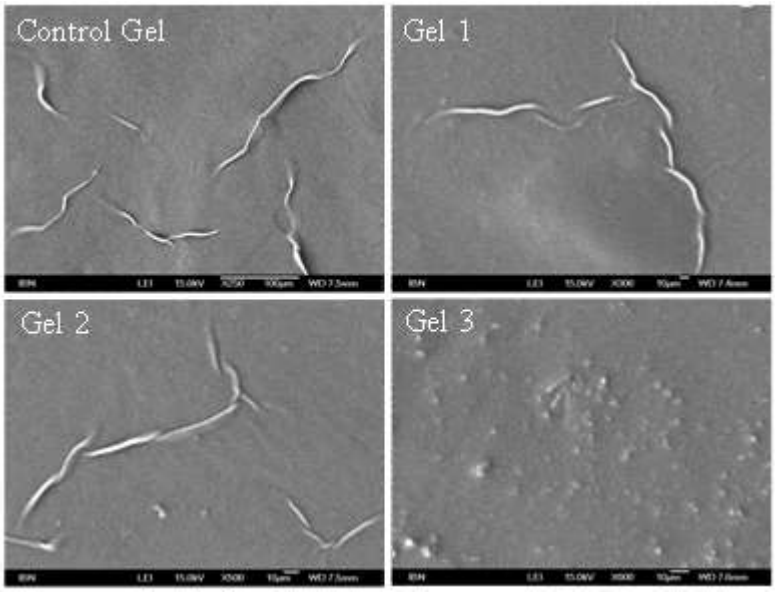

Figure 4.11 SEM images of Control Gel (PLLA-PEG-PLLA and PDLA-PEG-PDLA at 1:1 molar ratio), Gel 1 (PLLA-PEG-PLLA, (PDLA-PC-PDLA and PDLA-PEG-PDLA at 1:0.15:0.85), Gel 2 (PLLA-PEG-PLLA, PDLA-PC-PDLA and PDLA-PEG-PDLA at 1:0.3:0.7) and Gel 3 (PLLA-PEG-PLLA and PDLA-PC-PDLA at 1:1).

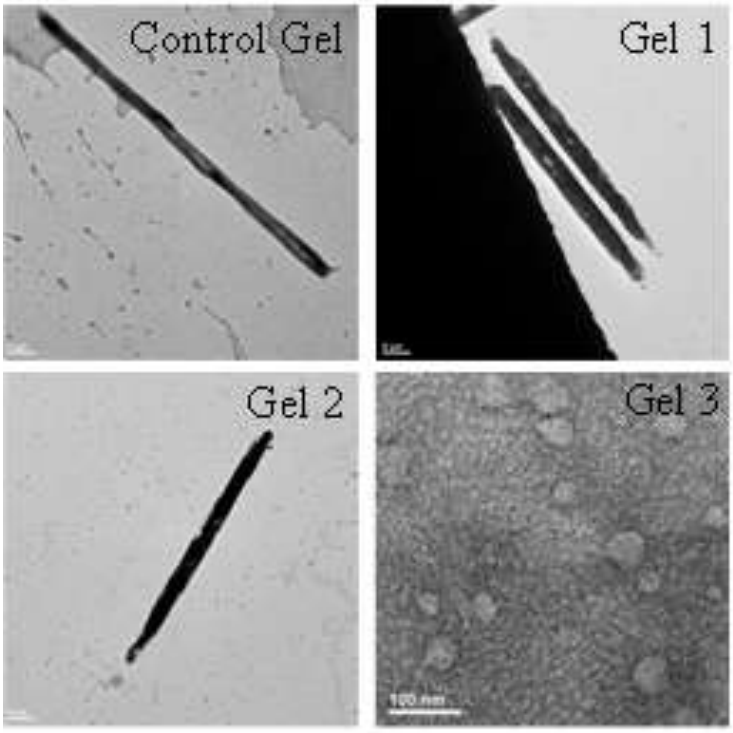

Figure 4.12 TEM images of Control Gel (PLLA-PEG-PLLA and PDLA-PEG-PDLA at 1:1 molar ratio), Gel 1 (PLLA-PEG-PLLA, (PDLA-PC-PDLA and PDLA-PEG-PDLA at 1:0.15:0.85), Gel 2 (PLLA-PEG-PLLA, PDLA-PC-PDLA and PDLA-PEG-PDLA at 1:0.3:0.7) and Gel 3 (PLLA-PEG-PLLA and PDLA-PC-PDLA at 1:1).

4.3.3 Antimicrobial activities *in vitro*

4.3.3.1 Killing efficiency

The antimicrobial activities of gel complexes were evaluated against various pathogenic microbes including *S. aureus* (Gram-positive), *E. coli* (Gram-negative) and *C. albicans* (fungus). PC2 was used at concentrations below 25,000 mg/L to form antimicrobial gels as it did not induce significant hemolysis and cytotoxicity at this concentration (Figures 4.2 and 4.3). The control gel formed from PLLA-PEG-PLLA with PDLA-PEG-PDLA and PC2 alone at 25000 mg/L showed no activity (Figure 4.13, Table 4.1). In sharp contrast, the stereocomplex gels made from PLLA-PEG-PLLA, PC2 and PDLA-PEG-PDLA at 1:0.15:0.85 molar ratio (i.e. Gel 1, PC2=10000 mg/L) completely suppressed bacterial growth and killed the bacteria (i.e. *S. aureus* and *E. coli*) at ~100% efficiency. A gel with an increased amount of PC2 to 20000 mg/L (i.e. Gel 2, ratio=1:0.3:0.7) was needed to inhibit *C. albicans* growth and completely kill the fungus.

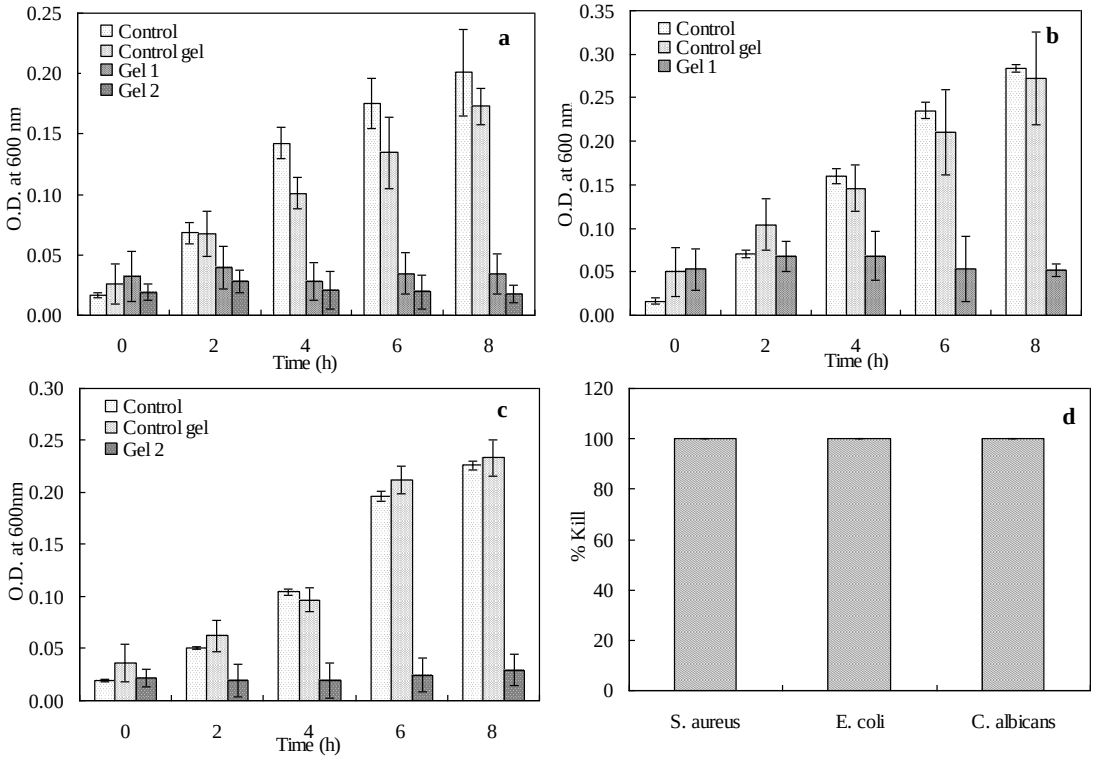

Figure 4.13 Antimicrobial activities of cationic hydrogels against various microbes: Growth inhibition of a: *S. aureus* (Gram-negative bacteria) (a); *E. coli* (Gram-negative bacteria) (b) and *C. albicans* (yeast) (c); % killing efficiency of different microbes (Gel 1 for *S. aureus* and *E. coli*, Gel 2 for *C. albicans*) (d). The number of colony forming unit (CFU) was recovered and counted in Killing efficiency= (cell count of control-survivor count on cationic hydrogel)/cell count of control ×100.

In order to demonstrate the clinical potential of these antimicrobial hydrogels, they were tested against clinically isolated microbes such as methicillin-resistant *S. aureus* (MRSA, Gram-positive), *vancomycin-resistant enterococci* (VRE, Gram-positive), *A. baumannii* (Gram-negative, resistant to most antibiotics), *K. pneumoniae* (Gram-negative, resistant to carbapenem) and *C. neoformans* (fungus). The hydrogels were found to completely inhibit growth and showed a near perfect killing efficiency on all cell lines tested (Figure 4.14).

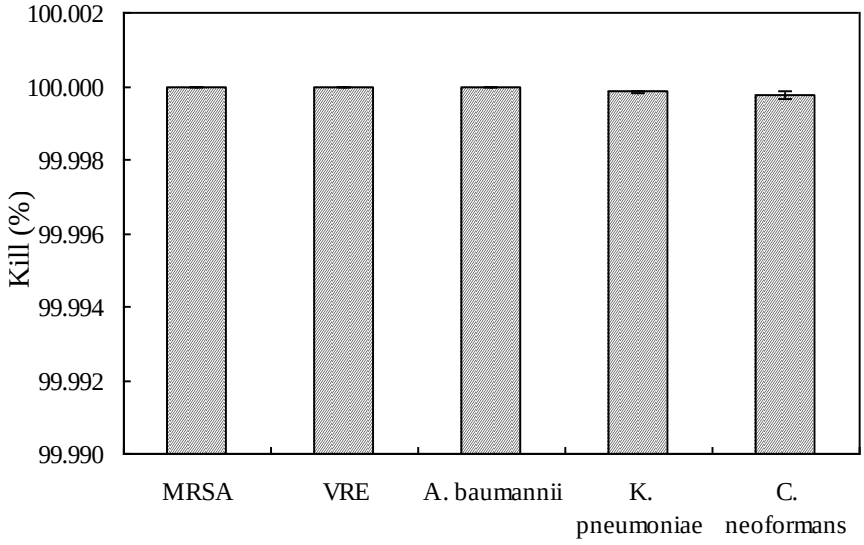

Figure 4.14 Killing efficiency of stereocomplex cationic hydrogels against various clinically isolated microbes**,** including methicillinresistant S. aureus (MRSA, gram-positive), vancomycinresistant enterococci (VRE, gram-positive), P. aeruginosa (gram-negative), A. baumannii (gram-negative, resistant to most antibiotics), K. pneumoniae (gram-negative, resistant to carbapenem), and C. neoformans.

4.3.3.2 Antimicrobial mechanism

The antimicrobial mechanism was determined to be cell wall/membrane lysis. This determination was supported by morphological changes of *S. aureus, E. coli* and *C. albicans* after incubation with the antimicrobial gels for 2 hrs. As shown in Figure 4.15, the untreated microbial cells or cells treated with the control gel remained smooth and in round (*S. aureus* and *C. albicans*) or rod-like (*E. coli*) shapes. In sharp contrast, cellular deformation and rough surfaces could clearly be seen after treatment with an antimicrobial gel for 2 hrs. Additionally, lysed cells and debris were also observed in the treated microbes. In the case of *E. coli,* numerous vesicle-like structures were formed presumably from gel-cell membrane integration (white arrows in Figure 4.15 b). Further highlighting the catastrophic membrane failure mechanism was the release of cytoplasts

in *C. albicans* after antimicrobial gel exposure (Figure 4.15 c). Based on these observations, we hypothesize that the anionic cell surface was associated with cationic polycarbonate blocks at many points on the gel surface *via* electrostatic interaction, which might further allow hydrophobic components in the gel to interact with lipid domains of cell membrane, thus causing terminal cell damage. Similarly, an "anion sponge" model for antimicrobial mechanism of hydrogel was proposed by Peng Li and his group [126]. According to this model, anionic microbial membrane was attracted and suctioned into the internal nanopores of the cationic hydrogels, disrupting microbial membrane integraty and causing microbial cell death.

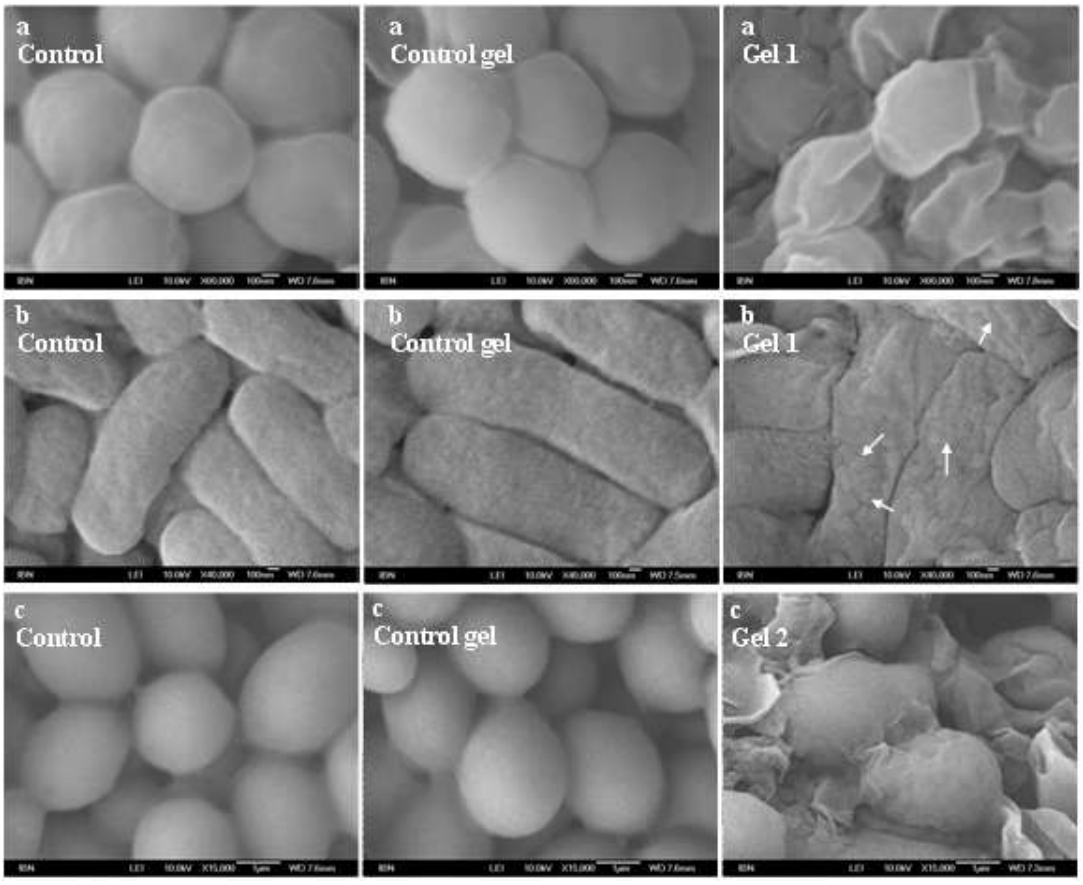

Figure 4.15 SEM images of *S. aureus* (a), *E. coli* (b) and *C. albicans* (c) before (Control) and after incubation with Control Gel, Gel 1 (*S. aureus* and *E. coli*), and Gel 2 (*C. albicans*) for 2 hours. Size of the bars: a,b-100 nm; c-1 μm.

4.3.3.2 Drug resistance stimulation study

It has been reported that repeated exposure of microbes to antimicrobial agents at concentration under their lethal dose contribute to drug resistance development [213]. This phenomenon was stimulated by monitoring the MIC of E. coli, survive and re-grow from sub-MIC treatment with ciprofloxacin, gentamicin and hydrogel (Gel 1) over 10 passages. As shown in Figure 4.16, bacterial developed drug resistance against different antimicrobial agents at different passages. MIC of E. coli with ciprofloxacin started to increase at passage 3 and shoot up to 10 times increase at passage 10 and MIC increase of E. coli with gentamicin was observed even at passage 2 and continuously increased 6.7 times by passage 10. In sharp contrast, no resistance was observed for bacterial treated with hydrogel (Gel 1) and killing efficiency was remained as 100% throughout the course of treatment. This can be attributed to the different antimicrobial mechanism adopted by the various antimicrobial agents. More importantly, we can infer that macromolecular antimicrobial agents offer greater advantages over conventional antibiotics in preventing drug-resistance development by adopting the membrane disruption mechanism. Same observation was reported by Wiradharma et al in microbes treated with macromolecular peptides [214].

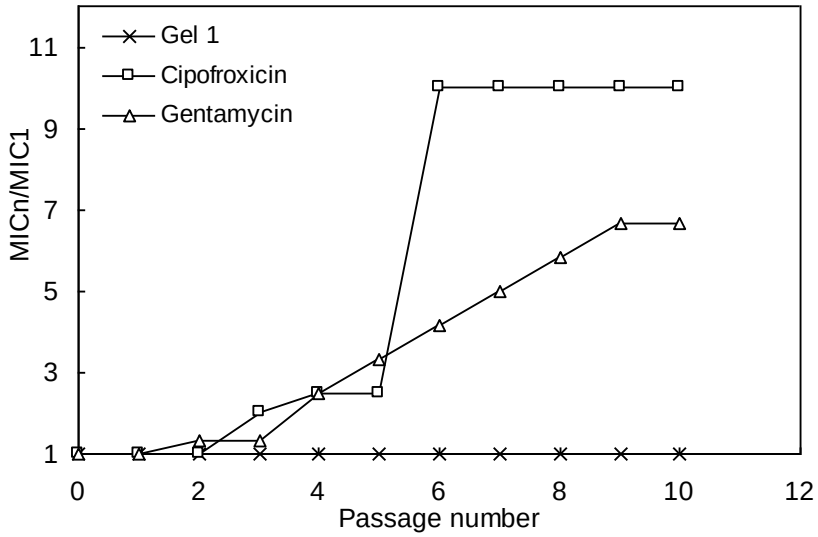

Figure 4.16 Changes in MIC against different antimicrobial agents upon repeated exposure with sub-lethal concentration. E. coli was used as a model microorganism and repeatedly exposed to antimicrobial agents at sub MIC concentration. MIC of gentamicin, ciprofloxacin and cationic hydrogels was monitored for consecutive 10 passages to monitor the MIC changes.

4.3.4 Antibiofilm activities *in vitro*

4.3.4.1 Biomass and XTT assay

To further investigate the antibiofilm activity of hydrogel complex, biofilm of *S. aureus*, MRSA, *E. coli* and *C. albicans* were cultured and formed in 96-well plate for 7 days [215]. Stereocomplex hydrogels prepared from PLLA-PEG-PLLA, PC2 and PDLA-PEG-PDLA at 1:0.15:0.85 molar ratio (i.e. Gel 1, PC2=10000 mg/L) and 1:0.3:0.7 molar ratio (i.e. Gel 2, PC2=20000 mg/L) were able to remove more than 60% of biomass (Figure 4.17 a1-a4) with a killing efficiency higher than 80% (Figure 4.17 b1-b4) as compare to control.

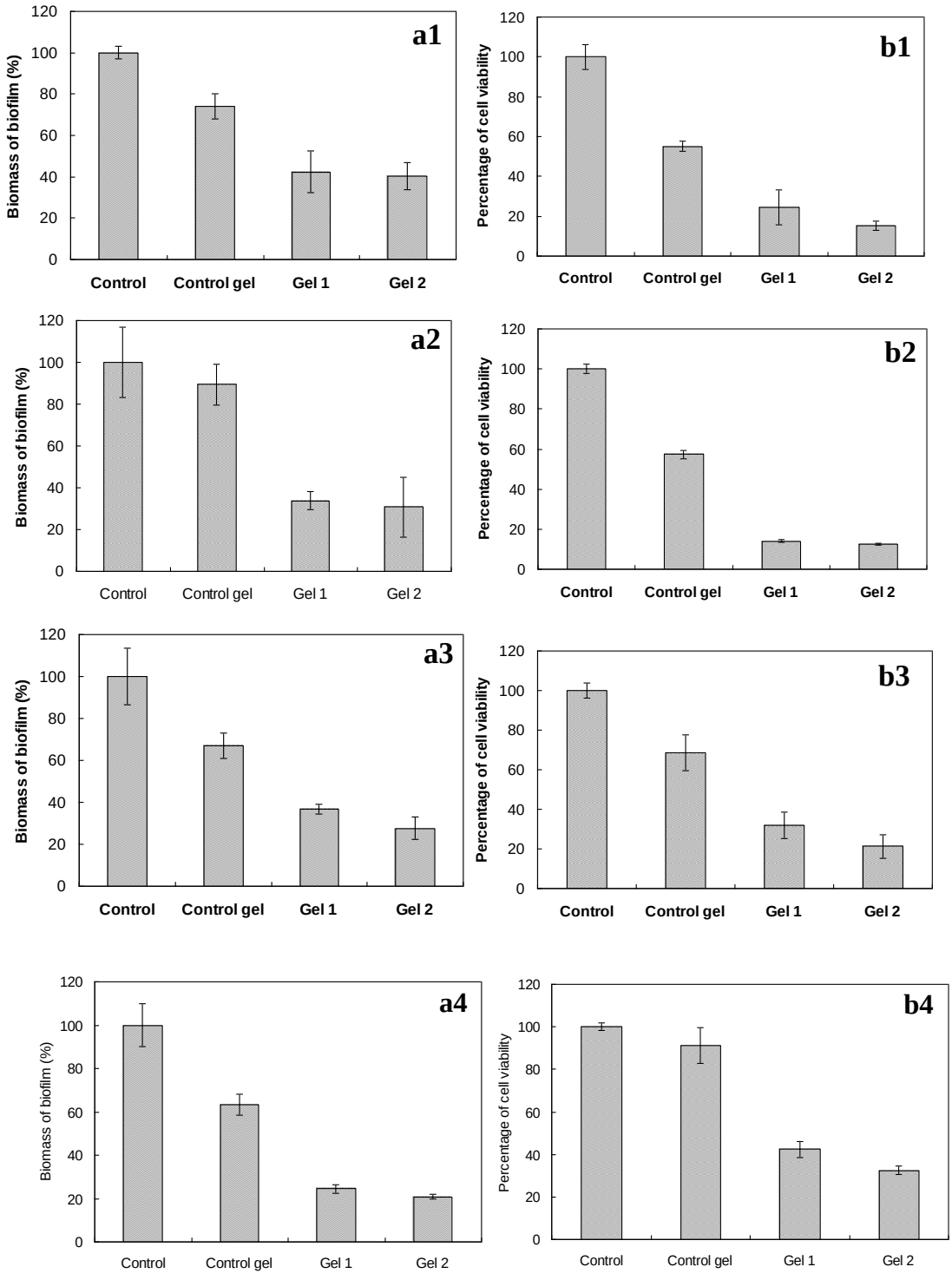

Figure 4.17 Anti-biofilm activities of cationic hydrogels against various microbes: biomass reduction (a1-4) and cell viability (b1-4) in *S. aureus* (1), MRSA (2), *E. coli* (3) and *C.albicans* (4). Biofilms of different microorganisms were formed for 7 days and treated with hydrogels for 24 hours. The results were expressed as a percentage of the cell viability without treatment.

4.3.4.2 SEM observations

Biofilm dispersion was further proved by the SEM images of the biofilms before and after the treatment (Figure 4.18). Typical biofilm structures were shown in both control and control gel group. In sharp contrast, biomass of the biofilm treated with cationic hydrogel was significantly decreased. A small portion of cells were left with cell membrane drastically disrupted morphologies similar to those observed in Figure 4.17 b1-b4.

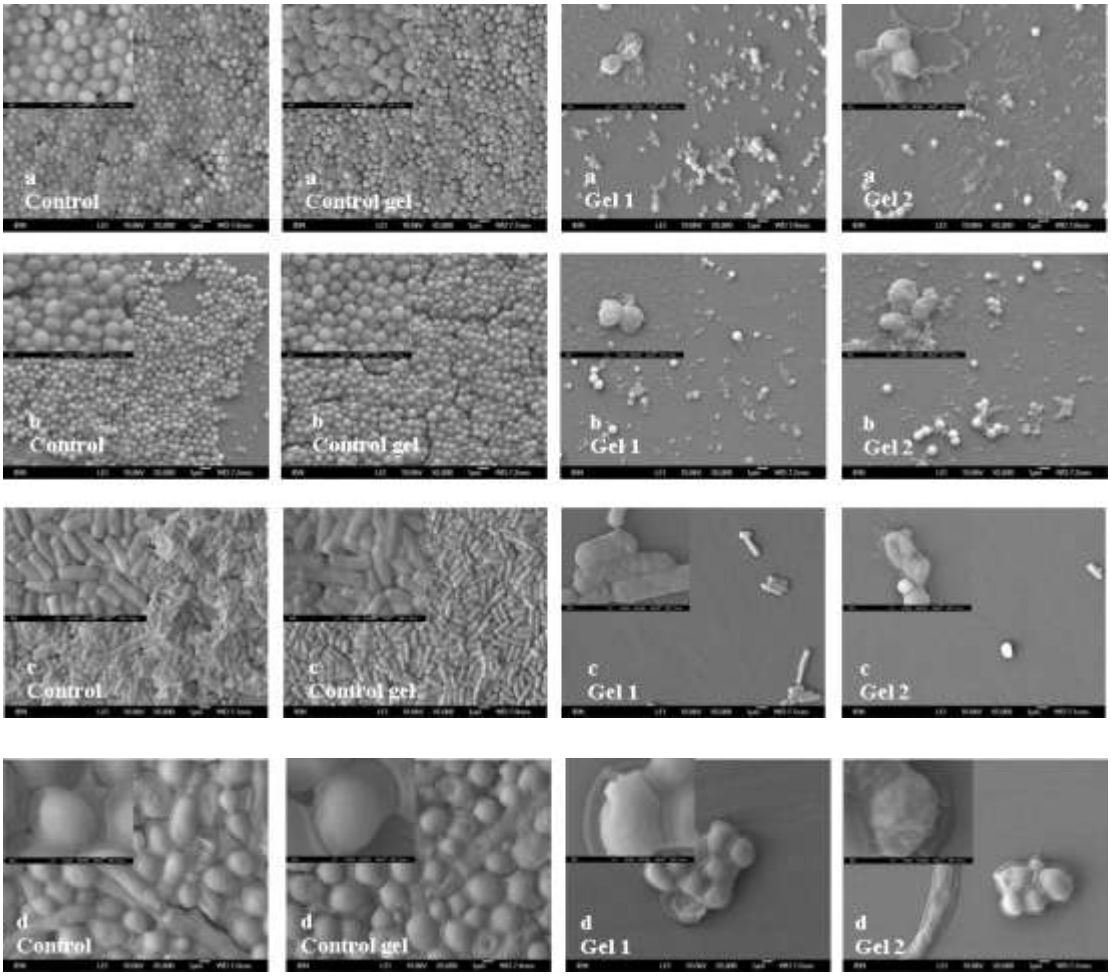

Figure 4.18 SEM images of *S. aureus* (a), MRSA (b), *E. coli* (c) and *C. albicans* (d) before (Control) and after incubation with Control gel, Gel 1 and Gel 2 for 24 hours. Size of the bars: 1 μm; inserted Control and Control gel samples: 1 μm; inserted Gel 1 and Gel 2 samples: 100 nm.

4.3.5 Antibiofilm activities *in vivo*

4.3.5.1 Fungal recovery assay

Candida albicans was recovered from 5 corneas of each group. Compared to the corneas of the control group, which normalized to be 100%, fungi recovery of the cornea was significantly lower in the Amphotericin B and gel 3 group (*P<0.05*, Figure 4.19). Photos were taken before and after the treatment for all the experimental groups.

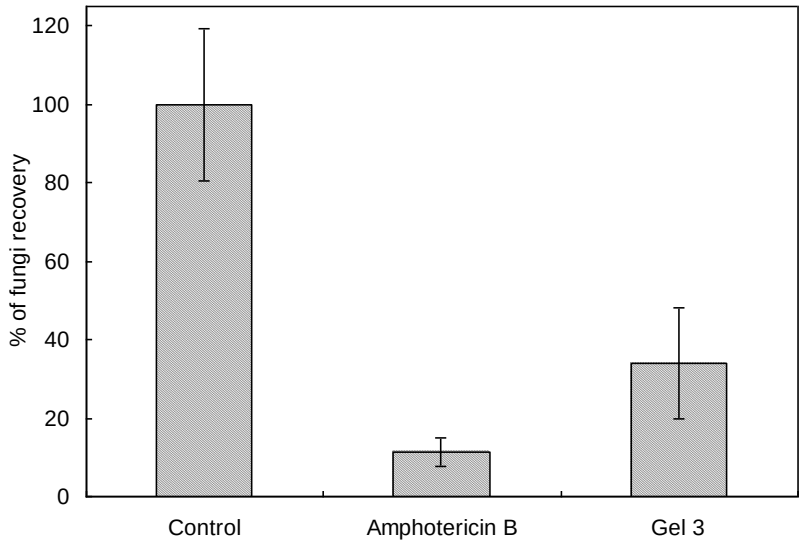

Figure 4.19 Fungi recovery from cornea of all treatment groups (Control, Amphotericin B and gel 3). Data normalized to control group. Fungus were recovered from the eye ball and incubated at 22 ℃ for 48 hours before counting the colony forming unit (CFU). The percentage of fungi recovery was expressed as the number of CFU revived from treatment groups as compare to those revived from control group to determine the survival of *Candida albicans*.

4.3.5.2 Histopathology

Photographs of the infected eyes with keratitis were taken before and after the treatment with control group, AMB and antimicrobial hydrogels (Figure 4.20). Significant

improvement was observed for the groups treated with AMB and antimicrobial hydrogel as compared to control group. Furthermore, the depth of fungal invasion was observed after staining (Figure 4.21 A). Compared to the hyphae invasion in control group, both AMB and antimicrobial hydrogel reduced the maximal depth of hyphae invasion into the corneas, and the difference between AMB and antimicrobial hydrogel was not significant. Representative sample of the cornea histopathologies are shown in Figure 4.21.

As shown in Figure 4.21 B, no evidence of drug-related adverse effects in the uninfected eyes was observed. There was no significant difference between the treatment groups and control group with respect to inflammation, indicating the no clinically apparent toxicity of the treatments used.

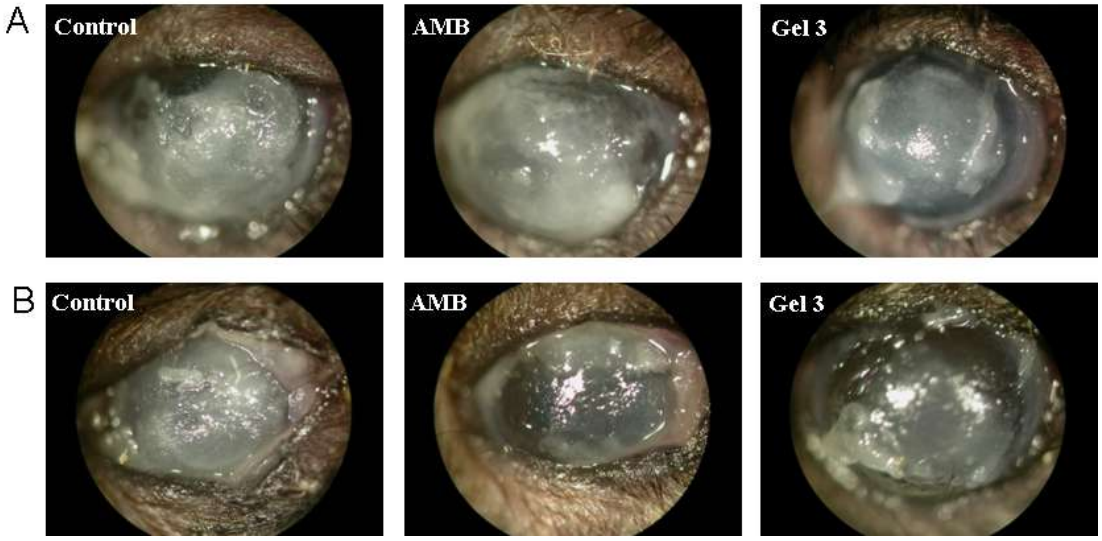

Figure 4.20 Typical clinical presentation of *C. albicans* keratitis mice eyes before and after treatment with control, Amphotericin B and gel 3. A. Keratitis before treatment; B. Keratitis after being treated with different groups hourly for 8 hours.

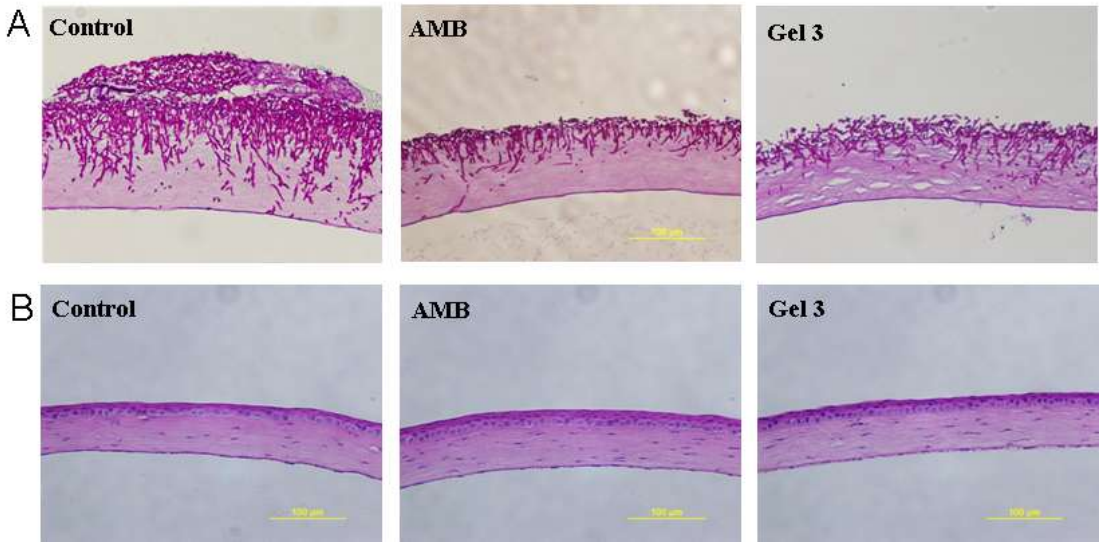

Figure 4.21 Representative example of histopathologies of treated and healthy corneas. Antibiofilm activity and selectivity were shown in A. Keratitis after being treated with control gel, AMB and cationic gel 3; Safety of the hydrogel was tested on health eye treated with control gel, AMB and cationic gel 3 (B).

4.4 Conclusion

In conclusion, we have designed and synthesized antimicrobial and antibiofilm stereocomplex hydrogel with distinctive supramolecular structures from the cationic polycarbonate polymers and PLA-PEG-PLA. We have demonstrated that the formation of the stereocomplex strongly enhanced its antimicrobial activities. These hydrogel possess a broad spectrum of superior antimicrobial activity with an inhibition above 99.9% for various types of pathogens, including clinic isolated gram-positive, gram-negative bacteria, fungi and yeast, yet induce relatively low cytotoxicity. Moreover, it was demonstrated that gel 1 and gel 2 has efficiently inhibited growth of fungi biofilm with low MIC values and clear fungal biofilm both *in vitro*. Compared to costly and unstable Amphotericin B, gel 1 and gel 2 are easy to prepare and can be stored for routine topical use with long shelf life. More importantly, preliminary keratitis treatment findings

suggest that topical solution of cationic hydrogel is safe and as efficacious as that of Amphotericin B, the most commonly used agent for the treatment of Candida keratitis. With an excellent biocompatibility, we believe that these hydrogel will be widely applicable for combating infections and provide a great platform for the applications in clinical biofilm dispersion.

CHAPTER 5. CONCLUSION AND FUTURE PERSPECTIVES

5.1 Conclusion

The common theme, discussed and analyzed throughout the thesis, has been the design and optimization of well-defined hydrogel systems for different specific applications. Herein we described the synthesis, characterization and development of two different types of hydrogels for tissue engineering and antimicrobial therapeutics, respectively.

In tissue engineering, a novel strategy, chemically incorporating micelles into the hydrogel system, has been proven to provide an alternative approach to tune the physical properties of the hydrogels as well as the subsequent cell behavior inside the hydrogels. **In Aim (1)**, we have shown that the swelling ratio and porosity of the hydrogel increased with increasing micelle content from 0% to 80%. These hydrogels are biodegradable as demonstrated by a reduction in storage modulus over 28 days. Moreover, in **Aim (2)**, subsequent cell matrix interactions showed that cell viability in the hydrogel with 20% micelle content was significantly higher the hydrogel without micelles. The same observation was seen for gene transfection efficiency in the hydrogel with 20% micelle content, which was significantly higher when compared to the control hydrogel without micelle. Our bolaamphiphile polymer was much more efficient as a gene carrier compared to the ‘golden standard’ of PEI. Thus we have successfully proven our hypothesis that incorporating micelle into the hydrogels is a good strategy to control cellular behavior in a 3D hydrogel environment for tissue engineering.

In antimicrobial therapeutics, a new hydrogel formulation with macromolecular cationic polymers encapsulated via stereocomplexation has been designed and evaluated. These hydrogels exhibited excellent antimicrobial and antibiofilm activities both *in vitro* and were shown to greatly improve fungal keratitis *in vivo*. **In Aim (1)**, the screening of three cationic polymers with different cationic and hydrophobic length demonstrated that hydrophobic/hydrophilic balance is of great importance in the design of antimicrobial polymer without undesirable cytotoxicity. Diffraction peak in X-Ray diffraction study confirmed the hydrogel formation through stereocomplexation and rheology study showed shear-thinning property of the hydrogel. Furthermore, supramolecular structure was observed under SEM and TEM with a ribbon-like structure clearly seen. **In Aim (2)**, hydrogels with different amounts of cationic polymer incorporated were tested against both *S. aureus* (G-positive), *E. coli* (G-negative) and *C. albicans* (fungus) and showed outstanding antimicrobial activities with killing efficiency near to 100%. SEM observation of the microorganisms in both control and treatment group revealed a membrane disruption mechanism by the polymers. These hydrogels were also tested against various clinically isolated drug-resistant pathogens including methicillin-resistant *S. aureus* (MRSA, Gram-positive), *vancomycin-resistant enterococci* (VRE, Gram-positive), *A. baumannii* (Gram-negative, resistant to most antibiotics), *K. pneumoniae* (Gram-negative, resistant to carbapenem) and *C.* neoformans and found to yield 99.99% of killing efficiency. Our study on antibiofilm has shown that these hydrogels were capable of dispersing biofilms formed from *S. aureus* (G-positive), MRSA, *E. coli* (G-negative) and *C. albicans* (fungus) with the majority of the biofilm removed and cells lysed. **In Aim (3)**, these hydrogels were applied on a fungal keratitis model and showed

comparable treatment effect with the commercially available antibiotic Amphotericin B, in both reducing fungi recovery and hyphae invasion yet induced no toxicity on the healthy eyes. Thus we successfully proved our hypothesis that incorporating cationic polymer into hydrogel system served as an effective platform to treat microorganisms and biofilms infections both *in vitro* and *in vivo*.

5.2 Future perspectives

This work has contributed not only to the development of new strategies for hydrogel applications in tissue engineering and antimicrobial therapeutics, but also identified potential opportunities in interdisciplinary subject of hydrogel for biomedical applications that can be further investigated.

Firstly, through our preliminary study performed in Chapter 3, we have confirmed that in addition to the many strategies that have been previously studied to improve PEG hydrogels for tissue engineering, incorporating nanostructured micelle into PEG hydrogels is a novel and feasible method to tune the physical properties of hydrogel, thus these hydrogels serve as an excellent platform for cell and gene delivery. Growth factor delivery for tissue engineering has been widely reported in the literature, for example, transforming growth factor beta (TGF-ß) superfamily including TGFß1, TGFß2 and TGFß3 have been widely studied in inducing chondrogenesis of MSCs under certain culture conditions [216, 217], Chung et al have significantly improved bone regeneration with the addition of recombinant bone morphogenetic protein-2 (BMP-2) [218]. However, delivery of therapeutic gene coded for these growth factors provided even greater

guidance in differentiation [219]. Herein, we propose that further investigations can be pursued with a wide coverage of therapeutic gene delivery coded for these growth factors to determine whether nanostructured PEG hydrogel is indeed a broadly applicable formulation for cell and gene delivery in tissue engineering.

Secondly, the success of tissue engineering is greatly dependent on the scaffold design. Consequently, more synthetic material development will have a significant impact on tissue engineering. For instance, environmentally responsive materials and the subsequently developed cell-responsive hydrogels will be an interesting scaffold to investigate. In addition, development in biological science, including understanding of more novel specific cell ligands, cell-cell interaction within the scaffold and cell-matrix, are of great importance in improving communications between natural tissues and artificial scaffolds. Last but not least, due to the potentially extensive applicability of the hydrogel system in biomedical area, it is essential to develop new well-defined hydrogels with their specific end-application in mind. As different applications require specific physical and biochemical properties of the hydrogel scaffold, such as stiffness, degradation rate and bioactive cues, this aspect should be taken into consideration in the future studies to fine tune hydrogel properties for specific tissue engineering studies both *in vitro* and *in vivo*.

Although currently increasing antimicrobial polymers has been synthesized and identified, in order to establish and explore the full potential of novel synthetic polymers as major treatments for infectious disease, several issues need to be carefully addressed. Firstly, it

is crucial to fine tune the structural parameter of the polymers, including cationic charge density, hydrophobicity and defined architecture (branched or linear), to obtain optimal antimicrobial activity and selectivity. As biocompatibility is another important aspect of polymer used in clinic settings, designing antimicrobial polymers with desired degradation rate and non-toxic degradation products deserves equal attention in research studies. Secondly, successful development of fast and reliable evaluation method of antimicrobial activity is a weapon for screening synthetic polymers. Currently, there are quite a few uncertainties in the universal utilization of broth microdilution method to determine MIC value of antimicrobial agents. These factors include the nature of microorganism in size, shape and growth curve, growth media and incubation time in culturing different microorganisms and even test condition difference employed by various research laboratories. Thus there is a pressing need to establish and validate standardized test for antimicrobial screening and ensuring rapid clinical translation is another important aspect to be taken into consideration.

Despite the huge potential of these polymers shown *in vitro*, there is still a long way to go in order to evaluate their safety and efficiency *in vivo*. Therefore, more effort needs to be devoted to develop proper infectious animal disease model and clinical trials for evaluation of molecular distribution, efficiency and toxicity of these polymers. These models can closely mimic the pathological environments in human body and provide accurate prediction in using novel antimicrobial polymers. Furthermore, the exact mechanism of antimicrobial activity of these polymers remains unclear, more research

need to be done to explore the mechanism behind and hopefully shed light on the development of antimicrobial polymers for targeted microorganisms.

In hydrogel for antimicrobial applications, although potential and advantages of hydrogels with cationic polycarbonate polymer incorporated has been shown in Chapter 4, it is critical to evaluate how formulating polymers interact with and affect the efficiency of incorporated therapeutics such as antibiotics, AMP and polymers in the scaffold. This can be done by monitoring MIC level of antibiotics in the presence/absence of scaffold exponents. Moreover, currently no hydrogel system has been tested to be used in clinic due to compatibility of the polymer systems. Thus *in vivo* studies are urgently needed to test the hydrogel stability and more importantly, toxicity.

In conclusion, finding of this thesis have effectively supported that PEG hydrogel scaffolds can be rationally designed for both tissue engineering and antimicrobial therapeutics. Pending proper material designing, advanced development of biological science and successful modification of the hydrogel scaffolds may intensely facilitate the widespread use of hydrogel scaffolds in various biomedical applications.

REFERENCES

[1] Farris S, Schaich KM, Liu LS, Piergiovanni L, Yam KL. Development of polyion-complex hydrogels as an alternative approach for the production of bio-based polymers for food packaging applications: a review. Trends in food science & technology. 2009;20:316-32.

[2] Kozlovskaya V, Kharlampieva E, Mansfield ML, Sukhishvili SA. Poly (methacrylic acid) hydrogel films and capsules: Response to pH and ionic strength, and encapsulation of macromolecules. Chemistry of materials. 2006;18:328-36.

[3] Nagaoka S, Nakao A. Clinical application of antithrombogenic hydrogel with long poly (ethylene oxide) chains. Biomaterials. 1990;11:119-21.

[4] Li W, Zhao H, Teasdale P, John R, Zhang S. Synthesis and characterisation of a polyacrylamide–polyacrylic acid copolymer hydrogel for environmental analysis of Cu and Cd. Reactive and Functional Polymers. 2002;52:31-41.

[5] Chung C, Burdick JA. Influence of three-dimensional hyaluronic acid microenvironments on mesenchymal stem cell chondrogenesis. Tissue Eng Part A. 2008;15:243-54.

[6] Liu Y, Cai S, Shu XZ, Shelby J, Prestwich GD. Release of basic fibroblast growth factor from a crosslinked glycosaminoglycan hydrogel promotes wound healing. Wound Repair Regen. 2007;15:245-51.

[7] Hubbell JA. Biomaterials in tissue engineering. Nature Biotechnology. 1995;13:565-76.

[8] Smidsrød O, Skjaok-Brk G. Alginate as immobilization matrix for cells. Trends in biotechnology. 1990;8:71-8.

[9] Francis Suh JK, Matthew HWT. Application of chitosan-based polysaccharide biomaterials in cartilage tissue engineering: a review. Biomaterials. 2000;21:2589-98.

[10] Bosnakovski D, Mizuno M, Kim G, Takagi S, Okumura M, Fujinaga T. Chondrogenic differentiation of bovine bone marrow mesenchymal stem cells (MSCs) in different hydrogels: influence of collagen type II extracellular matrix on MSC chondrogenesis. Biotechnology and Bioengineering. 2006;93:1152-63.

[11] Brännvall K, Bergman K, Wallenquist U, Svahn S, Bowden T, Hilborn J, et al. Enhanced neuronal differentiation in a three‐dimensional collagen‐hyaluronan matrix. Journal of neuroscience research. 2007;85:2138-46.

[12] Lee HJ, Lee JS, Chansakul T, Yu C, Elisseeff JH, Yu SM. Collagen mimetic peptide-conjugated photopolymerizable PEG hydrogel. Biomaterials. 2006;27:5268-76.

[13] Benoit DSW, Durney AR, Anseth KS. Manipulations in hydrogel degradation behavior enhance osteoblast function and mineralized tissue formation. Tissue Eng. 2006;12:1663-73.

[14] Liu SQ, Rachel Ee PL, Ke CY, Hedrick JL, Yang YY. Biodegradable poly (ethylene glycol)–peptide hydrogels with well-defined structure and properties for cell delivery. Biomaterials. 2009;30:1453-61.

[15] Wang Q, Wang J, Lu Q, Detamore MS, Berkland C. Injectable PLGA based colloidal gels for zero-order dexamethasone release in cranial defects. Biomaterials. 2010;31:4980-6.

[16] Kuo SM, Liou CC, Chang SJ, Wang YJ. Synthesis and characterizations of hydrogel based on PVA-AE and HEMA. Journal of Polymer Research. 2001;8:169-74.
[17] Lin CC, Anseth KS. PEG hydrogels for the controlled release of biomolecules in regenerative medicine. Pharm Res. 2009;26:631-43.
[18] Peppas NA, Hilt JZ, Khademhosseini A, Langer R. Hydrogels in biology and medicine: from molecular principles to bionanotechnology. Adv Mater. 2006;18:1345-60.
[19] West JL, Hubbell JA. Polymeric biomaterials with degradation sites for proteases involved in cell migration. Macromolecules. 1999;32:241-4.
[20] Bryant SJ, Anseth KS. The effects of scaffold thickness on tissue engineered cartilage in photocrosslinked poly (ethylene oxide) hydrogels. Biomaterials. 2001;22:619-26.
[21] Peppas NA. Hydrogels and drug delivery. Current opinion in colloid & interface science. 1997;2:531-7.
[22] Nuttelman CR, Tripodi MC, Anseth KS. Synthetic hydrogel niches that promote hMSC viability. Matrix biology. 2005;24:208-18.
[23] Lutolf MP, Weber FE, Schmoekel HG, Schense JC, Kohler T, Muller R, et al. Repair of bone defects using synthetic mimetics of collagenous extracellular matrices. Nature Biotechnology. 2003;21:513-8.
[24] Kraehenbuehl TP, Zammaretti P, Van der Vlies AJ, Schoenmakers RG, Lutolf MP, Jaconi ME, et al. Three-dimensional extracellular matrix-directed cardioprogenitor differentiation: systematic modulation of a synthetic cell-responsive PEG-hydrogel. Biomaterials. 2008;29:2757-66.
[25] Hoffman AS. Hydrogels for biomedical applications. Adv Drug Deliv Rev. 2002;54:3-12.
[26] Percec V, Bera TK, Butera RJ. A new strategy for the preparation of supramolecular neutral hydrogels. Biomacromolecules. 2002;3:272-9.
[27] Takamura A, Ishii F, Hidaka H. Drug release from poly (vinyl alcohol) gel prepared by freeze-thaw procedure. Journal of Controlled Release. 1992;20:21-7.
[28] Hubbell JA. Hydrogel systems for barriers and local drug delivery in the control of wound healing. Journal of Controlled Release. 1996;39:305-13.
[29] Panda P, Ali S, Lo E, Chung BG, Hatton TA, Khademhosseini A, et al. Stop-flow lithography to generate cell-laden microgel particles. Lab on a Chip. 2008;8:1056-61.
[30] Kloxin AM, Kasko AM, Salinas CN, Anseth KS. Photodegradable hydrogels for dynamic tuning of physical and chemical properties. Science. 2009;324:59-63.
[31] Noro A, Yamagishi H, Matsushita Y. Thermoreversible morphology transition from block-type supramacromolecules via hydrogen bonding in an ionic liquid. Macromolecules. 2009;42:6335-8.
[32] Lutolf MP, Hubbell JA. Synthesis and physicochemical characterization of end-linked poly(ethylene glycol)-co-peptide hydrogels formed by Michael-type addition. Biomacromolecules. 2003;4:713-22.
[33] Hiemstra C, van der Aa LJ, Zhong Z, Dijkstra PJ, Feijen J. Rapidly in situ-forming degradable hydrogels from dextran thiols through Michael addition. Biomacromolecules. 2007;8:1548-56.
[34] Zheng Shu X, Liu Y, Palumbo FS, Luo Y, Prestwich GD. In situ crosslinkable hyaluronan hydrogels for tissue engineering. Biomaterials. 2004;25:1339-48.

[35] Liu SQ, Ee PLR, Ke CY, Hedrick JL, Yang YY. Biodegradable poly(ethylene glycol)-peptide hydrogels with well-defined structure and properties for cell delivery. Biomaterials. 2009;30:1453-61.
[36] Lutolf M, Hubbell J. Synthesis and physicochemical characterization of end-linked poly (ethylene glycol)-co-peptide hydrogels formed by Michael-type addition. Biomacromolecules. 2003;4:713-22.
[37] Park J, Lim E, Back S, Na H, Park Y, Sun K. Nerve regeneration following spinal cord injury using matrix metalloproteinase‐sensitive, hyaluronic acid‐based biomimetic hydrogel scaffold containing brain‐derived neurotrophic factor. J Biomed Mater Res Part A. 2010;93:1091-9.
[38] Chung EH, Gilbert M, Virdi AS, Sena K, Sumner DR, Healy KE. Biomimetic artificial ECMs stimulate bone regeneration. J Biomed Mater Res Part A. 2006;79:815-26.
[39] Burdick JA, Anseth KS. Photoencapsulation of osteoblasts in injectable RGD-modified PEG hydrogels for bone tissue engineering. Biomaterials. 2002;23:4315-23.
[40] Hodde JP, Patel UH. Medical Composition Including an Extracellular Matrix Particulate. Google Patents; 2010.
[41] Metters A, Anseth K, Bowman C. Fundamental studies of a novel, biodegradable PEG-b-PLA hydrogel. Polymer. 2000;41:3993-4004.
[42] Vårum KM, Kristiansen Holme H, Izume M, Torger Stokke B, Smidsrød O. Determination of enzymatic hydrolysis specificity of partially N-acetylated chitosans. Biochimica et Biophysica Acta (BBA)-General Subjects. 1996;1291:5-15.
[43] LeRoux MA, Guilak F, Setton LA. Compressive and shear properties of alginate gel: effects of sodium ions and alginate concentration. Journal of Biomedical Materials Research. 1999;47:46-53.
[44] Suggs LJ, Mikos AG. Development of poly (propylene fumarate-co-ethylene glycol) as an injectable carrier for endothelial cells. Cell transplantation. 1999;8:345.
[45] Saito N, Okada T, Horiuchi H, Murakami N, Takahashi J, Nawata M, et al. A biodegradable polymer as a cytokine delivery system for inducing bone formation. Nature Biotechnology. 2001;19:332-5.
[46] Wichterle O, Lim D. Hydrophilic gels for biological use. Nature. 1960;185:117-8.
[47] DeForest CA, Anseth KS. Advances in Bioactive Hydrogels to Probe and Direct Cell Fate. Annual Review of Chemical and Biomolecular Engineering. 2012;3:421-44.
[48] Lai KK, Fontecchio SA. Use of silver-hydrogel urinary catheters on the incidence of catheter-associated urinary tract infections in hospitalized patients. American Journal of Infection Control. 2002;30:221-5.
[49] Adams TST, Crook T, Cadier MAM. A late complication following the insertion of hydrogel breast implants. Journal of plastic, reconstructive & aesthetic surgery. 2007;60:210-2.
[50] Kim B, Peppas NA. Poly (ethylene glycol)-containing hydrogels for oral protein delivery applications. Biomedical Microdevices. 2003;5:333-41.
[51] Marklein RA, Burdick JA. Controlling stem cell fate with material design. Adv Mater. 2010;22:175-89.
[52] Kirker KR, Luo Y, Nielson JH, Shelby J, Prestwich GD. Glycosaminoglycan hydrogel films as bio-interactive dressings for wound healing. Biomaterials. 2002;23:3661-71.

[53] Riley SL, Dutt S, de la Torre R, Chen AC, Sah RL, Ratcliffe A. Formulation of PEG-based hydrogels affects tissue-engineered cartilage construct characteristics. Journal of Materials Science: Materials in Medicine. 2001;12:983-90.
[54] Langer R. Perspectives and challenges in tissue engineering and regenerative medicine. Adv Mater. 2009;21:3235-6.
[55] Hubbell JA. Morphogen and material engineering in regenerative medicine. Wound Repair Regen. 2010;18:A72-A72.
[56] Murry CE, Keller G. Differentiation of embryonic stem cells to clinically relevant populations: lessons from embryonic development. Cell. 2008;132:661-80.
[57] Takahashi K, Yamanaka S. Induction of pluripotent stem cells from mouse embryonic and adult fibroblast cultures by defined factors. Cell. 2006;126:663-76.
[58] Giannios J, Delis S, Alexandropulos N. Use of induced pluripotent stem cells (IPSC) encoded with anti-grp78 shrna induces apoptosis/type i pcd after a gene-silencing bystander effect for circumvention of vinorelbine-induced angiogenesis, and inhibition of metastatic spread in advanced gist. Gut. 2011;60:A110-A110.
[59] Pittenger MF. Multilineage potential of adult human mesenchymal stem cells. Science. 1999;284:143-7.
[60] Toma C, Pittenger MF, Cahill KS, Byrne BJ, Kessler PD. Human mesenchymal stem cells differentiate to a cardiomyocyte phenotype in the adult murine heart. Circulation. 2002;105:93-8.
[61] Sila-Asna M, Bunyaratvej A, Maeda S, Kitaguchi H, Bunyaratavej N. Osteoblast differentiation and bone formation gene expression in strontium-inducing bone marrow mesenchymal stem cell. Kobe J Med Sci. 2007;53:25-35.
[62] Heng BC, Cao T, Lee EH. Directing stem cell differentiation into the chondrogenic lineage in vitro. Stem Cells. 2004;22:1152-67.
[63] Chen FH, Tuan RS. Mesenchymal stem cells in arthritic diseases. Arthritis Research & Therapy. 2008;10:223-34.
[64] Cushing MC, Anseth KS. Hydrogel cell cultures. Science. 2007;316:1133-4.
[65] Chang CW, van Spreeuwel A, Zhang C, Varghese S. PEG/clay nanocomposite hydrogel: a mechanically robust tissue engineering scaffold. Soft Matter.6:5157-64.
[66] Kim BS, Choi JS, Kim JD, Yeo TY, Cho Y. Improvement of Stem Cell Viability in Hyaluronic Acid Hydrogels Using Dextran Microspheres. J Biomater Sci-Polym Ed.21:1701-11.
[67] Sun XD, Jeng L, Bolliet C, Olsen BR, Spector M. Non-viral endostatin plasmid transfection of mesenchymal stem cells via collagen scaffolds. Biomaterials. 2009;30:1222-31.
[68] Veronese FM, Monfardini C, Caliceti P, Schiavon O, Scrawen MD, Beer D. Improvement of pharmacokinetic, immunological and stability properties of asparaginase by conjugation to linear and branched monomethoxy poly(ethylene glycol). J Control Release 1996;40:199-209.
[69] Bryant SJ, Anseth KS. Controlling the spatial distribution of ECM components in degradable PEG hydrogels for tissue engineering cartilage. J Biomed Mater Res A 2003;64A:70-9.
[70] Shin H, Ruhe PQ, Mikos AG, Jansen JA. In vivo bone and soft tissue response to injectable, biodegradable oligo(poly(ethylene glycol) fumarate) hydrogels. Biomaterials. 2003;24:3201-11.

[71] Hern DL, Hubbell JA. Incorporation of adhesion peptides into nonadhesive hydrogels useful for tissue resurfacing. Journal of Biomedical Materials Research. 1998;39:266-76.
[72] Nair LS, Laurencin CT. Biodegradable polymers as biomaterials. Progress in Polymer Science. 2007;32:762-98.
[73] Yoon JJ, Chung HJ, Park TG. Photo-crosslinkable and biodegradable pluronic/heparin hydrogels for local and sustained delivery of angiogenic growth factor. J Biomed Mater Res A. 2007;83A:597-605.
[74] Liu SQ, Tian QA, Wang L, Hedrick JL, Hui JHP, Yang YY, et al. Injectable biodegradable poly(ethylene glycol)/RGD peptide hybrid hydrogels for in vitro chondrogenesis of human mesenchymal stem cells. Macromol Rapid Commun. 2010;31:1148-54.
[75] Lei YG, Segura T. DNA delivery from matrix metal lop roteinase degradable poly(ethylene glycol) hydrogels to mouse cloned mesenchymal stem cells. Biomaterials. 2009;30:254-65.
[76] Smith IO, Liu XH, Smith LA, Ma PX. Nanostructured polymer scaffolds for tissue engineering and regenerative medicine. Wiley Interdiscip Rev-Nanomed Nanobiotechnol. 2009;1:226-36.
[77] Murakami Y, Yokoyama M, Okano T, Nishida H, Tomizawa Y, Endo M, et al. A novel synthetic tissue-adhesive hydrogel using a crosslinkable polymeric micelle. J Biomed Mater Res Part A. 2007;80A:421-7.
[78] Hwang NS, Varghese S, Elisseeff J. Derivation of chondrogenically-committed cells from human embryonic cells for cartilage tissue regeneration. Plos One. 2008;3.
[79] Minina E, Wenzel HM, Kreschel C, Karp S, Gaffield W, McMahon AP, et al. BMP and Ihh/PTHrP signaling interact to coordinate chondrocyte proliferation and differentiation. Development. 2001;128:4523-34.
[80] Day TF, Guo XZ, Garrett-Beal L, Yang YZ. Wnt/beta-catenin signaling in mesenchymal progenitors controls osteoblast and chondrocyte differentiation during vertebrate skeletogenesis. Developmental Cell. 2005;8:739-50.
[81] Ichinose S, Tagami M, Muneta T, Sekiya I. Morphological examination during in vitro cartilage formation by human mesenchymal stem cells. Cell and Tissue Research. 2005;322:217-26.
[82] Kamiya N, Watanabe H, Habuchi H, Takagi H, Shinomura T, Shimizu K, et al. Versican/PG-M regulates chondrogenesis as an extracellular matrix molecule crucial for mesenchymal condensation. Journal of Biological Chemistry. 2006;281:2390-400.
[83] Park JS, Woo DG, Yang HN, Lim HJ, Park KM, Na K, et al. Chondrogenesis of human mesenchymal stem cells encapsulated in a hydrogel construct: Neocartilage formation in animal models as both mice and rabbits. J Biomed Mater Res Part A. 2010;92A:988-96.
[84] Shen BJ, Wei AQ, Tao HL, Diwan AD, Ma DDF. BMP-2 enhances TGF-beta 3-mediated chondrogenic differentiation of human bone marrow multipotent mesenchymal stromal cells in alginate bead culture. Tissue Eng Part A. 2009;15:1311-20.
[85] Mehlhorn AT, Schmal H, Kaiser S, Lepski G, Finkenzeller G, Stark GB, et al. Mesenchymal stem cells maintain TGF-beta-mediated chondrogenic phenotype in alginate bead culture. Tissue Eng. 2006;12:1393-403.

[86] Trippel SB, Ghivizzani SC, Nixon AJ. Gene-based approaches for the repair of articular cartilage. Gene Ther. 2004;11:351-9.
[87] Yao YC, Zhang F, Zhou RJ, Su K, Fan JB, Wang DA. Effects of combinational adenoviral vector-Mediated TGF beta 3 transgene and shRNA silencing type I collagen on articular chondrogenesis of synovium-derived mesenchymal stem cells. Biotechnology and Bioengineering. 2010;106:818-28.
[88] Thomas CE, Ehrhardt A, Kay MA. Progress and problems with the use of viral vectors for gene therapy. Nat Rev Genet. 2003;4:346-58.
[89] Wang Y, Ke CY, Beh CW, Liu SQ, Goh SH, Yang YY. The self-assembly of biodegradable cationic polymer micelles as vectors for gene transfection. Biomaterials. 2007;28:5358-68.
[90] Bardi G, Malvindi MA, Gherardini L, Costa M, Pompa PP, Cingolani R, et al. The biocompatibility of amino functionalized CdSe/ZnS quantum-dot-Doped SiO2 nanoparticles with primary neural cells and their gene carrying performance. Biomaterials.31:6555-66.
[91] Krajcik R, Jung A, Hirsch A, Neuhuber W, Zolk O. Functionalization of carbon nanotubes enables non-covalent binding and intracellular delivery of small interfering RNA for efficient knock-down of genes. Biochem Biophys Res Commun. 2008;369:595-602.
[92] Gristina AG. Biomaterial-centered infection: microbial adhesion versus tissue integration. Science. 1987;237:1588-95.
[93] Schierholz J, Beuth J. Implant infections: a haven for opportunistic bacteria. Journal of Hospital Infection. 2001;49:87-93.
[94] Trampuz A, Widmer AF. Infections associated with orthopedic implants. Current opinion in infectious diseases. 2006;19:349.
[95] An Y, Alvi F, Kang Q, Laberge M, Drews M, Zhang J, et al. Effects of sterilization on implant mechanical property and biocompatibility. The International journal of artificial organs. 2005;28:1126.
[96] Ligon BL. Penicillin: its discovery and early development. Elsevier; 2004. 15:52-7.
[97] Gilbert P, Collier PJ, Brown M. Influence of growth rate on susceptibility to antimicrobial agents: biofilms, cell cycle, dormancy, and stringent response. Antimicrobial agents and chemotherapy. 1990;34:1865-8.
[98] Silver L, Bostian K. Discovery and development of new antibiotics: the problem of antibiotic resistance. Antimicrobial agents and chemotherapy. 1993;37:377-83.
[99] Levy SB. The challenge of antibiotic resistance. Scientific American. 1998;278:32-9.
[100] Whitney CG, Farley MM, Hadler J, Harrison LH, Lexau C, Reingold A, et al. Increasing prevalence of multidrug-resistant Streptococcus pneumoniae in the United States. New England Journal of Medicine. 2000;343:1917-24.
[101] Steiner H, Hultmark D, Engström Å, Bennich H, Boman H. Sequence and specificity of two antibacterial proteins involved in insect immunity. Nature. 1981;292:246-8.
[102] Wang Z, Wang G. APD: the antimicrobial peptide database. Nucleic Acids Research. 2004;32:D590-D2.
[103] Zasloff M. Antimicrobial peptides of multicellular organisms. Nature. 2002;415:389-95.

[104] Wiradharma N, Khoe U, Hauser CAE, Seow SV, Zhang S, Yang YY. Synthetic cationic amphiphilic α-helical peptides as antimicrobial agents. Biomaterials. 2011;32:2204-12.
[105] Devine DA, Hancock REW. Cationic peptides: distribution and mechanisms of resistance. Current pharmaceutical design. 2002;8:703-14.
[106] Tew GN, Liu D, Chen B, Doerksen RJ, Kaplan J, Carroll PJ, et al. De novo design of biomimetic antimicrobial polymers. Proceedings of the National Academy of Sciences. 2002;99:5110-4.
[107] Kenawy ER, Worley S, Broughton R. The chemistry and applications of antimicrobial polymers: a state-of-the-art review. Biomacromolecules. 2007;8:1359-84.
[108] Engler AC, Wiradharma N, Ong ZY, Coady DJ, Hedrick JL, Yang YY. Emerging trends in macromolecular antimicrobials to fight multi-drug-resistant infections. Nano Today. 2012;7:201-22.
[109] Gabriel GJ, Maegerlein JA, Nelson CF, Dabkowski JM, Eren T, Nüsslein K, et al. Comparison of facially amphiphilic versus segregated monomers in the design of antibacterial copolymers. Chemistry-A European Journal. 2009;15:433-9.
[110] Zhou C, Qi X, Li P, Chen WN, Mouad L, Chang MW, et al. High potency and broad-spectrum antimicrobial peptides synthesized via ring-opening polymerization of α-aminoacid-N-carboxyanhydrides. Biomacromolecules. 2009;11:60-7.
[111] Kuroda K, Caputo GA, DeGrado WF. The role of hydrophobicity in the antimicrobial and hemolytic activities of polymethacrylate derivatives. Chemistry-A European Journal. 2009;15:1123-33.
[112] Liu L, Xu K, Wang H, Tan PKJ, Fan W, Venkatraman SS, et al. Self-assembled cationic peptide nanoparticles as an efficient antimicrobial agent. Nat Nanotechnol. 2009;4:457-63.
[113] Demerec M. Origin of bacterial resistance to antibiotics. Journal of Bacteriology. 1948;56:63-74.
[114] Gonzalez M, Bischofberger M, Pernot L, Van Der Goot F, Freche B. Bacterial pore-forming toxins: the (w) hole story? Cellular and molecular life sciences. 2008;65:493-507.
[115] Wimley WC. Describing the mechanism of antimicrobial peptide action with the interfacial activity model. ACS chemical biology. 2010;5:905-17.
[116] Qian S, Wang W, Yang L, Huang HW. Structure of transmembrane pore induced by Bax-derived peptide: evidence for lipidic pores. Proceedings of the National Academy of Sciences. 2008;105:17379-83.
[117] Gazit E, Miller IR, Biggin PC, Sansom MSP, Shai Y. Structure and orientation of the mammalian antibacterial peptide cecropin P1 within phospholipid membranes. Journal of molecular biology. 1996;258:860-70.
[118] Hosaka S, Ozawa H, Tanzawa H, Kinitomo T, Nichols RL. In vivo evaluation of ocular inserts of hydrogel impregnated with antibiotics fop trachoma therapy. Biomaterials. 1983;4:243-8.
[119] Pugach JL, DiTIZIO V, MITTELMAN MW, BRUCE AW, DiCOSMO F, Khoury AE. Antibiotic hydrogel coated Foley catheters for prevention of urinary tract infection in a rabbit model. The Journal of urology. 1999;162:883-7.
[120] Wu P, Grainger DW. Drug/device combinations for local drug therapies and infection prophylaxis. Biomaterials. 2006;27:2450-67.

[121] Yu H, Xu X, Chen X, Lu T, Zhang P, Jing X. Preparation and antibacterial effects of PVA‐PVP hydrogels containing silver nanoparticles. Journal of applied polymer science. 2007;103:125-33.
[122] Masters KSB, Leibovich SJ, Belem P, West JL, Poole‐Warren LA. Effects of nitric oxide releasing poly (vinyl alcohol) hydrogel dressings on dermal wound healing in diabetic mice. Wound Repair Regen. 2002;10:286-94.
[123] Salick DA, Kretsinger JK, Pochan DJ, Schneider JP. Inherent antibacterial activity of a peptide-based β-hairpin hydrogel. Journal of the American Chemical Society. 2007;129:14793-9.
[124] Salick DA, Pochan DJ, Schneider JP. Design of an Injectable β‐Hairpin Peptide Hydrogel That Kills Methicillin‐Resistant Staphylococcus aureus. Adv Mater. 2009;21:4120-3.
[125] Tsao CT, Chang CH, Lin YY, Wu MF, Wang JL, Han JL, et al. Antibacterial activity and biocompatibility of a chitosan–γ-poly (glutamic acid) polyelectrolyte complex hydrogel. Carbohydrate Research. 2010;345:1774-80.
[126] Li P, Poon YF, Li W, Zhu HY, Yeap SH, Cao Y, et al. A polycationic antimicrobial and biocompatible hydrogel with microbe membrane suctioning ability. Nat Mater. 2010;10:149-56.
[127] Watnick P, Kolter R. Biofilm, City of Microbes. J Bacteriol. 2000;182:2675-9.
[128] Costerton JW, Montanaro L, Arciola CR. Bacterial communications in implant infections: a target for an intelligence war. The International journal of artificial organs. 2007;30:757-63.
[129] Gristina A. Biomaterial-centered infection: microbial adhesion versus tissue integration. Science. 1987;237:1588-95.
[130] Neut D, van de Belt H, Stokroos I, van Horn JR, van der Mei HC, Busscher HJ. Biomaterial-associated infection of gentamicin-loaded PMMA beads in orthopaedic revision surgery. J Antimicrob Chemother. 2001;47:885-91.
[131] Neut D, van Horn JR, van Kooten TG, van der Mei HC, Busscher HJ. Detection of Biomaterial-Associated Infections in Orthopaedic Joint Implants. Clinical Orthopaedics and Related Research. 2003;413:261-8
[132] Gottenbos B, Grijpma DW, van der Mei HC, Feijen J, Busscher HJ. Antimicrobial effects of positively charged surfaces on adhering Gram-positive and Gram-negative bacteria. J Antimicrob Chemother. 2001;48:7-13.
[133] Cheng G, Xue H, Zhang Z, Chen S, Jiang S. A Switchable Biocompatible Polymer Surface with Self-Sterilizing and Nonfouling Capabilities. Angew Chem Int Ed. 2008;47:8831-4.
[134] Rhoads DD, Wolcott RD, Percival SL. Biofilms in wounds: management strategies. J Wound Care. 2008;17:502-8.
[135] Ward K, Olson M, Lam K, Costerton J. Mechanism of persistent infection associated with peritoneal implants. Journal of medical microbiology. 1992;36:406-13.
[136] Nickel J, Ruseska I, Wright J, Costerton J. Tobramycin resistance of Pseudomonas aeruginosa cells growing as a biofilm on urinary catheter material. Antimicrobial agents and chemotherapy. 1985;27:619-24.
[137] Stewart PS, William Costerton J. Antibiotic resistance of bacteria in biofilms. The Lancet. 2001;358:135-8.

[138] Stewart PS. Mechanisms of antibiotic resistance in bacterial biofilms. International journal of medical microbiology. 2002;292:107-13.
[139] BROWN MRW, ALLISON DG, GILBERT P. Resistance of bacterial biofilms to antibiotics a growth-rate related effect? Journal of Antimicrobial Chemotherapy. 1988;22:777-80.
[140] Costerton JW, Lewandowski Z, Caldwell DE, Korber DR, Lappin-Scott HM. Microbial biofilms. Annual Reviews in Microbiology. 1995;49:711-45.
[141] Stoodley P, Sauer K, Davies D, Costerton J. Biofilms as complex differentiated communities. Annual Reviews in Microbiology. 2002;56:187-209.
[142] Chang CW, van Spreeuwel A, Zhang C, Varghese S. PEG/clay nanocomposite hydrogel: a mechanically robust tissue engineering scaffold. Soft Matter. 2010;6:5157-64.
[143] Dvir T, Timko BP, Kohane DS, Langer R. Nanotechnological strategies for engineering complex tissues. Nat Nanotechnol. 2011;6:13-22.
[144] Kolambkar YM, Dupont KM, Boerckel JD, Huebsch N, Mooney DJ, Hutmacher DW, et al. An alginate-based hybrid system for growth factor delivery in the functional repair of large bone defects. Biomaterials. 2011;32:65-74.
[145] Kisiday J, Jin M, Kurz B, Hung H, Semino C, Zhang S, et al. Self-assembling peptide hydrogel fosters chondrocyte extracellular matrix production and cell division: Implications for cartilage tissue repair. Proc Natl Acad Sci U S A. 2002;99:9996-10001.
[146] Frisman I, Seliktar D, Bianco-Peled H. Nanostructuring of PEG-fibrinogen polymeric scaffolds. Acta Biomater. 2009;6:2518-24.
[147] Liu SQ, Tian Q, Wang L, Hedrick JL, Hui JHP, Yang YY, et al. Injectable biodegradable poly (ethylene glycol)/RGD peptide hybrid hydrogels for in vitro chondrogenesis of human mesenchymal stem cells. Macromol Rapid Commun. 2010;31:1148-54.
[148] Riessen R, Rahimizadeh H, Blessing E, Takeshita S, Barry JJ, Isner JM. Arterial gene transfer using pure DNA applied directly to a hydrogel-coated angioplasty balloon. Human gene therapy. 1993;4:749-58.
[149] Merdan T, Kopeček J, Kissel T. Prospects for cationic polymers in gene and oligonucleotide therapy against cancer. Adv Drug Deliv Rev. 2002;54:715-58.
[150] Trentin D, Hall H, Wechsler S, Hubbell JA. Peptide-matrix-mediated gene transfer of an oxygen-insensitive hypoxia-inducible factor-1 alpha variant for local induction of angiogenesis. Proc Natl Acad Sci U S A. 2006;103:2506-11.
[151] Lei P, Padmashali RM, Andreadis ST. Cell-controlled and spatially arrayed gene delivery from fibrin hydrogels. Biomaterials. 2009;30:3790-9.
[152] Trentin D, Hubbell J, Hall H. Non-viral gene delivery for local and controlled DNA release. J Control Release. 2005;102:263-75.
[153] Khan M, Ang CY, Wiradharma N, Yong LK, Liu S, Liu L, et al. Diaminododecane-based cationic bolaamphiphile as a non-viral gene delivery carrier. Biomaterials. 2012;33:4673–80.
[154] Pratt RC, Nederberg F, Waymouth RM, Hedrick JL. Tagging alcohols with cyclic carbonate: a versatile equivalent of (meth)acrylate for ring-opening polymerization. Chem Commun. 2008:114-6.
[155] Astafieva I, Zhong XF, Eisenberg A. Critical micellization phenomena in block polyelectrolyte solutions. Macromolecules. 1993;26:7339-52.

[156] Stevens MM, George JH. Exploring and engineering the cell surface interface. Science. 2005;310:1135-8.
[157] Deshmukh M, Singh Y, Gunaseelan S, Gao DY, Stein S, Sinko PJ. Biodegradable poly(ethylene glycol) hydrogels based on a self-elimination degradation mechanism. Biomaterials. 2010;31:6675-84.
[158] Dikovsky D, Bianco-Peled H, Seliktar D. The effect of structural alterations of PEG-fibrinogen hydrogel scaffolds on 3-D cellular morphology and cellular migration. Biomaterials. 2006;27:1496-506.
[159] Dadsetan M, Hefferan TE, Szatkowski JP, Mishra PK, Macura SI, Lu L, et al. Effect of hydrogel porosity on marrow stromal cell phenotypic expression. Biomaterials. 2008;29:2193-202.
[160] Webb DJ, Horwitz AF. New dimensions in cell migration. NATURE CELL BIOLOGY. 2003;5:690-2.
[161] Khan M, Ang CY, Wiradharma N, Yong LK, Liu S, Liu L, et al. Diaminododecane-based cationic bolaamphiphile as a non-viral gene delivery carrier. Biomaterials. 2012;33:4673-80.
[162] Fischer D, Bieber T, Li Y, Elsässer HP, Kissel T. A novel non-viral vector for DNA delivery based on low molecular weight, branched polyethylenimine: effect of molecular weight on transfection efficiency and cytotoxicity. Pharm Res. 1999;16:1273-9.
[163] Wieland JA, Houchin-Ray TL, Shea LD. Non-viral vector delivery from PEG-hyaluronic acid hydrogels. J Control Release. 2007;120:233-41.
[164] Xie YB, Yang ST, Kniss DA. Three-dimensional cell-scaffold constructs promote efficient gene transfection: implications for cell-based gene therapy. Tissue Eng. 2001;7:585-98.
[165] Merdan T, Kopecek J, Kissel T. Prospects for cationic polymers in gene and oligonucleotide therapy against cancer. Adv Drug Deliv Rev. 2002;54:715-58.
[166] Fischer D, Li YX, Ahlemeyer B, Krieglstein J, Kissel T. In vitro cytotoxicity testing of polycations: influence of polymer structure on cell viability and hemolysis. Biomaterials. 2003;24:1121-31.
[167] Health CDoP. Methicillin-Resistant Staphylococcus aureus (MRSA). 2010.
[168] Taubes G. The bacteria fight back. Science. 2008;321:356-61.
[169] Davies J, Davies D. Origins and evolution of antibiotic resistance. Microbiology and Molecular Biology Reviews. 2010;74:417-33.
[170] Klevens RM, Edwards JR, Richards CL, Horan TC, Gaynes RP, Pollock DA, et al. Estimating health care-associated infections and deaths in US hospitals, 2002. Public Health Reports. 2007;122:160-6.
[171] Costerton JW, Montanaro L, Arciola CR. Bacterial communications in implant infections: a target for an intelligence war. Int J Artif Organs. 2007;30:757-63.
[172] Lewis K. Multidrug tolerance of biofilms and persister cells. Curr Top Microbiol Immunol. 2008;322:107-31.
[173] Kharidia R, Liang JF. The activity of a small lytic peptide PTP-7 on Staphylococcus aureus biofilms. J Microbiol. 2011;49:663-8.
[174] Steiner H, Hultmark D, Engstrom A, Bennich H, Boman HG. Sequence and specificity of two antibacterial proteins involved in insect immunity. Nature. 1981;292:246-8.

[175] Wang Z, Wang G. APD: the Antimicrobial Peptide Database. Nucleic Acids Res. 2004;32:D590-2.
[176] Liu L, Xu K, Wang H, Tan PK, Fan W, Venkatraman SS, et al. Self-assembled cationic peptide nanoparticles as an efficient antimicrobial agent. Nat Nanotechnol. 2009;4:457-63.
[177] Fjell CD, Hiss JA, Hancock REW, Schneider G. Designing antimicrobial peptides: form follows function. Nat Rev Drug Discov. 2012;11:37-51.
[178] Gabriel GJ, Som A, Madkour AE, Eren T, Tew GN. Infectious Disease: Connecting Innate Immunity to Biocidal Polymers. Materials Science and Engineering: R: Reports. 2007;57:28-64.
[179] Palermo E, Kuroda K. Structural determinants of antimicrobial activity in polymers which mimic host defense peptides. Appl Microbiol Biotechnol. 2010;87:1605-15.
[180] Li P, Poon YF, Li W, Zhu HY, Yeap SH, Cao Y, et al. A polycationic antimicrobial and biocompatible hydrogel with microbe membrane suctioning ability. Nat Mater. 2011;10:149-56.
[181] Zhou C, Li P, Qi X, Sharif AR, Poon YF, Cao Y, et al. A photopolymerized antimicrobial hydrogel coating derived from epsilon-poly-L-lysine. Biomaterials. 2011;32:2704-12.
[182] Tsao CT, Chang CH, Lin YY, Wu MF, Wang JL, Han JL, et al. Antibacterial activity and biocompatibility of a chitosan-gamma-poly(glutamic acid) polyelectrolyte complex hydrogel. Carbohydr Res. 2010;345:1774-80.
[183] Salick DA, Kretsinger JK, Pochan DJ, Schneider JP. Inherent antibacterial activity of a peptide-based beta-hairpin hydrogel. J Am Chem Soc. 2007;129:14793-9.
[184] Jeong B, Bae YH, Lee DS, Kim SW. Biodegradable block copolymers as injectable drug-delivery systems. Nature. 1997;388:860-2.
[185] Hiemstra C, Zhong Z, Li L, Dijkstra PJ, Feijen J. In-Situ Formation of Biodegradable Hydrogels by Stereocomplexation of PEG−(PLLA)8 and PEG−(PDLA)8 Star Block Copolymers. Biomacromolecules. 2006;7:2790-5.
[186] Kim SH, Tan JPK, Fukushima K, Nederberg F, Yang YY, Waymouth RM, et al. Thermoresponsive nanostructured polycarbonate block copolymers as biodegradable therapeutic delivery carriers. Biomaterials. 2011;32:5505-14.
[187] Lee Y, Fukushima S, Bae Y, Hiki S, Ishii T, Kataoka K. A Protein Nanocarrier from Charge-Conversion Polymer in Response to Endosomal pH. J Am Chem Soc. 2007;129:5362-3.
[188] Hales M, Barner-Kowollik C, Davis TP, Stenzel MH. Shell-Cross-Linked Vesicles Synthesized from Block Copolymers of Poly(d,l-lactide) and Poly(N-isopropyl acrylamide) as Thermoresponsive Nanocontainers. Langmuir. 2004;20:10809-17.
[189] Lutz J-F, Akdemir Ö, Hoth A. Point by Point Comparison of Two Thermosensitive Polymers Exhibiting a Similar LCST: Is the Age of Poly(NIPAM) Over? J Am Chem Soc. 2006;128:13046-7.
[190] Srinivasan M. Fungal keratitis. Current opinion in ophthalmology. 2004;15:321-7.
[191] Poggio EC, Glynn RJ, Schein OD, Seddon JM, Shannon MJ, Scardino VA, et al. The incidence of ulcerative keratitis among users of daily-wear and extended-wear soft contact lenses. New England Journal of Medicine. 1989;321:779-83.
[192] Tanure MAG, Cohen EJ, Sudesh S, Rapuano CJ, Laibson PR. Spectrum of fungal keratitis at Wills eye hospital, Philadelphia, Pennsylvania. Cornea. 2000;19:307-12.

[193] Marangon FB, Miller D, Giaconi JA, Alfonso EC. In vitro investigation of voriconazole susceptibility for keratitis and endophthalmitis fungal pathogens. American journal of ophthalmology. 2004;137:820-5.
[194] Lazarus HM, Blumer JL, Yanovich S, Schlamm H, Romero A. Safety and pharmacokinetics of oral voriconazole in patients at risk of fungal infection: a dose escalation study. The Journal of Clinical Pharmacology. 2002;42:395-402.
[195] Johnson LB, Kauffman CA. Voriconazole: a new triazole antifungal agent. Clinical Infectious Diseases. 2003:630-7.
[196] Dupuis A, Tournier N, Le Moal G, Venisse N. Preparation and stability of voriconazole eye drop solution. Antimicrobial agents and chemotherapy. 2009;53:798-9.
[197] Lalitha P, Shapiro BL, Srinivasan M, Prajna NV, Acharya NR, Fothergill AW, et al. Antimicrobial susceptibility of Fusarium, Aspergillus, and other filamentous fungi isolated from keratitis. Archives of ophthalmology. 2007;125:789-93.
[198] O'day DM, Head WS, Robinson RD, Clanton JA. Corneal penetration of topical amphotericin B and natamycin. Current eye research. 1986;5:877-82.
[199] Teo J, Tan T, Hon P, Lee W, Koh T, Krishnan P, et al. ST22 and ST239 MRSA duopoly in Singaporean hospitals: 2006–2010. Epidemiology and Infection. 2012;1:1-5.
[200] Peeters E, Nelis HJ, Coenye T. Comparison of multiple methods for quantification of microbial biofilms grown in microtiter plates. Journal of microbiological methods. 2008;72:157-65.
[201] Roehm NW, Rodgers GH, Hatfield SM, Glasebrook AL. An improved colorimetric assay for cell proliferation and viability utilizing the tetrazolium salt XTT. Journal of immunological methods. 1991;142:257-65.
[202] Goldblum D, Frueh BE, Sarra GM, Katsoulis K, Zimmerli S. Topical caspofungin for treatment of keratitis caused by Candida albicans in a rabbit model. Antimicrobial agents and chemotherapy. 2005;49:1359-63.
[203] Prakash G, Sharma N, Goel M, Titiyal JS, Vajpayee RB. Evaluation of intrastromal injection of voriconazole as a therapeutic adjunctive for the management of deep recalcitrant fungal keratitis. American journal of ophthalmology. 2008;146:56-9.
[204] O'Day DM. Orally administered antifungal therapy for experimental keratomycosis. Transactions of the American Ophthalmological Society. 1990;88:685.
[205] Kamber NE, Jeong W, Waymouth RM, Pratt RC, Lohmeijer BGG, Hedrick JL. Organocatalytic Ring-Opening Polymerization. Chemical Reviews. 2007;107:5813-40.
[206] Kim SH, Tan JPK, Nederberg F, Fukushima K, Yang YY, Waymouth RM, et al. Mixed Micelle Formation through Stereocomplexation between Enantiomeric Poly(lactide) Block Copolymers. Macromolecules. 2008;42:25-9.
[207] Nederberg F, Lohmeijer BGG, Leibfarth F, Pratt RC, Choi J, Dove AP, et al. Organocatalytic Ring Opening Polymerization of Trimethylene Carbonate. Biomacromolecules. 2006;8:153-60.
[208] Pratt RC, Lohmeijer BGG, Long DA, Lundberg PNP, Dove AP, Li H, et al. Exploration, Optimization, and Application of Supramolecular Thiourea−Amine Catalysts for the Synthesis of Lactide (Co)polymers. Macromolecules. 2006;39:7863-71.
[209] Mukose T, Fujiwara T, Nakano J, Taniguchi I, Miyamoto M, Kimura Y, et al. Hydrogel Formation between Enantiomeric B‐A‐B‐Type Block Copolymers of Polylactides (PLLA or PDLA: A) and Polyoxyethylene (PEG: B); PEG‐PLLA‐PEG and PEG‐PDLA‐PEG. Macromolecular Bioscience. 2004;4:361-7.

[210] Moughton AO, O'Reilly RK. Thermally induced micelle to vesicle morphology transition for a charged chain end diblock copolymer. Chemical Communications. 2010;46:1091-3.
[211] Tan JPK, Kim SH, Nederberg F, Appel EA, Waymouth RM, Zhang Y, et al. Hierarchical supermolecular structures for sustained drug release. Small. 2009;5:1504-7.
[212] Petzetakis N, Dove AP, O'Reilly RK. Cylindrical micelles from the living crystallization-driven self-assembly of poly(lactide)-containing block copolymers. Chem Sci. 2011;2.
[213] Džidić S, Šušković J, Kos B. Antibiotic resistance mechanisms in bacteria: biochemical and genetic aspects. Food Technology and Biotechnology. 2008;46:11-21.
[214] Wiradharma N, Khan M, Yong LK, Hauser CAE, Seow SV, Zhang S, et al. The effect of thiol functional group incorporation into cationic helical peptides on antimicrobial activities and spectra. Biomaterials. 2011;32:9100-8.
[215] Cazander G, van de Veerdonk MC, Vandenbroucke-Grauls CMJE, Schreurs MWJ, Jukema GN. Maggot excretions inhibit biofilm formation on biomaterials. Clinical Orthopaedics and Related Research®. 2010;468:2789-96.
[216] James AW, Xu Y, Lee JK, Wang R, Longaker MT. Differential Effects of TGF-β1 and TGF-β3 on Chondrogenesis in Posterofrontal Cranial Suture–Derived Mesenchymal Cells In Vitro. Plastic and reconstructive surgery. 2009;123:31-43.
[217] Mehlhorn AT, Schmal H, Kaiser S, Lepski G, Finkenzeller G, Stark G, et al. Mesenchymal stem cells maintain TGF-β-mediated chondrogenic phenotype in alginate bead culture. Tissue Eng. 2006;12:1393-403.
[218] Chung YI, Ahn KM, Jeon SH, Lee SY, Lee JH, Tae G. Enhanced bone regeneration with BMP-2 loaded functional nanoparticle–hydrogel complex. Journal of Controlled Release. 2007;121:91-9.
[219] Storrie H, Mooney DJ. Sustained delivery of plasmid DNA from polymeric scaffolds for tissue engineering. Adv Drug Deliv Rev. 2006;58:500-14
[220] Kim SH, Tan JPK, Nederberg F, Fukushima K, Colson J, Yang CA, et al. Hydrogen bonding-enhanced micelle assemblies for drug delivery. Biomaterials. 2010;31:8063-71.
[221] Pratt RC, Lohmeijer BGG, David A, Lundberg PNP, Dove AP, Li H, et al. Exploration, optimization, and application of supramolecular thiourea-amine catalysts for the synthesis of lactide (co) polymers. Macromolecules. 2006;39:7863-71.
[222] Ong ZY, Fukushima K, Coady DJ, Yang YY, Ee PLR, Hedrick JL. Rational design of biodegradable cationic polycarbonates for gene delivery. Journal of Controlled Release. 2011;152:120-6.

APPENDICES

Appendix A: Synthetic procedures and molecular characterization of VS-PEG-CPC and cationic bolaamphiphile

A.1 Materials and methods

Materials

All reagents were purchased from Sigma-Aldrich and used as received unless otherwise noted. Tetra acrylate PEG (Mn 10,000 g/mol) and tetra sulfhydryl PEG (Mn 10,000 g/mol) were purchased from Sunbio Corporation (South Korea). SH-PEG-OH (Mn 5000 g/mol, PDI 1.03) was purchased from RAPP Polymere GmbH (Germany). Sparteine was stirred over CaH2, distilled in vacuum twice, and then stored in glove box. N-(3,5-trifluoromethyl)phenyl-N'-cyclohexylthiourea (TU) was prepared according to our previous protocol [154]. TU was dissolved in dry THF, stirred with CaH2, filtered, and freed of solvent *in vacuo*.

Synthesis of VS-PEG-PC polymer

The functional carbonate monomers, MTC-OEt and MTC-urea, were prepared according to the protocol reported in the previous work [154, 220].

Synthesis of VS-PEG-OH

In a nitrogen gas atmosphere, triethylamine (23 μL, 0.16 mmol) was added to a solution of HS-PEG-OH (0.2 g, 0.04 mmol) in MeOH (5 mL). And then, the resulted solution was

to dryness. Finally, the crude product was purified by column chromatography added dropwise to a solution of divinyl sulfone (124 μL, 1.2 mmol) in MeOH (5 mL) under stirring. The reaction mixture was heated to 60 °C and reacted for 6 hours before concentrated on a Sephadex LH-20 column with THF as eluent, giving VS-PEG-OH as white powder (0.2 g, 100%). 1H-NMR (400 MHz, DMSO-d6, 22 °C) δ 6.69 (q, 1H, H of methine), 6.46 (d, 1H, H of methylene), 6.19 (d, 1H, H of methylene), 3.63 (s, 455H, H of PEG), 3.25 (m, 2H, -SCH2CH2O-), 2.86 (m, 4H, -CH2CH2SCH2CH2O-), 2.48 (m, 2H, -SO2CH2CH2S-).

Synthesis of VS-PEG-P[(MTC-OEt)-random-(MTC-urea)] (Scheme A.1)

In a glove box, a solution of VS-PEG-OH (0.26 g, 0.05 mmol) in CH2Cl2 (0.75 mL) was mixed with the solution of TU (18.5 mg, 0.05 mmol) in CH2Cl2 (0.75 mL), followed by adding sparteine (11.5 μL, 0.05 mmol), and the formed solution kept stirring for 10 min. Then, a solution of MTC-OEt (0.094 g, 0.5 mmol) and MTC-urea (0.081 g, 0.25 mmol) in CH2Cl2 (1.5 mL) was added to the reaction mixture and reacted for 16 hours before benzoic acid (15-20 mg) was added to quench the polymerization. The reaction mixture was purified by column chromatography on a Sephadex LH-20 column with THF as eluent, to give HS-PEG-P[(MTC-OEt)8-random-(MTC-urea)4] as off-white sticky solid (0.35 g, 86%).1H-NMR (400 MHz, DMSO-d6, 22 °C) δ 7.43 (s, 8H, PhH), 7.24 (s, 8H, PhH), 6.98 (s, 4H, PhH), 6.70 (q, 1H, H of methine), 6.47 (d, 1H, H of methylene), 6.21 (d, 1H, H of methylene), 4.17-4.32 (m, br, 72H, -CH2OCOO- and -COOCH2-), 3.69 (s, 455H, H of PEG), 3.45 (s, br, 8H, -CH2NHCO-), 3.24 (m, 2H, -SCH2CH2O-), 2.87 (m, 4H, -CH2CH2SCH2CH2O-), 2.48 (m, 2H, -SO2CH2CH2S-), 1.22 (s, 60H, -CH3).

Gel permeation chromatograph (GPC)

GPC analysis for block copolymers was carried out with a Waters HPLC system equipped with a 2690D separation module with two Styragel HR1 and HR4E (THF) 5 mm columns (size: 300 × 7.8 mm) in series and a Waters 410 differential refractometer detector. THF was used as the mobile phase with a flow rate of 1 mL/min. A calibration curve was constructed using a series of polystyrene standards (molecular weight: 1,350-151,700), from which number-average molecular weights and polydispersity indices were calculated.

^{1}H NMR spectroscopy

^{1}H NMR analyses of monomers and block copolymers were performed on a Bruker Advance 400 NMR spectrometer at 400 MHz at room temperature (25 ± 2°C). The ^{1}H NMR measurement parameters: acquisition time of 3.2 s, pulse repetition time of 2.0 s, 30 ° pulse width, 5208-Hz spectral width, and 32 K data points. Chemical shifts were referred to the solvent peaks (δ = 7.26 and 2.50 ppm for CDCl3 and DMSO-d6, respectively).

A.2 Results and discussion

Synthesis of VS-PEG-PC polymer

Vinyl sulfone-functionalized PEG-*b*-polycarbonate (VS-PEG-PC) containing ethyl and urea functional pendant groups were synthesized by ROP of two monomers derived from 2,2-bis(methylol)propionic acid bearing pendant functional ethyloxycarbonyl groups

(MTC-OEt) or pendant funcational urea groups (MTC-urea) using vinyl sulfone-terminated PEG (VS-PEG-OH) as a macroinitiator (Scheme A.1). VS-PEG-OH was obtained from reacting HS-PEG-OH (Mw 5,000 g/mol) with a large excess amount of divinyl sulfone (molar reatio of HS-PEG-OH:divinyl sulfone is 1:30), and then the excess divinyl sulfone was removed by column chromatography on a Sephadex LH-20 column using methanol as eluent. In the polymerization reaction, parteine and TU, instead of 1,8-diazabicyclo[5.4.0]undec-7-ene (DBU), are used as catalysts because DBU can cause precipitation of MTC-urea monomer. The polymer with vinly sulfone group was obtained in high yield and narrow molecular weight distribution (PDI 1.12, shown in Figure A.1). The composition of VS-PEG-polycarbonate polymer was estimated from ^{1}H NMR spectrum (Figure A.2). All peaks attributed to vinyl sulfone group, PEG, MTC-OEt and MTC-urea were clearly observed in the proton spectrum. Quantitative comparisons between the integral intensities of the peak of ethylene groups of PEG, phenyl hydrogen of MTC-urea and methyl groups of MTC-OEt and MTC-urea gave the composition of the polymer, and there were 8 MTC-OEt units and 4 MTC-urea units in the VS-PEG-polycarbonate polymers as shown in Scheme 1. In addition, the polymer molecular weight estimated from ^{1}H NMR spectroscopy (Figure A.2) was consistent with that obtained from the M_n values from GPC, relative to polystyrene standards (data not shown).

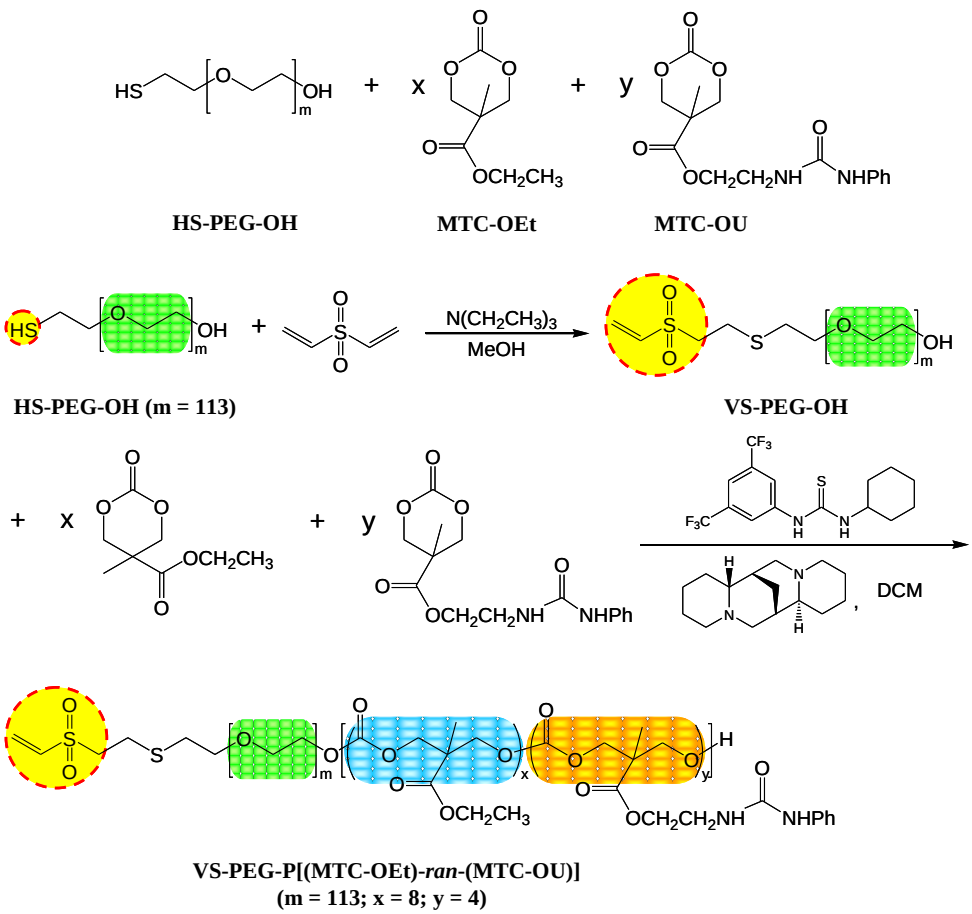

Scheme A.1 Synthetic schemes of VS-PEG-polycarbonate.

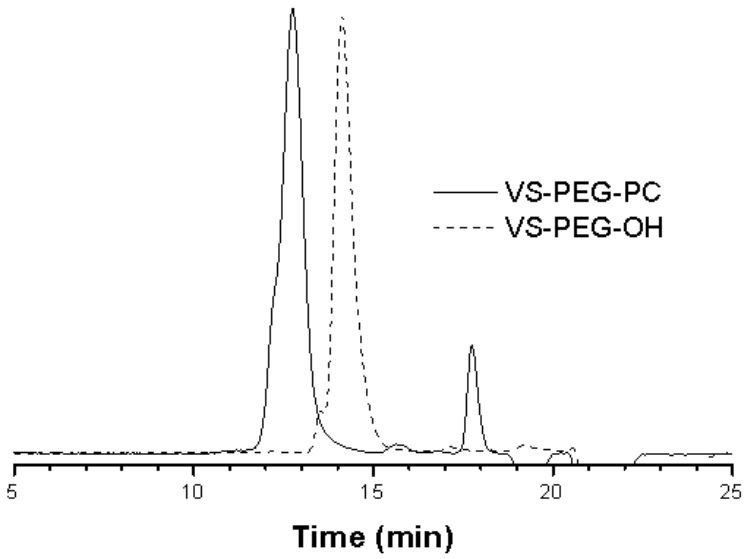

Figure A.1 GPC diagram of VS-PEG-PC (M_n = 10,120, M_w/M_n = 1.12).

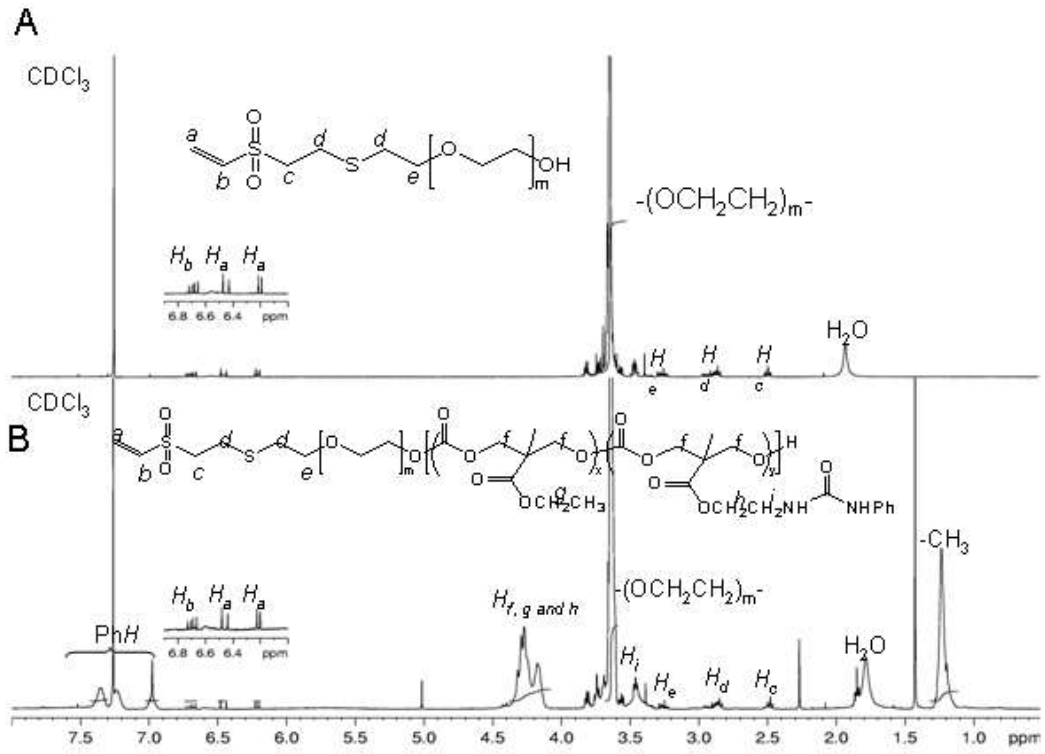

Figure A.2 Characterization of VS-PEG-OH, VS-PEG-polycarbonate (VS-PEG-PC) and its self-assemblies: $_1$H NMR spectra of (A) VS-PEG-OH and (B) VS-PEG-PC in $CDCl_3$.

Appendix B: Synthetic procedures and molecular characterization of cationic bolaamphiphile

Synthesis of cationic bolaamphiphile

The detailed synthesis and characterization for the cationic bolaamphiphile (Scheme 3.3) has been shown elsewhere [153]. This bolaamphiphile was synthesized using a three-step, two-pot procedure where pentaethylenehexamine was used as the hydrophilic amine unit, whilst 1,12-diaminododecane was used as the hydrophobic unit. In brief, the hydrophobic component of the bolaamphiphile was prepared by reacting 1,12-diaminododecane with a thiol ester, methyl-3-mercaptopropoinate, via nucleophilic substitution in a one-pot procedure at 80 ℃ for 24 hours in order to form the bolaamphiphile precursor molecule. Next using a ring-opening mechanism the precursor molecule was reacted with epichlorohydrin (glycidyl) to form the linker unit that was further connected to the hydrophilic pentaethylenehexamine unit via nucleophilic substitution to give rise to the final cationic bolaamphiphile. Successful synthesis of the precursor molecule and cationic bolaamphiphile were evidenced primarily by their IR spectra in conjunction with 1H NMR and 13C spectra. The 1H NMR spectrum of the cationic bolaamphiphile showed the presence of the hydrophobic diaminododecame as indicated by a broad set of peaks in the range of δ = 1.6-1.00 ppm. In addition, a peak at δ = 3.70 ppm was observed, which was assigned to the distinct methine proton (-CH2-CH(OH)CH2-) of the glycidyl linker unit. The presence of this peak proved the hydrophilic pentaethylenehexamine unit was connected to the hydrophobic diaminododecane unit via the glycidyl linker unit. Lastly, various sets of peaks were seen in the range of δ = 3.30-2.30 ppm, which were

mainly assigned to the methylene protons of the bolaaphiphile molecule. Bolaamphiphile: υmax/cm-1 3360 strong (sharp) [υ(N-H)]; 3310 strong (sharp) [υ(N-H)]; 2960 medium (sharp) [υ(C-H)]; 2830 medium (sharp) [υ(C-H)]; 1660 strong (sharp) [υ(C=O)]; 1120 weak (sharp) [υ(C-OH)]. δH (400 MHz, D2O) 3.70 (1H, m, -CH2-CH(OH)CH2-); 3.30-2.20 (2H, t, NH2-CH2-CH2-NH-, -CH2-CH2-CH2-NH-C(=O)-CH2-CH2-S-, -CH2-CH(OH)CH2-) and 1.60-1.00 ppm (-(O=)C-NH-CH2-(CH2)10-CH2-NH-C(=O)-).

Appendix C: Synthetic procedures and molecular characterization of P(D/L)LA-PEG-P(D/L)LA and cationic polymer PDLA-CPC-PDLA

Materials

L-lactide and D-lactide were obtained from Purac Biochem Gorinchem NL and recrystallized three times from toluene and dried in vacuum prior to use. Diol functional poly(ethylene glycol) macro-initiators were dried by azeotropic distillation with toluene and dried at 50 ℃ under reduced pressure. Dry toluene and dichloromethane (DCM) were obtained from a drying column using a setup from Innovative Systems Inc., with a 60 Å 230-400 Mesh ASTM Silicon Gel Whatman column. (-)-Sparteine (Sigma-Aldrich, 99%) and 1,8-diazabicyclo[5.4.0]undec-7-ene (DBU, Sigma-Aldrich, 98%) were distilled over calcium hydride. 1-(3,5-Bis(trifluoromethyl)phenyl)-3-cyclohexcylthiourea (TU), benzyl bis(2,2-hydroxymethyl)propionate (BnMPA), 2-(3-chloropropyl)oxycarbonyl-2-methyl trimethylene carbonate (MTC-CP), and 2-(3-bromopropyl)oxycarbonyl-2-methyl trimethylene carbonate (MTC-BP) were synthesized as previously reported elsewhere [221, 222]. All other chemicals and solvents were purchased from Sigma-Aldrich and used as received.

Polymer characterization

^{1}H and ^{13}C-NMR spectra were acquired on a Bruker Avance 400 instrument operated at 400 and 100 MHz, respectively. Gel Permeation Chromatography (GPC) in THF was performed at 30 ºC using a Waters chromatograph equipped with four 5 μm Waters columns (300 mm × 7.8 mm) connected in series (HR1, HR2, HR4E and HR5E), a

Waters 2410 refractive index (RI) detector and a 996 photodiode array detector, and calibrated with polystyrene standards (560 to 2 $\times 10^6$ g/mol).

Synthesis of PLA-PEG-PLA triblock copolymers (Scheme C.1).

These triblock copolymers were prepared *via* organocatalytic ring-opening polymerization (ROP). Diol functional poly(ethylene glycol) (PEG) having a number average molecular weight (Mn) of 6000 g/mol (PEG1) or 8000 g/mol (PEG2) was used as an initiator for the ROP of either L-lactide or D-lactide using a mixture of 1-(3,5-bis(trifluoromethyl)-phenyl)-3-cyclohexylthiourea (TU) and (-)-sparteine as catalysts in methylene chloride. As an example, PEG2 (Mn = 8K, 0.40 g, 0.05 mmol) was dissolved in 2 ml of methylene chloride. In a separate vial, L-lactide (0.20 g, 1.38 mmol) was charged along with catalysts TU (0.025 g, 0.007 mol) and (-)-sparteine (0.016 g, 0.007 mol), and dissolved in methylene chloride. The L-lactide solution was added to the PEG2 initiator solution and the polymerization was followed for 6 hours by ^{1}H NMR, at which time the L-lactide consumption was complete. The product was precipitated in ether, isolated by filtration, and dried. The non-charged triblock copolymer was characterized by ^{1}H NMR and GPC.

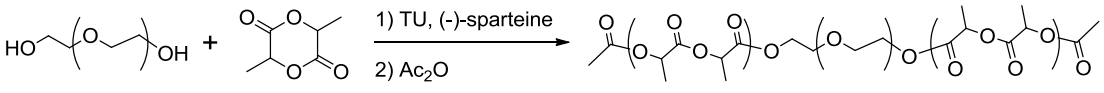

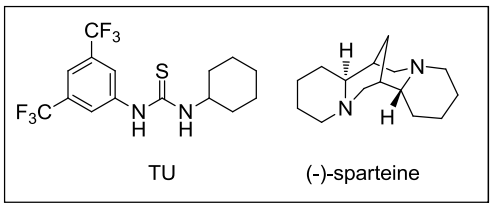

Scheme C.1 Typical synthesis of polylactide-*b*-poly(ethylene glycol)-*b*-polylactide (PLA-PEG-PLA) triblock copolymer.

Synthesis of PDLA-CPC-PDLA triblock copolymers (Scheme C.2)

Synthesis of precursor polymers

The precursor triblock copolymers were prepared by sequential ROPs of a MTC-PrCl or MTC-PrBr monomer to form the precursor core block, followed by polymerization of D-lactide to form the peripheral hydrophobic blocks. The initiator was a diol, BnMPA. The polymerization was catalyzed by TU and DBU in methylene chloride at room temperature (25 ± 2°C, 1 to 2 hours). Typically, MTC-PrCl (365 mg, 1.54 mmol), BnMPA (22.2 mg, 0.10 mmol), and TU (14.5 mg, 0.039 mmol) were dissolved in methylene chloride (1.0 mL), and this solution was transferred to a vial containing DBU (6.0 mg, 0.039 mmol) to start polymerization at room temperature (DP_1 = 16). After 5 hours (conversion of MTC-PrCl ~93%), the solution was transferred to a vial containing D-lactide (DLA) (261 mg, 1.81 mmol) to start the second polymerization. The second polymerization was stirred for 19 hours at room temperature (DP_2 = 18). Conversion of DLA was about 95%. Acetic anhydride (57 mg, 0.56 mmol) was added to the reaction mixture, and stirring was continued 96 hours, thereby forming an acetyl end-capped precursor triblock copolymer, Precursor I. The end-capped block copolymer was precipitated in cold methanol, centrifuged, and dried in vacuum. Yield of Precursor I: 497 mg (77%), GPC (THF): Mn 12700 g/mol, PDI 1.15, ^{1}H NMR (400 MHz, $CDCl_3$): δ 7.39-7.28 (m, Ar*H*), 5.23- 5.05 (m, PhCH_2, CH_{PDLA}), 4.40-4.17 (m, CH_2OCOO$_{poly(MTC\text{-}PrCl)}$, OC$H_{2\ poly(MTC\text{-}PrCl)}$), 3.65-3.53 (m, C$H_2Cl_{poly(MTC\text{-}PrCl)}$), 2.17-2.03 (m, C$H_{2\ poly(MTC\text{-}PrCl)}$, OC$H_{3\ end\ group}$), 1.64-1.46 (m, C$H_{3\ PDLA}$), 1.31-1.19 (m, C$H_{3\ poly(MTC\text{-}PrCl)}$).

Precursor II was prepared by the same protocol as that of Precursor I using MTC-PrBr (325 mg, 1.15 mmol) in place of MTC-PrCl, BnMPA (14.5 mg, 0.065 mmol), TU (11.9 mg, 0.032 mmol), DBU (5.1 mg, 0.033 mmol) and DLA (146 mg, 1.01 mmol) to yield the polymer with DP_1 = 18 and DP_2 = 16. Yield: 307 mg (63%), GPC (THF): Mn 4400 g/mol, PDI 1.08, ^{1}H NMR (400 MHz, $CDCl_3$): δ 7.40-7.28 (m, Ar*H*), 5.26-5.04 (m, PhCH_2, CH_{PDLA}), 4.41-4.16 (m, CH_2OCOO $_{poly(MTC\text{-}PrBr)}$, OC$H_{2\ poly(MTC\text{-}PrBr)}$), 3.53-3.37 (m, C$H_2$Br $_{poly(MTC\text{-}PrBr)}$), 2.25-2.14 (m, C$H_{2\ poly(MTC\text{-}PrBr)}$), 2.13 (s, OC$H_{3\ end\ group}$), 1.64-1.46 (m, C$H_{3\ PDLA}$), 1.33-1.19 (m, C$H_{3\ poly(MTC\text{-}PrBr)}$).

Quaternization with trimethylamine.

Trimethylamine gas (782 mg, 13.2 mmol) was charged to an acetonitrile solution (4 mL) of Precursor I (466 mg, [Cl] = 0.98 mmol) immersed in a dry-ice/acetone bath. The solution was then allowed to warm up to 50 ° C and kept stirring for 14 hours before acetonitrile and excess gasses were removed under vacuum. The concentrated residue was dried in vacuum (~88% quaternized). Yield of PDLA-CPC-PDLA 1: 461 mg (88%), GPC (DMF): Mn 8900 g/mol, PDI 1.17, ^{1}H NMR (400 MHz, MeOH-d_4): δ 7.44- 7.31 (m, Ar*H*), 5.27-5.03 (m, PhCH_2, CH_{PDLA}), 4.48-4.18 (m, CH_2OCOO$_{PC}$, OC$H_{2\ PC}$, OC$H_{2\ PC}$), 3.59-3.41 (br, N^+C$H_{2\ PC}$), 3.25-3.13 (br, N^+C$H_{3\ PC}$), 2.29-2.16 (br, C$H_{2\ PC}$), 2.09 (s, OC$H_{3\ end\ group}$), 1.60-1.40 (m, C$H_{3\ PDLA}$), 1.35-1.24 (m, C$H_{3\ PC}$).

PDLA-CPC-PDLA 2 (~89% quaternized) was prepared by the same procedure using Precursor II. Yield: 471 mg (81%), GPC (DMF): Mn 9400 g/mol, PDI 1.15. ^{1}H NMR (400 MHz, MeOH-d_4): δ 7.42-7.34 (m, Ar*H*), 5.26-5.04 (m, PhCH_2, CH_{PDLA}), 4.45-4.20

(m, CH_2OCOO$_{PC}$, OC$H_{2\ PC}$, OC$H_{2\ PC}$), 3.63-3.43 (br, N^+C$H_{2\ PC}$), 3.28-3.13 (br, N^+C$H_{3\ PC}$), 2.31-2.15 (br, C$H_{2\ PC}$), 2.09 (s, OC$H_{3\ \text{end group}}$), 1.62-1.40 (m, C$H_{3\ PDLA}$)), 1.36-1.24 (m, C$H_{3\ PC}$).

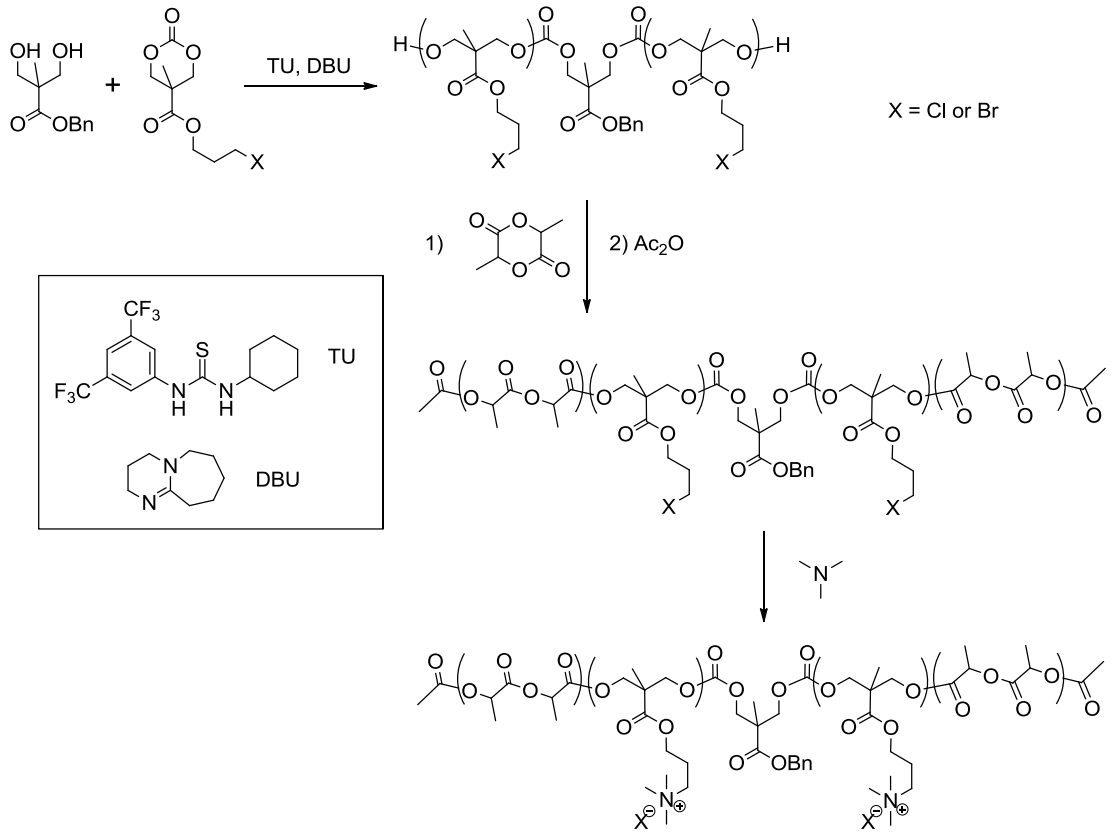

Scheme C.2 Typical preparation of poly(D-lactide)-*b*-cationic poly(carbonate)-*b*-poly(D-lactide) (PDLA-CPC-PDLA) triblock copolymers.